STOCHASTIC ANALYSIS OF HUMAN POSTURAL SWAY

A THESIS SUBMITTED TO
THE GRADUATE SCHOOL OF NATURAL AND APPLIED SCIENCES
OF
MIDDLE EAST TECHNICAL UNIVERSITY

BY

NACİ BARIŞ YARADANAKUL

IN PARTIAL FULFILLMENT OF THE REQUIREMENTS
FOR
THE DEGREE OF MASTER OF SCIENCE
IN
ENGINEERING SCIENCES

SEPTEMBER 2022

Approval of the thesis:

STOCHASTIC ANALYSIS OF HUMAN POSTURAL SWAY

submitted by **NACİ BARIŞ YARADANAKUL** in partial fulfillment of the requirements for the degree of **Master of Science in Engineering Sciences Department, Middle East Technical University** by,

Prof. Dr. Halil KALIPÇILAR
Dean, Graduate School of **Natural and Applied Sciences** _____

Prof. Dr. Murat Dicleli
Head of Department, **Engineering Sciences** _____

Assist. Prof. Dr. Senih Gürses
Supervisor, **Engineering Sciences, METU** _____

Examining Committee Members:

Prof. Dr. Yıldıray Ozan
Mathematics, METU _____

Assist. Prof. Dr. Senih Gürses
Engineering Sciences, METU _____

Prof. Dr. Dilek Keskin
Engineering Sciences, METU _____

Prof. Dr. Işık Hakan Tarman
Mechanical Engineering, METU _____

Prof. Dr. Mehmet Yetmez
Mechanical Engineering, Zonguldak Bülent Ecevit University _____

Date:

I hereby declare that all information in this document has been obtained and presented in accordance with academic rules and ethical conduct. I also declare that, as required by these rules and conduct, I have fully cited and referenced all material and results that are not original to this work.

Name, Surname: NACİ Barış Yaradanakul

Signature :

ABSTRACT

STOCHASTIC ANALYSIS OF HUMAN POSTURAL SWAY

Yaradanakul, NACİ Barış
M.S., Department of Engineering Sciences
Supervisor: Assist. Prof. Dr. Senih Gürses

September 2022, 116 pages

"The decisive step in the transition from ape to man", in other words, inherently unstable dynamics of human erect posture, is investigated throughout the thesis considering the random features with a spatiotemporal perspective employing stochastic dynamical system theory and statistical mechanics. During the investigation, mechanistic reasoning and control theory is not mentioned, but the complex dynamical output of four basic sensors somatosensory, vestibular, visual and proprioceptive, physicochemical actuator striated muscles, multidegree of freedom plant having redundancies depending on the task, and the nervous system, namely postural sway, is modeled as a black box that is characterized by CoP_x time series.

Keeping this objective in mind, the first chapter is devoted to the explanation of the loaded philosophical content of postural sway with a phylogenetic and ontogenetic point of view. Furthermore, the contrast between Newtonian determinism in time and Boltzmanian understanding of chance in space are considered in terms of the concept of time, its direction, causality, and entropy to clarify the spatiotemporal domain, in which the dynamics of interest to be analyzed with stochastic analytical tools. In this context, in Section 1.2, philosophical ideas that have been developed were employed

in an attempt to explain the particular problem by means of stochastic process and cybernetics to answer the question "What is the dice ruling the postural sway?".

Besides the philosophical content, Chapter 2 continued with neurophysiological reasons behind the never-ending postural sway, possibly serving for the ecological search of the equilibrium point (conservative level) and the boundaries of stability (operative level) with trial and error. For instance, the output of this complex system, CoP_x, two superposed oscillations at different frequencies constituting postural sway are explained considering the works of Zatsiorsky's rambling trembling decomposition, Gurfinkel's conservative and operative levels, Feldman's λ-threshold theory, and Hogan's virtual trajectory explanation; in spirit, all reconciling similar dualities. Considering the neurophysiological aspects in Section 2.2, measurement methods of postural sway are explained for the quantification of the problem.

Later, stochastic dynamics of the CoP_x signal are investigated in a pathwise manner with proposed stochastic differential equations starting from the visual verification of normality of decision makings, i.e., displacements. The first step is started with the integration of the Wiener process obeying $\sigma\left(\Delta t\right)^{1/2}\mathcal{N}(0,1)$. Due to the linearly increasing variance, which would result in falling down, linear mean reversion was imposed on the dice ruling the sway to constraint the variance inside the area under the foot. While the resulting process is named as Ornstein Uhlenbeck, it is linked to viscoelasticity known as Langevin Equation. For the analytical consideration of the two-level nature of postural sway, the double Ornstein Uhlenbeck process was defined. In this way, the baseline fluctuations around zero are converted into oscillations around θ_t which describes the rambling equilibria. The covariance function of the proposed system of differential equations having a double exponential form revealed distinct time scales consistent with the posture literature. A final improvement was performed by imposing a cubic nonlinearity on the model for the assessment of the multimodality of sway.

Keywords: postural sway, stochastic process, threshold dynamics

ÖZ

İNSAN DİK DURUŞUNUN OLASILIKSAL ANALİZİ

Yaradanakul, NACİ Barış
Yüksek Lisans, Mühendislik Bilimleri Bölümü
Tez Yöneticisi: Dr. Öğr. Üyesi. Senih Gürses

Eylül 2022 , 116 sayfa

Bu tezde insan dik duruşunun kararlı olmayan dinamiği olasılıksal özellikleri dikkate alınarak uzay zaman perspektifine sahip bir şekilde stokastik dinamik sistem teorisinin ve istatistiksel mekaniğin araçlarının kullanılmasıyla incelenmiştir. Araştırma sırasında mekanik yaklaşım ve kontrol teorisi göz önünde bulundurulmazmıştır. Fakat dört duyunun, eyleyici kasların, vücudun ve sinir sisteminin ortak çıktısı CoP_x sinyali üzerinden bir kara kutu olarak karakterize edilmiştir.

Tezin ilk kısmı postür salınımlarının felsefi içeriğe yoğunlaşmıştır. Bunun yanında Newton determinizmini Boltzmann anlayışıyla zaman, zamanın yönü, nedensellik anlamlarında karşılaştırılmasına yer verilmiştir. Kısım 1.2'de ise önceki kısımda geliştirilen fikirlerin incelenecek dinamik sistem üzerine uygulamalarından bahsedilmiştir. Ayrıca postür salınımlarını idare eden rastgelelik yapısını anlamaya yönelik girişimlerde bulunulmuştur.

Devamında gelen Kısım 2'de asla durmayan postür salınımlarının arkasındaki nörofizyolojik nedenler incelenerek devam edilmiştir. Söz konusu karmaşık sistemin temel çıktılarından olan CoP_x zaman serisinin ikili salınım yapısıyla ilgili Zatsiorksky,

Gurfinkel, Feldman ve Hogan'ın benzer çalışmaları açıklanmıştır. Devamında postür salınımlarının ölçüm prensipleri özetlenmiştir.

Takip eden Kısım 3'te ise CoP_x zaman serisini temsil eden stokastik diferansiyel denklemin formu aranmış ve hızların normal dağıldığı görsel olarak kanıtlanmıştır. Birinci aşamada difüzyon denklemi ve Wiener süreci kullanılmıştır. Fakat bu modellerin rastgeleliliği yakalasa bile varyansları sürekli olarak arttığı için uygun bir seçim olmadığına karar verilmiştir. Bu yüzden ikinci aşamada Ornstein Uhlenbeck süreci kullanılarak varyansın artışı kısıtlanmıştır. Daha sonra postür salınımlarının ikili yapısının incelenmesi gözetilerek çift Ornstein Uhlenbeck stokastik süreci tanımlanmıştır. Yeni tanımlanmış stokastik sürecin çift üstelli formu üzerinden postür literatürüyle tutarlı sonuçlar bulunmuştur. Son olarak ise kübik bir polinomun kullanılmasıyla CoP_x'in çok modlu olasılıksal dağılımına ulaşılmıştır.

Anahtar Kelimeler: postür salınımları, stokastik süreçler, eşik dinamikleri

to my family

ACKNOWLEDGMENTS

Albert Einstein defines the only rational way of education as being an example. So in the first place, I have to state my special thanks to my advisor Dr. Senih Gurses for being such a great example, as an old friend of mine, rather than providing a conventional education. Similarly, Dr. Yildiray Ozan for motivating me to learn mathematics and showing how a mathematician analysis the situation and acts to change. Also, I should state my sincere gratitude to Dr. Azize Hayfavi, who changed my life by accepting me for her class "Advanced Stochastic Calculus for Finance", together with her never-ending motivation for learning and teaching. From the very early days of my M.Sc. education, heavily depending on stochastic calculus, Ozenc Murat Mert was not only the teaching assistant of the course, but he answered all my questions about probability theory and stochastic calculus for three years.

Then I have to thank my family, Deniz, Figen, and Sinan Yaradanakul, together with my aunt Tijen Karakayali and Ayse Karakayali, the ones I live with, and also my friend Nazli Gokcen Guner. Without their support, especially without Tijen Karakayali and Gullu Comertoglu, the dissertation would definitely be an impossible task to complete.

Besides, I have to stress the role of my friend Ahmet Yesevi Kucuk for teaching me the scientific method from the very early days of my freshman year. Also, I have to thank my friend Cantug Fidan for his support and all the time we spent together. I deeply thank Umut Can Adıyaman and Saadet Coskun for their help in drawing the diagrams and for their friendship.

Last but not least, our research group members, Maryam Hassanpour, Elmira Pourreza, Berat Can Cengiz, Mehmet Imir, Ekin Varli, Gozde Yalcin, and Renan Arda Carlak are worth mentioning with my sincere and deepest gratitude.

TABLE OF CONTENTS

LIST OF TABLES

LIST OF FIGURES

FIGURES

LIST OF ABBREVIATIONS

B_t	White Noise
W_t	Wiener Process
X_t	Random Variable Representing CoP_x at t
GRF	Ground Reaction Force
CoP	Center of Pressure
CoP_x	Center of Pressure in Anterioposterior Direction
CoP_y	Center of Pressure in Mediolateral Direction
CoM	Center of Mass
CoM_x	Center of Mass in Anterioposterior Direction
CoM_y	Center of Mass in Mediolateral Direction
Rm	Rambling Trajectory
Tr	Trembling Trajectory
SDE	Stochastic Differential Equation

CHAPTER 1

INTRODUCTION

1.1 Phylosophical Content of the Subject

Friedrich Engels underlines the role of human erect posture as the first cornerstone for the establishment of civilization, *"the decisive step in the transition from ape to man"*, through the labor created with hands which converts the materials into wealth [7]. Engels asserts that by courtesy of raising on foot to stand upright in an agile manner, hands are departed from the ground and become free to execute motor tasks. Thanks to operational hands, which are not carrying load anymore, mankind rapidly differentiated from its ancestors, apes, as hands put forward the labor that is the source of all wealth. In this way, throughout the thousands of years of perfection of the human hand, which is *not only the organ of labor but also the product of the labor*, mankind created itself. As the hands became more dexterous, early human ancestors became able to build society. The surplus value was then created via hands-foot-eyes and brain through which exploited "wealth" became possible and would then be the promoter of the *civilized* society organization for tens of centuries. Throughout the gradual advancement, they started thinking; therefore, they had opinions to share. In this way, languages are developed parallel to the larynx for communication. Under the influence of labor created by hands and the stimulus of language, the human brain got ready for abstraction and deriving conclusions with clarity of consciousness. Consecutively, early human beings learned agriculture, performed metal working and poetry, settled trading and industries, and also performed art and science. In this way, nations are born, and tribal life morphed into states, so the domination of nature became possible. In short, until our time, humankind established civilized society on the path of searching for the truth and revealing the unknown with a never-ending motivation,

setting higher aims, and overcoming the obstacles faced. All advancements along the route became possible with the involvement of the hands, without which, would be impossible in the absence of erect posture.

Besides the attempts of different apes to rise on foot, they can not stand properly but only in a very clumsy way in case of urgency. Yet, man is the one and the only creature that exploits the proactive erect posture for the benefit of hands to build every single piece of civilization. Rather than its millions of years long phylogenetic development, i.e., evolution, individual infants spend more than one year to learn standing independently in an ontogenetic perspective compared to newborn quadripedal animals walking immediately in several minutes. In other words, they allocate the very first year of their lives to achieving the most complicated motor task among all living creatures. Either in a phylogenetic or ontogenetic point of view, the question arises in anyone's mind, "How is erect posture maintained?" which is not only the most fundamental building block of the enlightenment in terms of human society but the inevitable skill required for almost every single daily life activity along the lifespan.

As claimed by Engels, proactive rather than reactive erect posture, which is the accomplished motor skill, ends up with the advancement of different parts of the body. Particularly, the associated senses involved in the maintenance of the balance are enhanced, that are the exteroceptors, including somatosensory afferents located in plantar cutaneous (foot sole), vestibular apparatus, semicircular canals, and otolith organs, together with vision. As he cited, Charles Darwin proposes the same as "the law of correlation of growth" with the words *if man goes on selecting, and thus augmenting, any peculiarity, he will almost certainly unconsciously modify other parts of the structure, owing to the mysterious laws of the correlation of growth."* [8] together with many examples derived from the animal kingdom in his well-known work "The Origin of Species". It is clear that the dynamics of erect posture is associated with the exteroceptive senses, which collect information from the external world, and interoceptors named proprioception, gathering kinematic information related to joint angles and velocities, which are employed together to form the *self-perception*. Besides the senses, either exteroceptors or the interoceptors, actuators, namely striated muscles, the plant which is the body, and the greatest mystery of all times, the human brain and the nervous system are also shaped to work together collectively for the maintenance

of upright balance in a proactive manner despite a passive, reactive way of behavior.

Besides the temporal development of erect posture, either phylogenetic or ontogenetic, each distinct spatial segment contributing to balance must work together. Otherwise, the maintenance of bipedal stance becomes impossible in the absence of bidirectional information flow [9], either mechanical or electrochemical, between the actuators and senses. In other words, the quiet stance is the outcome of the states of distinct segments, including redundantly many striated muscles obeying the laws of biochemistry and four basic sensors in a multijoint plant together with the most complicated and mysterious product of nature, the human brain or neurological system including reflex loops and hierarchically structured divisions. Therefore, in addition to the temporal development of posture, a spatial analysis of segments that give birth to erect posture is the *sine qua non* for a concrete understanding.

Spatial analysis of states of different segments is a complicated problem, so it has to be handled carefully. René Descartes suggests four laws he strictly obeyed for methodological reasoning in his book *Discourse on the Method of Rightly Conducting One's Reason and Seeking Truth in the Sciences*[10]. Firstly, he advises never accepting the truth of anything unless there exists evident proof about its truth which keeps him away from hasty conclusions and prejudgements. Secondly, he suggests dividing the complete complex problem into as many parts as possible to deal with each separately. Thirdly, one should start from the simplest to the direction of more and more complicated for ordering the sequence of thoughts. Finally, he suggests checking every single aspect of the problem to be sure about noticing all points. Even if the method proposed by Descartes puts one reasoning into a well-grounded basis, segmentation of the complex dynamics, in our particular case of erect posture, into parts such as actuator, senses, or plant may lead to significant misinterpretations due to the existence of nonlinear crosstalks rather than linear, and bidirectional information flow rather than unidirectional, between distinct segments. Interestingly the information flow in the actuator, striated muscle is bidirectional [11],[12], which will be discussed in the next section. Furthermore, sensory fusion involves nonlinear relations[13],[14]. In other words, even if we would be able to explain every single aspect of all senses, actuators, plant, and nervous system, we can not fully comprehend all facets of quiet stance since it is more than the assembly of disjoint segments

due to the coupling between divisions. Under the existence of linear and nonlinear crosstalks, redundantly many degrees of freedom, mysteries of the central and peripheral nervous system, together with missing information about the core of the dynamics, probabilistic reasoning is inevitable rather than a deterministic Newtonian point of view in which everything is known, in other words, the missing information is nothing but zero. Besides those troubles, it is well known that deterministic Newtonian understanding can not explain adapting and learning dynamical systems whether the equations employed are linear or nonlinear [15], since the infinite future and past are well defined by initial conditions and boundary conditions, so even an infinitesimal deviation from certainly defined trajectory is impossible in the absence of missing information.

On the other hand, probabilistic analysis of spatial facets is named statistical mechanics, starting with the efforts of many talented scientists, including Ludwig Boltzmann [16], Albert Einstein [17], and Louis Bachelier [18] from various fields. Anyone studying statistical mechanics realizes that considerations are restricted in space, $S = K_B log(\Omega)$ or $p(E_i) = \frac{e^{E_i/K_BT}}{\sum_i e^{E_i/K_BT}}$ where only the arrow of time is present in the direction which entropy increases according to the *second law of thermodynamics*, besides its magnificent fertileness which is mentioned as *"It is the only physical theory of universal content, which I am convinced, that within the framework of applicability of its basic concepts will never be overthrown."* by Albert Einstein. Entropy, denoted with S, can be interpreted as a measure of surprise and ignorance. Still, it has nothing to do with time except the direction in which every spontaneous reaction increases the entropy, missing information, or surprise of the universe (union of system and surroundings). Therefore entropy can be deciphered as the accumulation of surprise as time progresses, even if the time is implicit in the relations. In other words, thermodynamics deals with the spontaneity of the reactions indicated by the arrow of time. However, it has nothing to say about temporal analysis, including the required time that the reaction is completed, even though the reaction necessitates an infinite amount of time since the temporal variable t is implicit. On contrary, in Newtonian description of the problem the spatial facets are missing, and all differential equations are solved over time explicitly as $\dot{\vec{x}} = \underline{f}(\vec{x})$ for some $\vec{x} \in R^n$ whether the function $\underline{f}(\vec{x})$ is linear or nonlinear. By employing a nonlinear $\underline{f}(\vec{x})$, one can consider

aperiodicity and initial condition sensitivity, so the model comes close to reality with a trade-off of abandoning explicit solutions of the differential equation. In this route, the most common intuitive interpretation is *Geometrical Way of Thinking*. Anyone interested in the subject may read the well-known introductory book written by Steven Strogatz for further information [19].

At this point, before going further and deeper, it is better to distinguish Newtonian mechanics, Newtonian time, against the concept of time in statistical mechanics which the direction of time is guided by the increasing entropy. Therefore the events following each other increase the total entropy of the universe rather than causality. In Newtonian mechanics, such as two celestial objects rotating around each other, anyone can not see any distinction if the arrow of time is reversed, where the consecutive events are linked with causality. In other words, from a Newtonian point of view, time is symmetric forward and backward through the reversion of causes and effects. Imagine watching a video where the earth rotates around the sun, a pendulum swinging back and forth, or an object following a parabolic trajectory in the presence of gravitational force. For all of those situations, nobody can notice if the film is reversed or not. Yet the reversion of a video showing turbulence or sprayed liquid from a vaporizer looks unusual. The main reason behind the difference is the existence of missing information between two distinct classes of dynamical systems. In the first kind, like celestial bodies, due to well-defined relations between a few particles, reversion of time does not have qualitative or quantitative effects. In terms of Shannon Information Theory [20], anything is known in this case. However, in the second kind of examples, due to the existence of almost infinite many particles in which all initial conditions and cross relations are ill-posed, time can not flow symmetrically. In those cases, entropy, i.e., missing information, increases following the arrow of time, giving rise to asymmetry in the direction of the time flow. Therefore rather than the position of each particle, against to the celestial body, everything can not be determined precisely. So that the method inevitably must depend on distributional properties to investigate the system. As longer times pass, even the distributional properties vanish, and the predictions deteriorate due to growing missing information. Yet, in a moderate time scale, the missing information, namely spatial facets, can be followed with statistical moments which are not considered in Newtonian mechanics of celes-

tial bodies. In this perspective, the nonlinearity of deterministic dynamics does not impose anything on the reversibility of time but changes the properties related to predictability which Lyapunov exponents can measure, basically the measurement of the rate of divergence of two paths starting arbitrarily close to each other. In other words, when the dynamics are selected to be nonlinear, one may find room for chance in the absence of missing information unless the initial condition of the trajectory is fully determined.

Therefore one can conclude that statistical mechanics involves spatial facets, but the time is missing; on the other hand, Newtonian mechanics involve time but miss the space. In order to benefit from the advantageous aspects of each, the next step must be fusing space with asymmetrical time to form a spatio-temporal domain where the range is the probability density function denoted as $p(x,t)$. Different than Newtonian trajectory $x(t)$, in a stochastic perspective domain has two distinct variables one is associated with space, and the other one governs the flow of time explicitly. Therefore investigation of the spatio-temporal domain is possible with partial differential equations. In this sense, the most basic relation explaining diffusion on the real line $x \in (\infty, -\infty)$ can be stated as Fick's second law, namely diffusion equation, and it can be expressed as $\frac{\partial p(x,t)}{\partial t} = D\frac{\partial^2 p(x,t)}{\partial x^2}$. The left-hand side of the relationship dictates the temporal evolution of probability density, and the partial derivative on the right-hand side is nothing but the spatial second-order derivative. The solution for the given initial condition, which is a Dirac delta located at zero $\delta(x)$, evolves into a Gaussian density in which the variance increases linearly with time $2Dt$, and the mean remains constant at zero. The initial condition can be interpreted within two distinct perspectives [21] (namely ergodicity [22]). The first one is an ensemble of indistinguishable particles located at the origin at $t = 0$ and diffusing for $t > 0$. The other interpretation is a single particle located at the origin; therefore, the distribution stands for its fate, so the probabilities represent its location at $t > 0$ standing for the realization of some certain fate. Yet, the solution says nothing about the pathwise features of a single particle, but it describes the evolution of an ensemble of particles or infinite possible fates of a single particle. Please note that in terms of distribution, dynamics is still deterministic due to deterministic moments, even though the fate of a single particle is random. While considering the difference between the pathwise

random appearance of the stochastic process against the deterministic evolution of distribution, a further explanation is required involving spatio-temporal aspects of the dynamical systems. To the best of our knowledge, the most concrete explanation of the relation can be found in Hegel's Philosophy of Nature. He clearly explains the relation between space and time by considering the fate of a particle and deterministic spatial distribution with a dynamical perspective with the words *"As space, in which time is suspended, the body is enduring, and as time, in which the indifferent subsistence of space is suspended, the body is transitory. ... In motion, time posits itself spatially as place, but this indifferent spatiality becomes just as immediately temporal: the place become another."*

Either philosophically or analytically, space and time must be fused together to comprehend the dynamical system of interest by benefiting the power of calculus [23], since "calculus is the limit of things that are easy to interpret" as defined by Clifford A. Pickover. In this respect, two necessities emerge. As it is known from the times of Newton, calculus is the only possible way for the quantitative handling of the problem, which is also seen in the words of Lord Kelvin that *"When you can measure what you are speaking about, and express it in numbers, you know something about it; but... when you cannot express it in numbers, your knowledge is of a meager and unsatisfactory kind."*. So firstly, the problem must be quantified, then a proper model involving calculus must be developed.

1.2 Implementing the Philosophical Ideas to the Particular Field

The main signals of human postural sway are the center of pressure, CoP, and the center of mass, CoM. CoP can be defined as the location of net force applied to the body through the foot and consists of two orthogonal coordinates at the horizontal plane, CoP_x and CoP_y at anteroposterior (forth-and-back) and mediolateral (right-and-left) directions respectively. The important distinction between anterioposterior and mediolateral directions is the difference in the stability of the sway. Firstly, the lateral (side) view (sagittal plane) of the posture seems like an inverted pendulum which is inherently unstable and can be expressed as an open kinematic chain. Yet the anterior (frontal) view of posture (frontal plane) looks like a four-bar linkage which is

stable and is a closed kinematic chain [24]. Therefore, either CoM and CoP or x and y directions are different than each other, and both aspects of the sway must be treated with various analytical methods and perspectives. On the other hand, the center of mass of the human body is mainly controlled through these two main signals because the human body is defined as an open kinematic chain touching the environment from the ground only, which will be discussed in the next chapter in detail. Even if CoP_x and CoM are dynamic outputs of the complex system, in the scope of the thesis, CoP_x is going to be used for the assessment of unstable manifold, and it is going to be investigated. For the investigation, consideration of the explanations of Soviet neurophysiologist Nikolai Bernstein (1896 - 1966) is inevitable, who is the founder of motor control. Bernstein asserts that motor actions never repeat themselves. As an example given by him, while hitting a nail with a hammer, any strike is different than the others. Another daily life example is drawing circles on a piece of paper. Anyone can notice that all circles drawn on paper looks different than each other, and a circle can never be repeated exactly. Besides the intrapersonal time-to-time variability, patterns vary in an intersubject manner among different people. Therefore analysis of motor output is only possible with associated probabilistic properties of time series rather than trajectories themselves.

Considering the difficulties of analyses with Newtonian deterministic methods, the employment of partial differential equations is also subject to problems for two main reasons. The first one is the impossibility of the great number of repetitions of the same experiment to construct an ensemble in order to reveal stochastic characteristics of sway. Secondly, the existence of signature characteristics of postural sway like fingerprints has already been reported [24], [25], [26], [27]. Therefore in the scope of the thesis, the output of the complex dynamics of postural sway, in a pathwise manner, is going to be analyzed with the tools of Cybernetics and Stochastic Calculus. Historically speaking, those two fields coincide with famous mathematician Norbert Wiener (1894 – 1964), who is the founder of cybernetics. So Wiener's life and his works have to be considered at this point of the dissertation.

Besides the contributions of Norbert Wiener to many fields in mathematics and physics, the process representing Brownian motion in stochastic calculus is named in his honor as the Wiener process and denoted with his initial W_t. Also, he is the founder of Cy-

bernetics, which his book named *"CYBERNETICS or control and communication in the animal and the machine"* [28], includes the exact definition of cybernetics crystal clear. Not surprisingly, just in the introduction chapter, Wiener defines a problem that he deals with, an analogous physiological problem, which is explained in detail in various chapters of the book. The story is about the time of onset of the second world war, 1940 summer. Motivated by the war and the power of german airforces, Wiener studied control theory with a group of engineers, scientists, and physicians to develop anti-aircraft artillery. During their work, they realize that artilleries must depend on two steps. The first step is the computation of the path of the aircraft, which must be constrained to a smaller control surface which the pilot stays conscious, and the plane is not disintegrated due to great accelerations. Then the second step is time prediction through extrapolation to aim the missile, where the trajectory of the missile will coincide with the plane for a successful annihilation. Luckily one of the group members, Dr. Vannevar Bush, has a computing machine for solving partial differential equations. While they are progressing in the artillery, they start to study control theory, bringing their attention to physiology. During their work, they realize the importance of the term "feedback", and either lack of feedback or excessive feedback may lead to significant deterioration under the presence of delays. After that, Wiener continues his explanation with a physiological example of "picking a pencil up", which may be treated similarly to the maintenance of the quiet stance. While one's hand is coming closer to the pen, the trajectory of the hand must be controlled with a feedback loop through the information coming from the exteroceptive, namely eyes, touch, etc., and interoceptive senses, proprioception which is mostly associated with the relative motion of the hand with respect to the body. If proprioceptive sense lacks (e.g., syphilis of the nervous system, named as tabes dorsalis seen at the later stages of syphilis, where the dorsal root of the spinal cord to which the sensory neurons enter has deteriorated), and if eyes are closed during a motor task execution (say, picking up the pen) then it ends up with ataxia [29]. They also searched for the opposite case where the excessive feedback deteriorates the process of picking the pencil up. Therefore they asked Arturo Rosenblueth, researcher, physician, and physiologist, for a physiological example of such a case where the hand oscillates while reaching the pencil due to destructive feedback. Dr. Rosenblueth immediately answers them with a well-known pathology "purpose tremor" associated with damage to the cerebellum. Please

consider holding a pen at the tip of your finger. Due to neural delays associated with the control of the pen, the task requires practice to accomplish. The related strategy is named "Drift and Act", leaving the pen free to drift in the basin of attraction until some point when control comes into play intermittently [30], [31]. Similarly, excessive or lacking feedback ends up with the failure of falling off of the pen, which can be learned by practice. After finding their physiologically analogous problem, they publish their findings [32]. While Wiener and colleagues are developing their method for handling the problem, they concluded that communication engineering and control engineering could not be treated separately, and both of them are centered on the characteristics of the messages, which is named time series in the statistics literature. Then they found out that there are two types of error in their prediction, a trade-off. The more the prediction device anticipates the event trajectory as an extreme smooth curve, the device becomes subject to greater sensitivity ending up with oscillations that die out in greater times in the presence of small disturbances. Therefore they grasp that "the best prediction" ends up with detrimental results, and good prediction is only associated with a good *"reasonable erroneous"* apparatus rather than feedback with a higher gain or better calculations. Besides, Wiener stresses that the problem has something in common with the Heisenberg uncertainty principle. In this way, they discuss the essence of optimal prediction, which can be understood with the methods of statistical mechanics. He continues with the words, *"Once we had clearly grasped that the solution of the problem of optimum prediction was only to be obtained by an appeal to the statistics of the time series to be predicted, it was not difficult to make what had originally seemed to be a difficulty in the theory of prediction into what was actually an efficient tool for solving the problem of prediction."*

Before beginning the interpretation of the method depending on stochastic calculus, the reader may benefit from a short conclusion related to the ideas demonstrated until now. Up to this point, the contrast between the deterministic Newtonian method and stochastic understanding is stressed. Firstly, the difference between the two is explained in terms of the flow of time. In deterministic Newtonian mechanics, time appears symmetric, unlike statistical mechanics, where entropy imposes the direction of time. More specifically, entropy can be defined as the measure of surprise, chance, or ignorance that accumulates as time progresses, so entropy induces an asymmetry

in terms of the direction of time. Moreover, the infinite past and infinite future are completely determined from a Newtonian perspective since the amount of missing information, i.e. entropy, is zero from a deterministic point of view. Yet, in statistical mechanics, due to the presence of missing information, any path can not be analyzed, but all trajectories have certain probabilities represented by the probability density function. In this way, under the presence of the room for chance where the future is not determined precisely, one can consider the adaptability of dynamics through "exploration and exploitation"[33], which is nothing different than learning. Besides that, Newtonian determinism only considers the time evolution of a single trajectory, and spatial facets of dynamical systems are not considered whether the equation of motion is linear or nonlinear. Yet, in statistical mechanics through entropy, the spatial characteristics are considered in terms of a probability density function, but time remains implicit in the relations. In other words, the variance or other statistical moments are missing in Newtonian mechanics and implicit in statistical mechanics. For the particular problem of the complex dynamical system, namely quiet stance, which is characterized by its output variable CoP_x time series, a probabilistic way of thinking is inevitable for the analysis of the statistical properties under interest rather than the paths themselves. Therefore, neither the deterministic approach, which considers temporal evolution of path, nor statistical mechanics in which space is visible but the time is implicit are proper. By considering Bernstein's ideas about nonrepeating features of patterns of motor behaviors, a statistical way of reasoning is necessary together with considering the asymmetric evolution of time to exploit the power of calculus and differential equations [23]. Moreover, because of the impossibility of the construction of an ensemble due to experimental constraints, methods have to be applied in a pathwise sense rather than distribution itself, such as $p_t = Dp_{xx}$. Therefore in the scope of the thesis, stochastic calculus is going to be employed, and the simplest general relation can be stated as follows. Besides that, please note that the stochastic process is chosen to be continuous [34], [35] due to experimental observations, which can also be grasped by daily life experiences intuitively. If the jumps were allowed to exist in CoP, then any people standing still may fall to the ground frequently, which is against common sense, as long as the reader does not remember the last time they fell down.

$$dX_t = \mu(t, X_t)dt + \sigma(t, X_t)dW_t \tag{1.1}$$

For a more intuitive understanding of the stochastic differential equation given in Equation 1.1, a time series related to CoP_x under eyes open condition during quiet stance is collected from the writer by a force plate, and it is presented below. The data is collected at a 100 Hertz [Hz] sampling rate for a duration of 180 seconds.

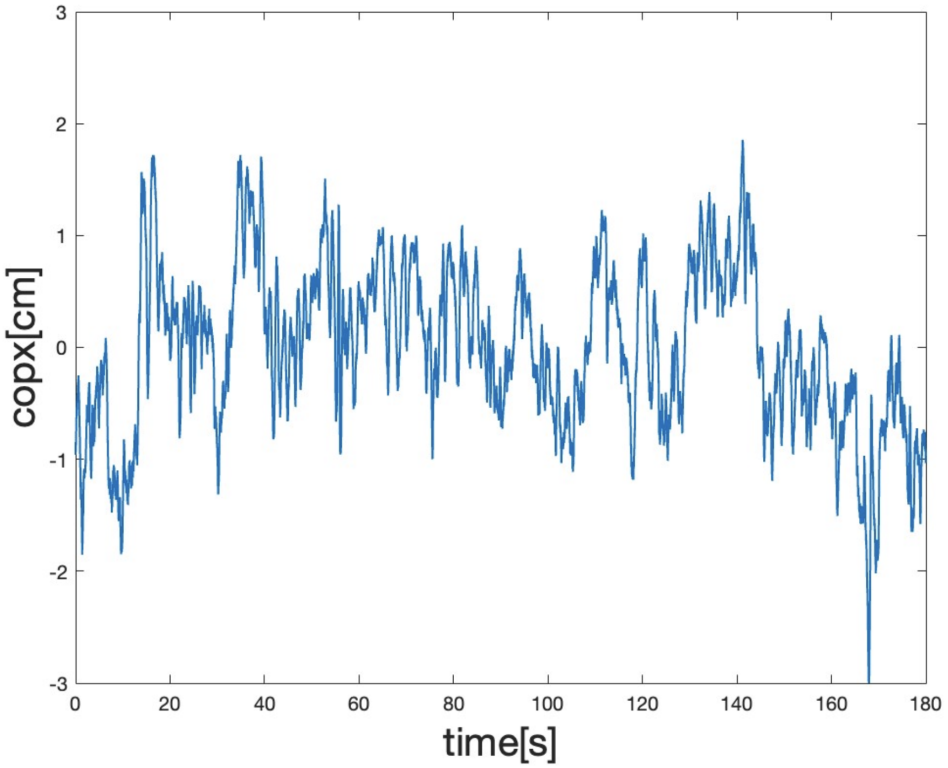

Figure 1.1: Representative CoP_x Data

The time series consists of $100 \times 180 = 18000$ data points, each of them is indexed with $i \in [0, 17999]$ and the location of CoP_x at that instant is denoted as X_i discretely. Furthermore, since the data collection frequency is 100 Hz, every time interval Δt is 0.01 second. Each Δt corresponds to a decision making which is the output of a black box representing the overall effect of actuators, plant, sensors, and all kinds of neurological structures, either peripheral or central (spinal or supra-spinal). Therefore, any decision-making in each Δt can be denoted as ΔX_t, which is written as dX_t at the limit of time $\Delta t \to 0$, since ΔX_t is nothing but the change of location of CoP_x in the corresponding time interval. Then the rest is modeling the decisions in continu-

ous time. Whether the infinite frequencies, i.e., $\Delta t \to 0$, are meaningful or not, it is necessary to exploit the power of calculus, as mentioned by Steven Strogatz [23]. In this way, one becomes able to write a differential equation representing the output of the black box, symbolizing human postural sway.

In the presence of missing information related to almost every single segment of the sway, ordinary differential equations in a Newtonian sense can not be used. Similarly, partial differential equations involving Brownian motion are not plausible as the explicit solutions are almost impossible to be found for more profound analysis and due to the impossibility of the generation of time series in a pathwise sense. Therefore stochastic differential equations involving pathwise features are employed to model and understand the dynamic properties of postural sway and, finally, to express ideas about the dynamics. Since the dynamical system of interest is too complex to interpret, writing down an equation of motion may be beneficial for further analysis of the particular dynamics, even if it models the posture as a black box. In other words, the differential equation written in the dissertation has no mechanical taste, which involves inverted pendulums, sensory reweightings, actuator dynamics, and so on, but the terms are borrowed from stochastic dynamical system theory. Still, the proposed form can be enhanced further, just like any other model inevitably incomplete by nature. Besides, there is still no attempt to write an equation of motion for the particular problem known to us at that time.

If we turn back to the interpretation of Equation 1.1, differential random variable dX_t obeys the laws of an abstract dice, which can be completely determined by its first and second moments. Then the decision-making in every single dt can be reduced to the outcome of rolled dice at the corresponding time intervals. This abstract dice making decisions has a mean $\mu(t, X_t)dt$ and standard deviation of $\sigma(t, X_t)dW_t$ where W_t is Wiener process and distributed standard normal. In other words, in discrete form the decision can be stated as ΔX_t and it obeys the law of Gaussian distribution $\mu(t, X_t)\Delta t + \sigma(t, X_t)\sqrt{\Delta t}\mathcal{N}(0, 1) = \mathcal{N}(\mu(t, X_t)\Delta t, \sigma^2(t, X_t)\Delta t)$. Anyone using Equation 1.1 is also able to decide the mean and standard deviation of dice as a function of not all history up to now but only the current time t, together with the last position of the CoP_x denoted as X_t. So that it is better to note that the relationship still has one-step memory so-called Markov property.

The postural sway searches the vast ocean of unknowns with trial and error in the presence of uncertainties and missing information, termed exploration, throughout the life from birth to death by rolling the dice delicately shaped in ontogenetic and phylogenetic development since the transition from apes to derive the information of a drop. The search is in its unique way, which never repeats the past, similar to a blind-folded child swinging the bat in random directions to find the hanging pinata [33]. Then the vital question of the dissertation can be asked without hesitation: **"What is the dice ruling the sway?"**.

CHAPTER 2

POSTURAL SWAY

2.1 Neurophysiological and Biomechanical Aspects of Postural Sway

Motor control is thought to be the origin of the neurological system in the animal kingdom. Daniel Wolpert explains the reason behind the brain is to produce adaptable and complex motions since movement is the only way we affect the world around us, either by speech, gestures, or writing; all are executed by the contraction of muscles controlled by the brain. He supports his ideas with an ecological example of a sea squirt that swims in its juvenile times and then implants itself onto a rock that it will never leave. Therefore after that stage, it no longer needs to produce motion, and the first thing it does is digestion of its brain for food [36]. Even though motor control has a driving role in the existence of life, the field emerges with the works of Bernstein and Lord Sherington in relatively recent times, at the beginning of the last century. While Lord Sherrington stresses its fundamental role with the words "to move things is all that mankind can do, for such sole executant is a muscle, whether whispering a syllable or in felling a forest", Bernstein is the first one to realize and express the random character of motor behavior and explained it with a simple example of hammering a nail. According to Bernstein, anyone hitting a nail with a hammer never repeats the same path twice, but always there exists a certain amount of variation in the execution of the complex task. The same can be seen in modern chess engines. Even if chess bots easily win against grand-masters, thanks to today's computation power, still any robot arm can not move pieces better than a child [37]. The main distinction is the complexity of the task and the presence of uncertainty compared to the discrete chess board with six distinct pieces; all are entirely defined. The complexity in motor control arises from the complex interrelations between disjoint elements

contributing to execution, such as biochemical probabilistic actuators, noisy sensors, a multijoint plant having redundant many degrees of freedom, and the nervous system existing with delays in the order of a few hundred milliseconds. While the actuator, striated muscles, obey the laws of statistical mechanics due to the chemical kinetics of cross-bridges, the plant has infinite many possibilities corresponding to the same task due to the redundant degree of freedoms. The problem is named "Degree of Freedom Problem" by Bernstein. When it comes to sensors, either exteroceptors or interoceptors, the presence of noise and feedback delays make the problem more complex. Furthermore, the noise is not only present in the sensor, but the motor commands are also subject to noise where the variance is proportional to the size of the control signal [38], similar to a geometric Brownian motion. In the presence of such uncertainties related to the core of the dynamics, simple biomechanical considerations are lacking for the explanation of the reality, yet an analysis requires the assessment of many different parts [39].

Besides the central role of motor control in animals, anyone may attempt to divide it into two subcategories as posture and movement. Even if their differentiation is a crucial question, a decisive answer is still absent [40]. Rather than two distinguished approaches discussed by Massion in his paper, successful execution of any task requires a well-defined movement and stabilized posture at the same time since posture serves two different crucial functions. While the first one is the antigravity function for maintenance of balance to keep the center of gravity inside the area spanned by the foot by providing necessary torques and muscle stiffness through probabilistic actuators, secondly it behaves as an interface between *self* and the *external world* for action and perception [24]. According to the definition of Alain Berthoz, "perception is simulated action" [41], so those two concepts have to be unified into one. Therefore they can be analyzed neither separately nor without informatic terms [42]. The necessity of a point of view involving information theory can be understood through developmental studies investigating infants who are learning independent stance and then walking in the absence of a reference signal, which makes the dynamics of erect posture completely different than linear time-invariant systems. In the field, Barella and Jeka are the ones who found the striking fact of the evolution of mechanical support into an informatic source. In the scope of the experiment, during the learning of

independent stance, the bar, analogous to a sofa or wall, serves as mechanical support at the beginning. During the continuation of development, the mechanical support morphs into an information source through somatosensory with the emergence of the light touch of the infant's hand, which is characterized by a change of force in magnitude, approximately from 5-8 Newtons into less than one Newton together with the appearance of a leading delay 200-300 ms for the achievement of quiet stance [43]. Therefore, the adaptable dynamics of stance capable of learning can not be viewed as a summation of deterministic reflexes, but an informatics and inevitably probabilistic understanding is necessary with employing the tools of statistical mechanics.

From a probabilistic point of view, motor variability, similar to Bernstein's hammer, can not be treated as an undesirable aftereffect of motor execution, but it has to be understood as the fundamental precondition of motor learning as long as it is the undeniable result of the noisy nervous system and probabilistic actuators as explained by Wu in his work inspired from songbird [44]. As asserted by him, juvenile birds are the ones having greater variability compared to adults in singing for the benefit of promoting the rate of learning. Besides that, in the presence of a potential mate, variability is significantly decreased, showing the proactive temporal regulation of variability. Thanks to the ecological influence, since the rate of variability is context specifically adjusted, Wu experimentally concludes that the subjects having greater variability at the initial phase of learning are the ones having greater learning rates. In this way, dynamics become adaptable and stable at the same time [45], associated with the "operative and conservative level of control" asserted by Gurfinkel. Similar phenomena can be exemplified in the pinata game. While at the beginning of the game, the stick has to be swung in random directions to locate the target with explorative purposes, after the first hit, random swings reduce into deterministic exploitation of the necessary trajectory for successful hits [33]. Besides the temporal adjustment of motor variability, it can be modified in desired directions spatially, given that there exist redundant freedoms in the system from the point of control of the given motor task [46]. In a spatial sense, the decomposition of the controlled dynamics into principal directions (manifolds) can be assessed with the "Uncontrolled Manifold Theory". Later in the field, the notion of synergies based on the principle of motor abundance, the uncontrolled manifold hypothesis as offering a computational

framework to identify and quantify synergies, and the equilibrium-point hypothesis described for a single muscle, single joint, and multi-joint systems [47] are fused in order to describe a coherent field of science [48]. Particularly, for the experiment of generating a required magnitude of force with two fingers (constructing a redundant system), good and bad variabilities can be understood. If the produced force by using two fingers fulfills the required level, the variation in the direction of produced force is called *good variability* due to unequal sharing of force between the two fingers. On the contrary, any variability deviating from the required level of force (orthogonal to the previous direction) points to *bad variance* [49], [50]. Furthermore, Mussa Ivaldi and colleagues have shown that the subjects are learned the directions that are less affected by noise during the experiment, and the subjects trained with additional noise generalized the training better for unseen movements. Then they asserted through changing the relation of the movement and noise, the experimenter can affect the way the subject behaves in the desired manner [51]. As long as the control of variability is possible either temporally or spatially, the infants learning independent stance can be given as an example to the ones who are constructing the spatio-temporal attractor during motor development [42] with "trial and error", or "exploration and exploitation" [33].

In adults, the remaining randomness continues to drive the never lasting postural sway, and it is attributed to two fundamental aspects. Firstly, rather than minimization of the sway, humans purposefully increase sway for the benefit of discovery of dynamic characteristics of erect posture, including the boundaries of stability [52], namely active search. So the sway can be linked to learning with the terms exploration and exploitation. Secondly, the sway can be attributed to some level of ignorance related to the current state, in other words, the impossibility of exact determination of position and velocity at any instant. Whether the reason behind sway is associated with the search or estimation error, neither can be expressed without the employment of informatic terms and tools of statistical mechanics, as long as the complex dynamics of sway during quiet stance are highly probabilistic within a well-defined region of space [53]. More specifically, estimation and sensorimotor integration is a challenging problem from a physiological point of view, as long as the complete determination of complex systems is not possible with an understanding of distinct parts. Particu-

larly speaking, the estimation of verticality during quiet stance is complex due to the multi-integration of many senses, i.e., somatosensory, vestibular, vision, etc., and proprioception inherently included [54]. In this way, the vestibular is not directly used to estimate the state of the head; instead, through a downward chain, it is employed for the estimation of the body orientation starting from the foot support through the trunk and finally the head (bottom-up construction) [55]. In this way, the noise in the vestibular signal becomes eliminated, so it is used by the brain for the internal reconstruction of self motions and the environment we interact with. Internal representation can also be analyzed with forward and inverse models that predict the sensory consequences and calculate the necessary feedforward control signals from the information of the desired trajectory, respectively [56]. Further, the subject is studied with an engineering perspective by Mergner and van der Kooij in order to reveal the characteristics of the control of erect posture, particularly in elder people [57] as they are suffering in the maintenance of balance. Moreover, the statistical features of sensorimotor integration are studied by Daniel Wolpert with Bayesian terms. In the studies, the Bayes theorem is employed to understand the effects of *"prior"* knowledge on accuracy in reaching task, which can only be understood with a probability distribution. In corresponding articles, they show that the greater the uncertainty related to the task, the more reliance on "prior" knowledge increases [58]. In this way, the effects and characteristics of noise in motor planning and prediction [59] can be studied by changing the sensory conditions in various motor tasks [60]. In the presence of noise, the gravitational vertical may not be the absolute vertical (absolute frame of reference) for the body to refer [61], [62], therefore Gurfinkel and colleagues showed that during superslow platform tilts, posture is stabilized by some system around a preselected and continuously updated a set of points determined by another system as a result of many sensory states rather than a single parameter or sensory input [63]. Please remind that those two systems are named "conservative" and "operative", respectively.

Historically speaking, Begbie (1967) is the first one to realize two superposed oscillations at 0.5-1 and 1.5-2.5 Hz only by visual inspection. A similar observation is made by Arnblard as the existence of two mechanisms one is operated below 2 Hz and strobe resistant, and the other one is above 4 Hz, which is strobe vulnera-

ble. Therefore the postural sway can be explained by at least two levels. On the subject, one of the most profound methods is the Rambling Trembling decomposition proposed by Zatsiorsky and Duarte [1]. After the application point of the net vertical force exerted to the foot CoP_x, CoP_y estimated by the force plate, the first step of Rambling Trembling analysis is the determination of the positions of CoP in the desired direction, x or y, when the equilibrium is instantly maintained. The details related to force equilibrium and an inverted pendulum representing the erect posture are presented in Appendix B. For that purpose, the instants at which the horizontal force at either direction is zero are selected, i.e., the $\sum F_{horizontal} = 0$ in the direction of interest. Then the position of CoP at that instant can be treated as an "Instant Equilibrium Point", since the force equilibrium in the corresponding direction is satisfied as shown in Figure 2.1a. After that, by using cubic splines, the instant equilibrium points are extrapolated in time which is named the "Rambling" trajectory denoted as Rm. Therefore the intersections of the rambling trajectory and CoP are instant equilibrium points presented in Figure 2.1b. As mentioned by Zatsiorsky, cubic splines have no physical meaning, but they only impose smoothness, whether it is a physical quantity or not. Still, the smoothness can be linked to minimum jerk criteria for motor execution [41]. The same is explained by Hogan, involving a different analytical point of view. As asserted by him, at moderate speeds, wear and tear in the neuromuscular system can not be responsible for the minimum jerk, even if it was, it would be difficult to reconcile. Instead, through the minimization of jerk, control is simplified by neglecting the higher order derivatives. Then, the information required to specify, store and predict the desired trajectory [64] can be kept smaller in this way. The same criterion can be explained by the minimization of effort too, and it means smoothness with kinematic terms [51]. In this way, CoP becomes pulled along a dynamically characterized rambling trajectory rather than a constant baseline by restoring forces, and the associated distance between CoP and the rambling trajectory is named "Trembling" trajectory denoted with Tr that is shown in Figure 2.1c. In other words, the body sways with respect to the preselected and continuously updated points assessed with rambling trajectory, so analytically $Rm + Tr := CoP$. Even if the approach is similar to Gurfinkel's operative and conservative systems, analytical methods differ. For further visual understanding, the figure showing rambling and trembling together with CoP is provided in Figure 2.1.

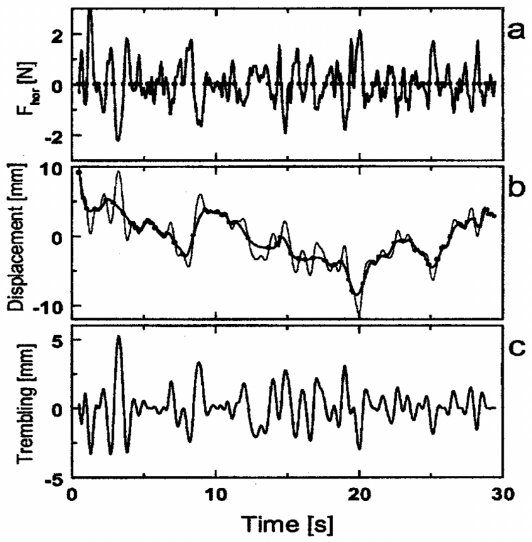

Figure 2.1: A Sample Path for Rambling and Trembling Trajectories [1]

Anyone may notice two main characteristics of rambling and trembling directly from Figure 2.1. Firstly, rambling has significantly greater variance compared to trembling, almost three times. Therefore most of the sway must be associated with the migrating reference point. Secondly, while the trembling determines the high-frequency behavior, rambling rules the navigation in greater periods, which can be seen either visually or from the power spectral densities in Figure 2.2 and phase portraits shared in Figure 2.4. In a similar perspective, Collins asserts the existence of two distinct control strategies, open loop and closed loop, at short and long time scales, respectively [29].

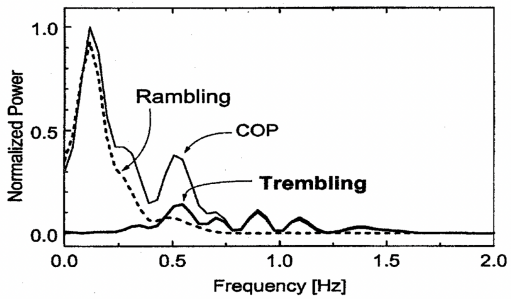

Figure 2.2: Power Spectral Densities of Rambling Trembling and CoP_x [1]

We can observe the frequency contents at low and high frequencies in the time domain by looking at Figure 2.1. Indeed Figure 2.2 represents the power spectral density function estimates of Rm, Tr and CoP_x trajectories. On the other hand, phase portraits are dynamical representations of time series under consideration by plotting displacement with respect to the velocity of the dynamical event. The phase portraits

of the decomposed CoP_x are given in the top right corner of Figure 2.2, which visualizes the frequency content and the scaling of the motion of each. Moreover, while the trembling trajectory is explained by restoring forces similar to elastic forces, due to intrinsic properties of muscles and the joints together with reflex loops, spinal-peripheral, mechanistic, etc., the reasons behind rambling are not that clear. However, it can be related to supraspinal divisions. Therefore one can say that the central nervous system can be the one responsible for selecting and updating the point at which the equilibrium will be maintained. Still, Zatsiorsky explicitly stresses that the reason behind rambling is still unknown [65], [66].

It is better to keep in mind that the rambling trembling analysis says nothing about mechanical sources and the reasons behind the dynamics of rambling. Also, it does not support either pendular motion [67], [68] around a fixed joint or the opposite perspective of free drift without corrections inside the margins of stability [69] similar to "drift and act" strategy [30]. Rather it supposes that the equilibrium is maintained around a preselected point represented by the rambling trajectory [2]. Furthermore, Zatsiorky investigated (first table of the article [2]) variances and covariances between Rm, Tr and CoP_x and found a slightly positive correlation between Rm and Tr; i.e. $\langle Rm \times Tr \rangle > 0$ (Rm and Tr are not linearly independent), which makes the variance $\langle CoP_x^2 \rangle$ less than the sum of individual variances of Rm and Tr according to relation $\langle CoP_x^2 \rangle \leq \langle (Rm + Tr)^2 \rangle = \langle Rm^2 \rangle + \langle Tr^2 \rangle + 2 \langle Rm \times Tr \rangle$ due to the cross-talk, $\langle Rm \times Tr \rangle \neq 0$. In this way, this simple method relying on force equilibrium and splines reveals many hidden quantities in experimental studies.

Even if, until now, the rambling is defined and its relation to CoP is discussed, the dynamical characterization of the rambling trajectory is not explained thoroughly yet. In the figure given below retrieved from Zatsiorsky [2], horizontal force applied at any instant is provided with the position of CoP as shown. Anyone looking at the figure notices at least two distinct poles rather than one, which is pointed by the arrows.

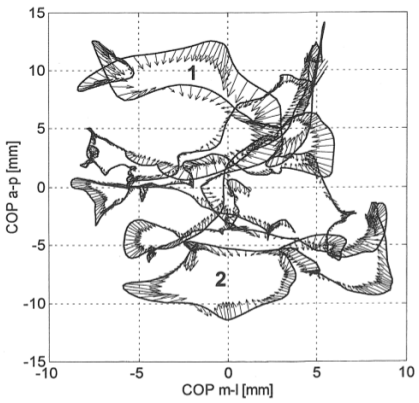

Figure 2.3: Force Field and CoP Time Series [2]

While the trembling trajectory has a single stable point around zero after detrending CoP with respect to the rambling trajectory, the rambling trajectory itself consists of more than one equilibrium point. Similar characterization is possible through phase portraits in that the position is plotted with respect to velocity. Phase portraits of CoP, rambling, and trembling are provided below [2].

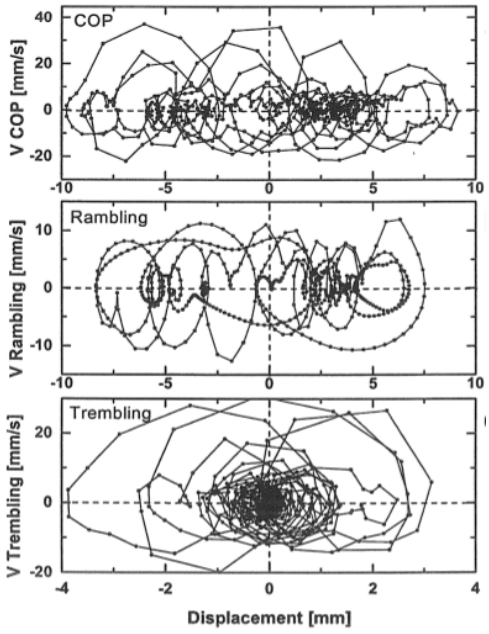

Figure 2.4: A Sample Path for Rambling and Trembling Trajectories [1]

In both of the figures, the multipolar structure of rambling is clearly visible, which shows the existence of more than one stable point. The same phenomenon represents itself as multimodality in the probability distribution function. If the aim is the probabilistic representation of dynamics of CoP, the multimodal behavior of rambling

has to be understood clearly, which is investigated experimentally by I.C. Lee, M.M. Pacheco, and K.M. Newell [70]. In the scope of the experiments, subjects hold a pole at various lengths to manipulate the stability of balance, similar to a wirewalker. With the help of the pole held, the CoP time series is captured and entrapped in distant regions. Even if they assert that the reason behind the migrating reference is still unknown, they counted the number of stable points by employing a kernel density estimation of CoP to count the number of peaks in the probability density function.

Furthermore, it is worth interpreting a few empirical studies Zatsiorsky himself contributed for a deeper comprehension of the rambling trembling decomposition.

The first striking experimental design is the one in which Zatsiorsky and colleagues manipulated the support surface area. In the scope of the experiment, they decreased the support surface to an area greater than the region spanned by CoP as shown in Figure 2.5. Interestingly, none of the different support conditions impose any problem related to balance if subjects basically ignore the decrement. Yet the area CoP covered increased, which led the subject to fail to stand. The results are interpreted as being consistent with the active search of sway, where the change is mainly observed in rambling rather than trembling. Besides that, they reported different studies where the sway area decreased at the surfaces elevated from the ground as it is perceived as a threat; still, they mention that the experimental setup is not considered a danger for subjects as it is very close to the ground and only making a step is sufficient and it is highly safe. This exploratory behavior is explained as an active search for stability boundaries in the absence of fear of fall, which has been estimated by constructing 83.35% confidence ellipses [3].

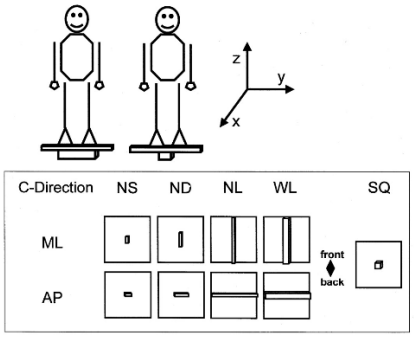

Figure 2.5: The Experimental Design for Support Surface Manipulation [3]

Secondly, in another setup, the experimenters let the subjects watch their own CoP live during the experiment. While they measured the area spanned by CoP time series in the first trial, for the latter trials, they defined two tasks, named easy and hard. The hard task is to keep the CoP inside the predefined region, which has fifty percent of the original area measured at the first trial, namely the challenging task. Moreover, in the easy task, they used a region one and a half times 150% greater compared to the original one. Either hard or easy tasks end up with greater sway, which shows that the sway is at its minimum in the original. After the decomposition of the CoP time series into rambling and trembling components, they have observed opposite effects in rambling and trembling, as shown in Figure 2.6. While in the easy task, the rambling increased due to greater active search, conversely during the hard task, the increasing trembling is explained by greater activation of ankle muscles inducing greater ankle stiffness for the accomplishment of the task. Therefore the writers associated rambling with the supraspinal process and trembling with the spinal peripheral part involving spinal reflexes, intrinsic properties of muscles, and elastic forces. In Figure 2.6, one can see that CoP is affected less than each of rambling and trembling due to respective opposite changes, so without the decomposition, the change in dynamical characteristics could not be easily noticed. Therefore, the experimental design is highly intuitive for the comprehension of rambling and trembling [4].

In contrast, according to another experimental paper, Latash and colleagues concludes that the supraspinal and peripheral distinction of rambling against trembling could be too simplistic according to the data collected from elder and young people. Even if they hypothesized that increased co-contraction in old people would increase trembling in the presence of sarcopenia due to decrement of α-motor neurons, deterioration of the central nervous system, sensory decline, and change of muscle properties, they observed that rambling is affected more than trembling in contrast to the proposed hypothesis [71].

In a fourth experiment, the ankle, hip joints, and trunks of subjects are constrained with plasters. During the consecutive bottom-up immobilization, the dynamical characteristics of sway are changed. Especially the most significant effect is seen when the ankle is immobilized. For the rest of the further constraints, only minor changes are observed. During trials, immobilization led to greater ankle activation, followed

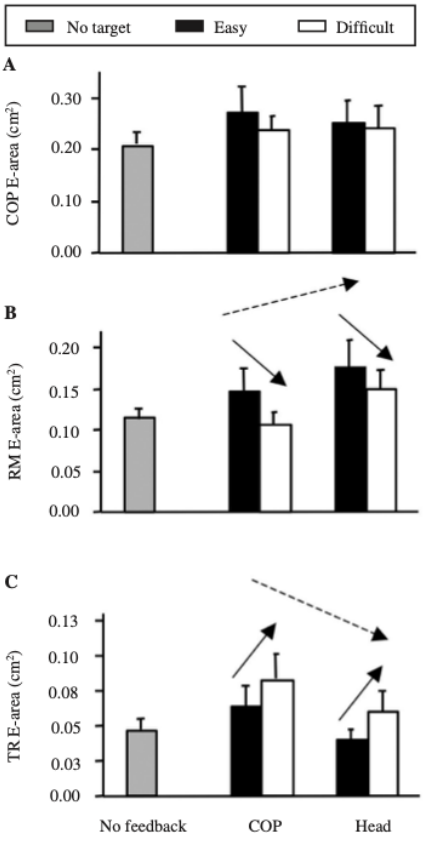

Figure 2.6: Effects of Easy and Challenging Task on the CoP, Rambling and Trembling Time Series [4]

by greater stiffness around the ankles. Therefore the trembling increased significantly. Yet no significant change is found in rambling under any constraint in AP direction (mediolateral direction is skipped as it is out of scope). Then they concluded that a single inverted pendulum might not be enough to explain sway since the trembling and CoP showed significant change after all of the knee, hip and trunk were constrained in terms of measured metrics in anterioposterior direction [71].

Besides the comprehensive experiments, rambling trembling decomposition can not be thought of on its own, but it can be linked to different approaches easily since it investigates the evolution of equilibrium point. Zatsiorsky [1] mentions that instant equilibrium points are the instants in which the force equilibrium at the horizontal plane is maintained. Therefore even if those are not exactly the same, Zatsiorsky says that there exists a certain analogy between Feldman equilibrium point [72] and rambling trembling decomposition. In the same text, "Feldman equilibrium point" is defined as a virtual trajectory that would be followed if the limb was massless, damp-

ing was zero, and external loads were absent by citing Latash's book [73]. Even if, at first glance, two approaches are similar, Zatsiorsky mentions two basic distinctions which are worth being aware of. Firstly he asserts that instant equilibrium points are purely biomechanical terms defined over force equilibrium $\sum F_{horizontal} = 0$ simply. Secondly, instant equilibrium points have nothing to do with the configuration of joints. Therefore, a short introduction to the Feldman equilibrium point may be beneficial for a better understanding of distinctions and similarities.

As known to us, the example given in Feldman's paper is the best for understanding the equilibrium point theory [5]. Please imagine that you are holding books, and suddenly the load is lifted over your hand. In this case, anyone can imagine the involuntary upward movement of the arm due to the unloading reflex. The original manipulandum experiment simulates this situation under laboratory conditions by estimating the angular position of the joint of interest and the corresponding resistive torque [74], [75]. During the experiment, a robot arm with two joints involving two torque motors (fully actuated) is handled. The endpoint of the robot arm is coupled with the plastered wrist of the subject, while the remaining two joints, the elbow, and shoulder, are left free. Therefore the experimental setup allows two degrees of freedoms to be controlled by two independent torque motors, which guarantees the solution for the system to be unique; i.e., for each angular position of the joint of interest corresponds to a unique resistive joint torque generated by the subject [76]. For every distinct set of experiments starting from a particular initial condition described with a unique pair of joint angular position and corresponding resistive joint torque, the path that the subject follows until the input torque is decreased to zero is unique. In Figure 2.7, the initial conditions where the subjects start the experiment are shown in black, whereas the white ones are employed for the experimental data measured on the unique paths that the subject follows for every given initial condition. After all, the dashed line in Figure 2.7 is obtained by interpolating the zero torque equilibrium points (zero EMG tonic activity) on the given space, pointing to passive characteristics of the joint of interest.

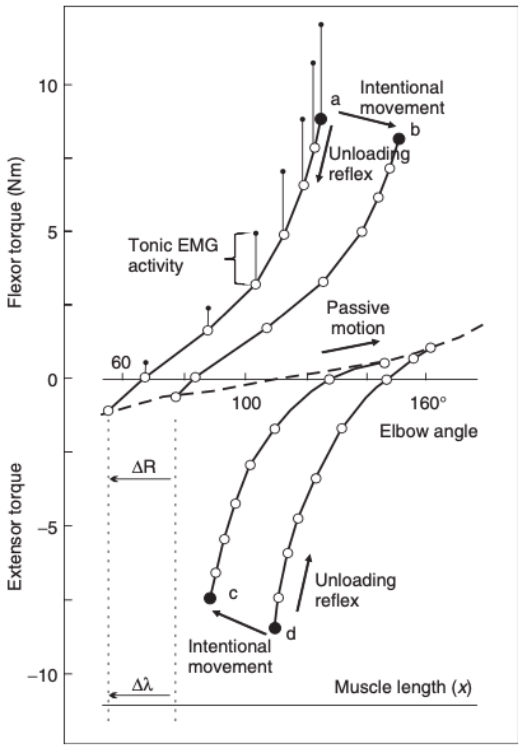

Figure 2.7: Feldman Equilibrium Point Experimental Results [5]

At the plane of angular position and resistive torque, it is possible to define a function describing the torsional spring $T_r = K_t\theta$, where T_r is the resistive torque, θ is the angular position, and K_t stands for the joint stiffness. In this case, the torsional spring curve is unique in the given plane; however, Figure 2.7 presents a family of curves. So another freedom is required in the constitutive equation of the torsional spring given above. Feldman proposes that the required freedom is nothing but the threshold set by the nervous system while changing the initial condition intentionally from a to b. Further, Feldman states that the freedom of the threshold serves as a system invariant which implies the way the brain controls voluntary motion. Therefore he concludes that by shifting the threshold, a movement is triggered against the previous posture where the former threshold was resisting the newborn generated motion. In other words, the one and only control variable, the threshold, is changed from posture stabilizing into a movement generator. Specifically, the problem is defined as "Posture - Movement Problem" by Feldman, and it has similarities with instant equilibrium points and rambling trajectory towards which CoP is pulled, where the task is the maintenance of posture.

Besides the Equilibrium Point Theory of Feldman, Zatsiorsky mentions another concept, "virtual trajectory", which is "similar in spirit" and is defined over Feldman equilibrium point [2]. Feldman himself mentions the same concept [5] as the gradual change of equilibrium position for the construction of equilibrium trajectory during the execution of the given motor task by citing Bizzi [77], Katayama and Kawato in 1993 [78] together with Flash and Hogan in 1984 [79]. Particularly Flash and Hogan employ a method depending on the calculus of variation to minimize jerk for smoothness while the limb is following a predefined virtual trajectory during a reaching task.

2.2 Measurement Methods and Quantification of Postural Sway

For the particular problem of answering "How is erect posture maintained?" before attempting a mathematical model, quantification of the problem is the first necessary step. Quantitative handling of erect posture during quiet stance, namely assessment of postural sway, is possible with two distinct time series. The first one is tracking the center of mass of the human body during quiet stance, which is located somewhere a few centimeters at the front of the lumbosacral joint, i.e., behind the belly button [9]. The location of the center of mass can be obtained by motion tracker systems using LEDs located at the various sites of the body and the cameras tracking the LEDs' positions to extract three-dimensional positions of the corresponding sites in time. An approximation of the position of the center of mass is possible by considering the weighted average of distinct parts of the body according to their respective masses. In the case of raising arms, moving the head, bending down, and so on, the location of center mass may change significantly relative to body segments, yet it can be neglected for quiet stance, so the center of mass is assumed to be motionless with respect to the body under small movements during quiet stance [9]. Besides, Mittelstaedt [80], [81] proposes the existence of a gravitoceptor around the center of mass, which makes it observable to the body whether it is controlled or not. Secondly, it is possible to experimentally measure the location of the resultant of reactive forces (Center of Pressure) applied to the body/foot by the ground; Ground Reaction Forces (GRF). The location is also relevant to the subject due to mechanoreceptors embedded in plantar cutaneous, which are measuring the pressure distribution on foot soles

whether it is controllable or not [14]. The associated signal is named as Center of Pressure (CoP), and it is measured by force plate which collects force and moment signals; i.e., F_x, F_y, F_z and M_x, M_y, M_z respectively, in a three-dimensional cartesian coordinate system. CoP_x and CoP_y are defined as $-M_y/F_z$, M_x/F_z respectively.

Please note that CoM and CoP signals have quantitatively and qualitatively different natures, which present themselves in the time domain, frequency domain, and the phase space representation of the postural sway dynamics. Besides there exists a hierarchical control relation between CoP and CoM [82]. The relation can be understood through an example of holding a pen vertically to the ground on the tip of the index finger. If the projection of CoM intersects with CoP at the horizontal plane; i.e., $\vec{CoP} - \vec{CoM} = \vec{0}$, the pen stands still. Yet any deviation from equality, $\vec{CoP} - \vec{CoM} \neq \vec{0}$ forms a moment arm inducing rotation to the pen. Then the person has to change the direction of the rotation induced to the pen by reverting the direction of the moment arm unless the pen is to fall down to the ground. The pen example constitutes an analogy to the quiet stance in which the location of CoP is governed by the active control of the foot instead of the active control of the hand [83], [84], [85], [86], [87]. By following the example of the pen CoP is the actively generated signal either by the foot or hand, whereas CoM is the passive entity controlled by the former [82]. In this way, CoP is the controlling variable responsible for keeping the controlled CoM in a confined region. Therefore, CoP must be faster than CoM motion, resulting in the body oscillations without falling. At any instant relative positions of $\vec{CoP}$ and $\vec{CoM}$ create a moment arm proportional to the distance $|\vec{CoP} - \vec{CoM}|$ which induces a tendency to the $\vec{CoM}$ in the reverse direction [88], [6]. In his paper related to stiffness control, Winter explicitly asserts that CoP oscillates at either side of CoM to keep it inside the confined region spanned by foot for the maintenance of balance. Please remind that $\vec{d} := \vec{CoP} - \vec{CoM}$ forms a couple which generates moment according to $\vec{M} = \vec{d} \times \vec{F_z}$ where F_z is the weight of the subject. In the article, Winter proves his ideas by employing the covariance between the distance $|CoP - CoM|$ and acceleration $|\ddot{CoM}|$ which is found to be between -0.96 and -0.99 by using a mechanical model involving an inverted pendulum [88], [6]. Please refer to Appendix B related to the inverted pendulum for detailed derivations.

Further models involving similar duality in terms of center of mass and center of

pressure can be found in the posture literature. In this point of view, CoM behaves similarly to rambling, and CoP oscillates around it just like trembling. In the subject, Zatsiorsky's articles comparing CoM, [89], [90] and rambling trembling decomposition are enlightening [2] so they are referred in Appendix B related to inverted pendulum. A further similarity with rambling trembling decomposition is observed in terms of smoothness, such that CoM is much smoother than CoP, which is the controlling variable. In other words, CoP is faster than CoM. In the subject recently published article written by Alice Nicolai is worth attention [91]. The writers employ the following stochastic differential equation.

$$dv_t^{CoP} = \left[\lambda(CoM_t - CoP_t) + \Gamma(-v_t^{CoP})\right] dt + \Sigma dW_t \tag{2.1}$$

While v is the velocity of CoP at the direction of interest, Λ, Γ, Σ are positive constants, and dW_t is the Wiener process which will be discussed later. According to the given stochastic differential equation, CoP is pulled toward CoM due to the negative sign in the first term. The next two terms have a form of Ornstein Uhlenbeck, i.e., Langevin equation, in terms of velocities where the ΣdW_t is Wiener process together with the second term keeping the variance of velocities bounded. The dynamics obeying Equation 2.1 never come to rest in this form in the absence of the zeroth order term of CoP_t, and it oscillates forever even if there was no noise term as long as CoM never stops.

From this perspective, the proposed model in the following chapter should consist of at least two processes. While the first one is for assessing the equilibrium points corresponding to rambling, the second process represents the random walk around the formerly defined equilibrium point like trembling. In this way, we attempt to model the main outcome of the human postural sway, CoP_x, that is proposed to be the composition of those two processes. In this context, the model should involve randomness due to the complexity of the dynamics and grasping the property of active search to create room for learning. Nevertheless, the CoP must remain in some certain area spanned by foot for the maintenance of balance; otherwise, the subject falls.

CHAPTER 3

DESCRIPTION OF THE STOCHASTIC DIFFERENTIAL EQUATION

This chapter aims to describe and design the dice ruling the decisions in the dynamics of postural sway, which are represented as differential increments of the stochastic process. So that, throughout the chapter, the stochastic differential equation will be improved progressively by modification of terms to grasp the various properties of postural sway and the representative time series CoP_x. In addition, please note that the model can be improved further for assessing different aspects of the dynamical system related to quiet stance and then motor tasks. Moreover, any of the steps do not involve control theory or neurophysiological aspects, and it also does not include a biomechanic perspective, but it uses terms of stochastic dynamical system theory by employing the tools of stochastic calculus. In other words, the models consider the dynamics of postural sway as a black box that has a dynamical output CoP_x denoted with a random variable X_t.

Before presenting the first step, it is better to describe the random variable X_t symbolizing the location of the output of postural sway CoP_x at any instant t. Basically, X_t denotes the random variable. Then the stochastic differential equation describes the temporal evolution of the random variable without a mechanical taste involving an inverted pendulum and related control theory. In this respect, X_t must have some particular distribution that is entirely different than a path evolving in time according to Newtonian mechanics, which is represented as $\dot{\vec{x}} = \underline{f}(\vec{x})$. Therefore even if X_t is a random variable described by its distribution, it is treated pathwise, which is a definite dichotomy [21]. While on one side fate of a single particle following a random trajectory is the first explanation; the other representation is a probability density spreading along one-dimensional space in time standing for an ensemble. In this way, the time

series of X_t related to a single experiment can be analyzed from a pathwise point of view by capturing randomness and missing information. So that another time series of CoP_x is presented in the figure given below for any naive reader to gain deeper insight in case they have not seen any data before. The data is collected with a 100 Hz sampling rate, again similar to Figure 1.1.

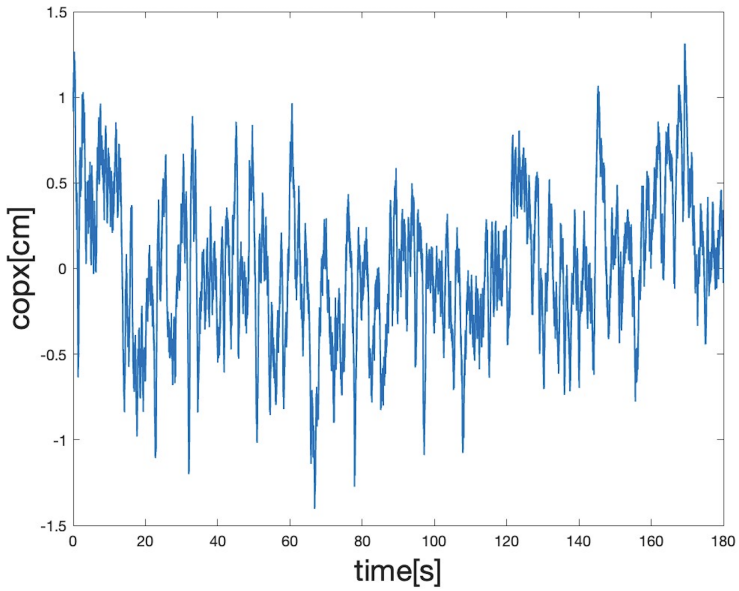

Figure 3.1: Another Representative CoP_x Data

Furthermore, in all steps, the displacements, steps, are assumed to be distributed normal for employment of the central limit theorem. Therefore Q-Q plots of six time series are provided below, which show the quartiles of velocities with respect to quartiles of Gaussian distribution in the range $\pm 3\sigma$ for the visual verification of the assumption. Further details of Q-Q plots are explained in Appendix A. Anyone can see that the quartiles at tails deviate from Gaussian, yet it is not discussed as it is out of scope for the dissertation, but a curious reader may refer to Mangalam's recently published article about tail behaviour of postural sway [92]. Simply the linear appearance implies that the collected data is distributed Gaussian in which the quartile values of data coincide with Gaussian quartiles. Furthermore one can check the kurtosis values of the same data after standardizing the distribution to $N(0, 1)$. Then the kurtosis values are found to be $\{3.24, 3.07, 3.18, 3.10, 3.06, 3.03\}$, and all are close enough to three. In the scope of the thesis, the behavior at the tails is not important as long as the dissertation does not involve analysis of extreme events during quiet stance. Still, the analysis of tail behavior can be read from the influential book of Taleb [93].

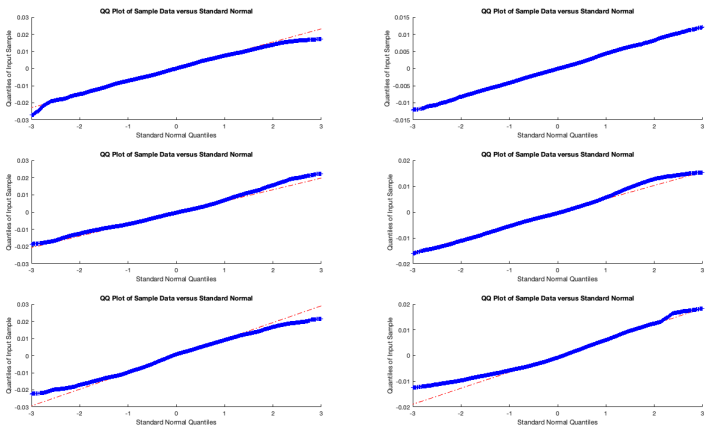

Figure 3.2: Q-Q Plots of Data

3.1 Step 0 White Noise

Zeroth step of the derivation of the stochastic differential equation is the simplest case which is White Noise. According to the perspective mentioned until now, White noise is throwing an abstract dice and determining the position of the associated random variable X_t accordingly. Even if the decisions, namely ΔX_t, can be interpreted as normal distributed random displacements for each time interval Δt relying on Figure 3.2, white noise can not be a proper model as long as it does not accumulate surprise, chance, and technically entropy. In other words, it corresponds to a zeroth-order differential equation, yet the summation of consecutive steps decided by rolled dice is necessary to assess the build-up of chance with time. In this way, integration comes into play at the limit of time partition, so the relation corresponds to at least a first-order differential equation. Then the velocities named decisions, can be denoted with $\Delta x = \sigma \Delta t \mathcal{N}(0, 1)$ in discrete form. The relation describes the random variable, and it can be thought of as an abstract dice determining the next step in each Δt. Then, the decisions, i.e., the steps, can be integrated at the limit of $\Delta t \to 0$, which yields the Wiener process. It is the most fundamental continuous process among all subjects in stochastic calculus, representing the diffusion of a single particle, i.e., Brownian motion. A sample figure representing white noise is not provided as it is known to anyone, and to keep the discussion short enough by considering the structure. Still the details of white noise is explained in Appendix A including its probability density and spectral content.

3.2 Step 1 Brownian Motion, Wiener Process

Firstly, it is better to start by describing the most straightforward stochastic process, namely the Wiener process. It is denoted with W_t, and the corresponding differential increments are dW_t, which will be integrated in a Riemann-Stieltjes sense rather than a well-known Riemann integral. About the subject, the best example is the calculation of the definite integral given below retrieved from Dr. Peyam's Youtube channel who is teaches subjects of probability theory and fractional calculus clearly [94].

The integral can be computed with the common method by defining $dg(x) := dx^2$, and then substitution of the derivative $dg(x) = g'(x)dx = 2xdx$. Yet this is not the only way, but the integral can be evaluated even if the integrator is a non-differentiable function which a sketch of proof is provided in Equation 3.1.

$$\int_0^1 x dx^2 = \lim_{N\to\infty} \sum_{i=1}^{N} \frac{i}{N} \left[\left(\frac{i}{N}\right)^2 - \left(\frac{i-1}{N}\right)^2 \right] = \lim_{N\to\infty} \left[\frac{2}{N^3} \sum_{i=1}^{N} i^2 - \frac{1}{N^3} \sum_{i=1}^{N} i \right] = \frac{2}{3} \quad (3.1)$$

After expanding squares, one can see that the integral can be computed without finding $g'(x)$. Therefore in the case of $g(x)$ is not differentiable; still, it is possible to evaluate the integral. Further details of Riemann-Stieltjes integral are not provided as it is out of scope in an applied sense. In the same respect, the Wiener process dW_t Gaussian distributed differential random variables has to be integrated over time. Then one can define the first step as follows.

$$dX_t = \sigma dW_t \quad (3.2)$$

Before describing the terms one by one and providing the integrated form of a solution, it may be beneficial for the reader to see the relation in discrete form, which makes the understanding easier for further discussion.

$$dX_t = \lim_{\Delta t \to 0} \sigma \underbrace{(\Delta t)^{1/2} N(0,1)}_{\Delta W_t} \tag{3.3}$$

The relation explicitly states the law that the random variable ΔX_t obeys. It can be seen that the decisions ΔX_t are random variables distributed $N(0, \sigma^2 \Delta t)$ where all steps in time are "independent identically distributed". According to the central limit theorem, the summation of N-many steps Δx where all steps have finite variance yields another normally distributed random variable. Please note that the central limit theorem is valid only if all random variables summed up have finite variance. Further, the random variable at any finite $t > 0$ has a variance equal to the summation of variances of all steps up to that time. Algebraically speaking, it means "closed under addition", which is necessary for consistency at the limit. Therefore the solution is distributed as $\int_0^T dX_t = \int_0^T \sigma dW_t = \sigma(W_T - W_0) \sim \mathcal{N}(0, \sigma^2 T)$.

As known to us, the most interesting part of the integral shown in Equation 3.3 is the square root of Δt. Firstly, at the limit of $\Delta t \to 0$, the square root converges to zero slower than an ordinary first power, linear Δt. Therefore the variation of ΔW_t becomes infinite in any "finite" time interval no matter how small it is. In the presence of infinite variation, the quadratic variation proportional to Δt becomes a positive finite value which is zero in ordinary calculus. Quadratic variation is defined as the summation of squared steps, and in this particular case, it evolves with $\sigma^2 \Delta t$. Since the variation of the Wiener process is infinite, the function is **everywhere continuous, nowhere differentiable**, so the integration necessitates Riemann-Stieltjes integral as mentioned before, where $g'(x)$ does not exist. In addition, quadratic variation is usually confused with variance, yet those concepts have totally different meanings. Even though the expectation of quadratic variation is equal to variance, they are distinct concepts, as quadratic variation is a path-wise property. However, the variance is a completely abstract statistical outcome that is about the ensemble of infinitely many paths, i.e., fates. So the concept of variance is related to distribution. The detailed discussion of distinction can be read in Shreve's book [95]. Besides that, another common confusion is the calculation of variance from a single path. It is also significantly misleading since the variance is a property related to whole distribution, and it is shown as the parabola $\pm 3\sigma\sqrt{t}$, in Figure 3.3. Therefore it is entirely different than

the squared difference of all data points from the mean of the entire time series, and the increasing standard deviation by following the parabola will be discussed later.

Secondly, the integral is somewhat half due to $\sqrt{\Delta t}$, which is unusual for anyone who knows calculus at the level of undergraduate education. Besides, it is the reason behind infinite variation; the branch of mathematics dealing with non-integer differentiation is named fractional calculus, which is still a developing field. Integer order derivatives can be easily generalized to real orders with the gamma function. In this respect, the fractional order of derivatives is an old discussion in which the subject can be traced back to the letters between Leibniz and L'Hopital, that Leibniz replied with the words *"...Thus it follows that* $d^{1/2}x$ *will be equal to* $x\sqrt{dx : x}$*"*. Non-integer differentiation is associated with fractals in this context. In Mandelbrot's paper [96], fractional Brownian motion is derived and defined as a generalization as $W_t \rightarrow W_t^H$ where the variance increases with $(\Delta t)^{2H}$ rather than Δt. In W_t Hurst exponent is $H = 1/2$, and this generalization is out of scope for the dissertation.

By keeping all in mind Equation 3.3 is the first step and constant σ is nothing but the scale of variance per unit time by considering $X \sim \mathcal{N}(0,1), a \in R \implies aX \sim \mathcal{N}(0,a)$. Therefore at any time T, the accumulated chance linearly increases to $\sigma^2 T$, which is the variance. In financial mathematics literature, σ is named volatility, and modeling $\sigma := \sigma(t, X_t, Y_t)$ is a field that may be studied lifelong since it is directly associated with risk and option pricing theory as it determines the rate of accumulation of surprise [97].

Equation 3.3 describes the rolled dice as Gaussian increments at each dt, and the distribution is $N(0, \sigma^2 dt)$. For further understanding, the next plot is inevitable, which shows many different trajectories generated in Matlab obeying the laws of the same process. Therefore every single path is independent and identically distributed.

Firstly, all the trajectories shown in the figure obey the laws of W_t for all $t \in [0, T]$. Please remind that it means $\Delta x = \sigma\sqrt{\Delta t} N(0,1)$ in discrete form. Even if some curves, such as the black one, look like it has a negative trend, there is no reason for the drift, but it is completely due to randomness. In this point of view, anyone who collected a single time series experimentally may misinterpret the data, which is nothing but being "fooled by randomness" termed by Nicholas Nassim Taleb [98].

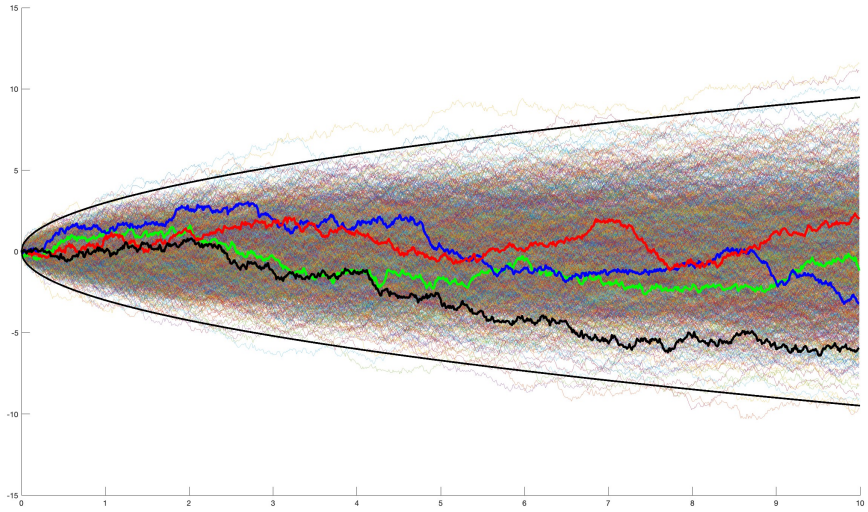

Figure 3.3: Sample Paths Generated for W_t and 99.73% Confidence Interval at $\pm 3\sigma\sqrt{t}$

Besides the black one, the green trajectory lies around zero, again for no reason but only due to chance. As it can be seen from the relation, there is no trend in W_t, so the mean of all trajectories apparently stays at zero for all time. Another point about the trajectories is their variance. Since a normal distribution can be characterized completely by the first and the second moments, the variance has to be analyzed in detail. It is already mentioned that the standard deviation of W_t is $\sigma\sqrt{t}$. Therefore three standard deviations 99.73% confidence interval is shown in the figure with the black parabola that 0.27% of trajectories barely stay outside the curve for any t. The branches of the parabola expanding away from each other is the best way to show the accumulation of surprise with the passing time, so-called the increment of the entropy. Since the trajectories are distributed Gaussian at any instant, the mean is always zero, and the variance increase with $\sigma^2 t$. Then anyone plotting the distribution for some $t \in [0, T]$ see a Gaussian distribution with $\mathcal{N}(0, \sigma^2 t)$ at that particular time t.

Besides all it is known that addition of a real number $a \in \mathbb{R}$ to a random variable only shifts the mean, but the variance remains unchanged $X \sim \mathcal{N}(0, \sigma^2), a \in \mathbb{R} \implies a + X \sim \mathcal{N}(a, \sigma^2)$. Therefore one can simply impose the deterministic drift (trend) to the process by an additional differential term μdt, then the differential equation has the form shown in the equation provided below for some $T > 0$.

$$dX_t = \mu dt + \sigma dW_t \implies X_T \sim \mathcal{N}(\mu T, \sigma^2 T) \tag{3.4}$$

Once again, the figure can be interpreted in two respects, which is the dichotomy mentioned. The first explanation is a single particle located at the origin at the initial time. In this respect, the trajectories generated represent possible fates for the particular agent. In addition, the trajectories can be explained as an ensemble of particles, such as a mole of gas particles. Then the trajectories stand for the individual particles that are independent and identically distributed [21]. In either case, the entropy accumulates with passing time. Furthermore, both interpretations have no difference, either qualitatively or quantitatively, as long as they are independent and identically distributed, commonly abbreviated as i.i.d.

Yet neither drifty one nor dW_t is not able to explain the evolution of CoP_x since the variance increases unboundedly. If the X_t has the form W_t, then the variance becomes infinite at the limit of $t \to \infty$. In this case, no human can maintain the balance after some intermediate t but falls to the ground as the CoP_x leaves the area spanned under foot. In mathematical words, at the limit of time, CoP_x can not stay inside any open interval represented by $(-M, M)$ for $M > 0$ as follows due to linearly increasing variance. For the particular problem, $(-M, M)$ represents the area spanned by foot that the probability of finding CoP_x inside goes to zero at the limit of time according to the squeeze theorem.

$$\lim_{t \to \infty} P\left(\mid X_t \mid < M\right) = 0 \tag{3.5}$$

or

$$0 \leq t_1 \leq t_2 \implies P\left(\mid X_{t_1} \mid < M\right) \geq P\left(\mid X_{t_2} \mid < M\right) \geq 0 \tag{3.6}$$

Therefore CoP_x can not be explained by W_t due to unboundedly increasing variance, but mean reversion is the first necessity that keeps the variance bounded for large t according to Equation 3.3. In other words, certain constraints have to appear in the equation to limit the variance at a reasonable value for the maintenance of erect posture. Therefore, the visually provided time series of CoP_x can not be threated as the diverging Markov paths shown in Figure 3.3.

Besides, in all steps of derivation, differential Wiener process dW_t is used as velocities, and intuitively decisions, which have constant power among all frequencies $\omega > 0$. Note that it is physically implausible as it requires infinite energy due to the non-decaying power spectrum at greater frequencies, as shown in Appendix A. Even if we know that W_t is absurd from a physiological perspective, it is employed to benefit from the analytical solutions. Otherwise, the model may come closer to reality by using band-limited white noise with losing analytical solutions, which is a definite trade-off that one side has to be selected. The same can be grasped from the infinite variation of process in any time interval, which makes the quadratic variation greater than zero, as mentioned before. Intuitively it is impossible to find endless variation in small Δt, as it requires an immense amount of energy.

Furthermore, in the absence of $\mu dt = 0$, the first moment stays constant along time. Analytically it can be expressed as $E(X_t) = E(X_u)$ such that $t > u > 0$. The property is named Martingale, and it is a crucial concept in stochastic calculus. Besides, in Newtonian deterministic calculus, the variance is always zero, and only the mean evolves in time which is the path itself. Therefore, the intersection of martingales and deterministic calculus is only a constant function $f(t) = c$ where $c \in \mathbb{R}$ in which the velocities are always zero. In this way, the fertileness of stochastic calculus can be seen, which is entirely different than ordinary calculus, thanks to dW_t.

3.3 Step 2 Mean Reversion

Please remind that the general equation is stated as $X_t = \mu(t, X_t)dt + \sigma(t, X_t)dW_t$ in Equation 1.1 where μ determines the rate of change of mean, and σ is associated with the scale of the standard deviation of the dice thrown for decision makings.

The analogy of dice is used for decisions since the steps governed by relation can be completely described by the first and second moments. In order to revert the paths diverging to infinity, the dice have to be constrained properly through the $\mu(t, X_t)$ term, but how? (For a detailed analysis, please refer to Appendix C)

If $\mu(t, X_t)$ is selected as a function of X_t, then the paths going further away from the mean can be directed back by imposing a bias on the dice in the desired direction. Still, some variance remains as long as the dice is not entirely constrained to stand still, but some room is left for dynamics. The bias can only be enforced through its first moment since the second moment is related to the square of ΔX_t, which has no direction due to the positive definite nature of even powers. The most straightforward choice is $\mu(X_t) := -X_t$, which is nothing but a linear mean reversion. Furthermore, the parameter $\lambda > 0$ may help to set the mean reversion rate. Therefore the following relation is written in the following way.

$$dX_t = -\lambda X_t dt + \sigma dW_t \tag{3.7}$$

Equation 3.7 can be interpreted as linear mean reversion, and the corresponding linear process is named Ornstein Uhlenbeck. Similar to the discussion in the last part, the process can be comprehended easily from discrete form, which explicitly shows the structure of the dice. Therefore discrete representation of Equation 3.7 is provided below.

$$\Delta X_t = \underbrace{-\lambda X_t \Delta t}_{\substack{\text{deterministic} \\ \text{mean reversion}}} + \underbrace{\sigma\sqrt{\Delta t} N(0,1)}_{\text{random part}} \tag{3.8}$$

Equation 3.8 shows the architecture of the dice at any instant t, which the decision depends on the current location as $X_t \sim \mathcal{N}(-\lambda X_t \Delta t, \sigma^2 \Delta t)$. If the current location of time series X_t is at zero, then the mean of the thrown dice is zero $-\lambda X_t dt = 0$, and $dX_t = dW_t$, so that the mean reversion disappears. However, as it goes further away from the equilibrium point zero, the dice apparently gain bias in the opposite direction due to the minus sign in front of it with a proportion of $-\lambda$. Therefore if the particle goes further away, it is pulled back to the mean due to the minus sign from

either direction. The corresponding stochastic differential equation is named Ornstein Uhlenbeck process, and it is named *"Fokker Plank Equation"* in the physics literature, as shown in the next relation.

$$\dot{x} = -\lambda x + \sigma B_t \tag{3.9}$$

Fokker Plank equation can be derived from the Ornstein Uhlenbeck process by differentiating both sides with respect to time. Therefore B_t is defined as dW_t/dt, which is nothing different than white noise, that is distributed standard normal. Therefore B_t represents the randomness due to the dice. Similarly, σ stands for the standard deviation of the noise and scales it accordingly. Another interpretation of the Fokker Plank equation is a parallel connected spring and damper, namely Kelvin-Voight, with an input of white noise. Since the spring always applies force according to $F = k(x - x_{th})$, the particle can not go far away from the equilibrium point in the presence of white noise input due to the accumulation of chance. Furthermore the existence of damper makes the equation first order rather than a zero order spring which get back to equilibrium position instantly as long as it does not have any room for time similar to zeroth step discussed before. Furthermore the existence of a damper makes the equation first order rather than a zero order spring which gets back to equilibrium position instantly as long as it does not have any room for time, similar to the zeroth step discussed before. Therefore the Fokker Plank equation can be written as $\dot{x} = -k/bx + \sigma B_t$, which explicitly shows the damping and stiffness. In this respect, the mean reversion rate is the ratio of stiffness to damping $\lambda := k/b$ with a physical unit of frequency $1/t$. Please note that increasing stiffness of spring k corresponds to greater mean reversion rate λ that presents itself as less deviation from equilibrium point and smaller variance respectively. Then any step of the Ornstein Uhlenbeck process can be interpreted as a biased decision because of the negative ratio of the distance from equilibrium, and it is proportional to λ in terms of its mean $\mathcal{N}(-\lambda(X_i - 0)\Delta t, \sigma\sqrt{\Delta t})$.

Another interpretation of the Ornstein Uhlenbeck process is possible with the *"Geometrical Way of Thinking"* proposed by Strogatz as mentioned before [19]. The analysis involves plotting $\dot{x}$ as a function of x in phase space, so the result is a line

with the intersection at zero and a slope of $-\lambda$ such that $\dot{x} = -\lambda x$. Zero represents the equilibrium point, i.e., rest length, and the negative slope shows the kind of stability at that point. As the slope is negative $-\lambda < 0$, the critical point is stable. In detail, the paths at the negative side $x < 0$ converge to zero with positive velocity $\dot{x}$, and the trajectories on the positive side do the same due to the opposite sign, which is negative $x > 0 \implies \dot{x} < 0$. Additionally, the second term σdW_t is nothing but the error and randomness around the line in the phase space. In this respect, the Ornstein Uhlenbeck process can be described as a search of the line consisting of a stable equilibrium point at a given location.

Besides that, the Ornstein Uhlenbeck differential equation has an analytical solution since it is a first-order linear non-homogeneous differential equation. Therefore the differential equation should be solved for a more concrete understanding, and the solution is provided below by following the procedure shown in Appendix C.

$$X_t = X_0 e^{-\lambda t} + \sigma e^{-\lambda t} \int_0^t e^{\lambda s} dW_s \tag{3.10}$$

In the equation, X_0 is the initial condition representing the current location, and s is the dummy variable for integration. Firstly the term $X_0 e^{-\lambda t}$ shows the exponential decay of the initial position to the origin. Besides that, the most interesting part is the second term. The integrator $e^{\lambda s}$ behaves as a time window for the past steps of dW_s for $0 < s < t$. The time window rules the influence of the distant and recent past in an exponential sense. In discrete form the past decisions and respective influences can be seen clearly such that $\sigma \sum_i e^{-\lambda i \Delta t} \sqrt{\Delta t} \mathcal{N}(0, 1)$ where all steps are independent identically distributed. Then the constant $e^{-\lambda t}$ normalizes the result of the integral for that particular t successfully since the integral of an exponential $e^{\lambda s}$ is again an exponential. It is worth noting that even if the bias is introduced through the mean as $-\lambda X_t$, in the solution, it ends up with normalization of variance to keep it bounded as desired. For a complete understanding, the solution can be traced step by step from Appendix C. Besides that, the positive constant σ is only for the scaling of the variance as it appears in front of the integral. Another way of expressing the second term is $\int_0^t e^{-\lambda(t-s)} dW_s$ to make the time window visible, which governs the influence of history. Even if it is skipped, a different time window can be observed

in fractional Brownian motion that is $\int_0^t (t-s)^{H-1/2} dW_s$, yet it is out of scope for the thesis. Still, the time windows differ significantly. In fractional Brownian, power relation ends up with a slow decay of correlations compared to exponential $e^{-\lambda(t-s)}$. Further, it gains a fractal structure due to scale independence of power law as $\alpha \in \mathbb{R}$ and $(\alpha t)^H / t^H = \alpha^H$ is independent of the time variable. However, this kind of scale independence can not be obtained with an exponential function.

Besides the solution, it is possible to compute the first and second moments of X_t since it is distributed normal, and the distribution can be completely characterized by those two moments. As there is no bias for drift, the mean can be intuitively found as zero. Furthermore, the bounded variance must be a constant independent of t. Therefore, the variance has to be proportional to the scaling of dice σ^2 and inversely proportional to the mean reversion rate λ, which is explained as the ratio of stiffness to damping in the Langevin equation. Even if the variance given below with an intuitive explanation detailed derivation can be found in Appendix C.

$$\langle X_t \rangle = 0 \tag{3.11a}$$

$$\langle X_t^2 \rangle = \frac{\sigma^2}{2\lambda} \tag{3.11b}$$

Moreover, by using the solution, the correlation function can be found. Please remind that the integrand $e^{-\lambda(t-s)}$ is mentioned as a time window determining the influence of past decisions. Therefore correlation function can be nothing different than $\rho(X_t X_u) = e^{-\lambda(t-u)}$, again a detailed derivation is provided in Appendix C. Then the Fourier transform of the deterministic correlation function can be computed to reach the frequency content of the process in the Fourier domain. The relation is named Power Spectral Density and it is equal to $\frac{\lambda}{\pi(\lambda^2+\omega^2)}$ where ω is the frequency with a physical dimension $[1/s]$.

Please note that only λ presents itself in correlation function and power spectral density, but both of them are independent of σ. This result is expected since σ is only the scale for the variance, so it can not do anything different than determining the area under the power spectrum. In contrast, λ governs the decay rate of spectral power at greater frequencies since power spectral density can be interpreted as *partition of*

variance over frequencies. Therefore σ affects only the area under the power spectral density.

In this perspective, path-wise effects of each parameter have to be provided. The best way known to us is using a three-by-three table, each plot having distinct λ and σ for any row and column. The following figure is provided below, which has to be investigated in a detailed way. During the creation of the table, the same set of random variables is used, by setting the random seed, kernel, for a better comparison among different parameter settings. In the figure λ increases from right to left and σ increases from bottom to top.

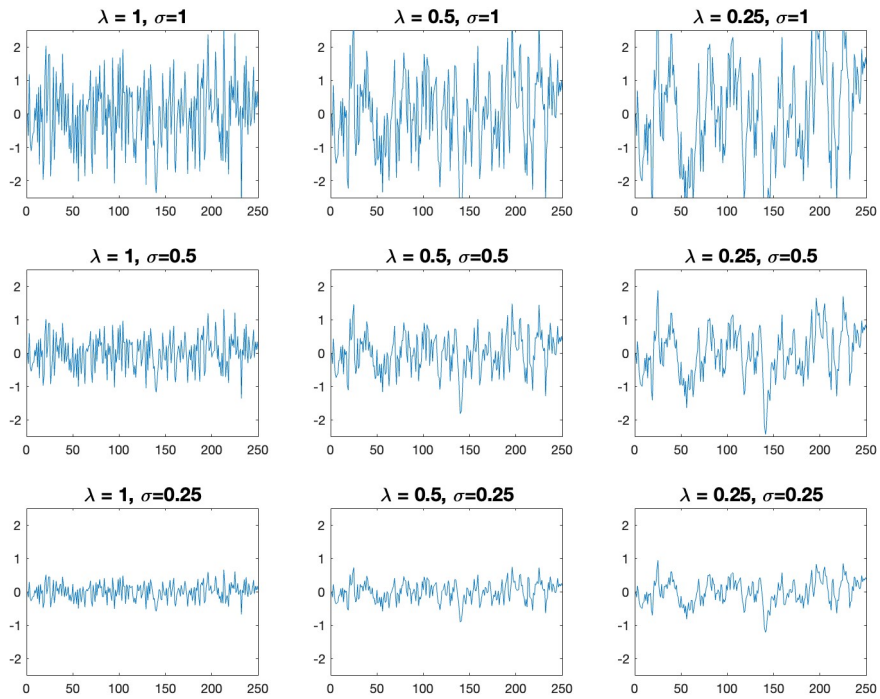

Figure 3.4: Paths Generated with Different Values of λ and σ

Please note that as σ increases, the difference between the maximum and the minimum becomes larger, which is mentioned as σ scales the variance of increments. Also, σ enlarges the interval spanned by the path faster than λ as the variance is proportional to the square of sigma but inversely proportional to the first power of λ according to Equation 3.11b. Moreover, σ is found to have no effect on the decay of the power spectrum in the frequency domain, which is clearly visible to the naked eye. However, the frequency content changes due to λ varying on rows. As λ increases the

power spectrum shift toward smaller frequencies according to $\frac{\lambda}{\pi(\lambda^2+\omega^2)}$. Please have a look at the figure once again before continuing, especially the row at the bottom, for a visual understanding.

Moreover, the mean of the Ornstein Uhlenbeck process can be shifted easily. Please remind that X_t is pulled toward zero due to the minus sign. Therefore if one multiplies $-\lambda$ with $(X_t - \theta)$, than the process becomes pulled toward θ, since $(X_t - \theta) > 0$ if $X_t > \theta$ and vice versa. So, in either case, the dice become biased for pulling toward θ rather than zero. It can be thought analogous to threshold, rest length, of the spring in Fokker Plank, so the corresponding Fokker Plank equation can be apparently stated as $\dot{x} = -\frac{k}{b}(x - x_{th}) + \sigma B_t$.

3.4 Step 3 Double Ornstein Uhlenbeck

At the end of the last step, the equilibrium point of the spring shifted from zero to x_{th}, and the corresponding value is denoted as θ. In this way, the stochastic process shown in Equation 3.7 is rewritten in the following form. As mentioned before, the dice gained a definite bias toward the long-term mean θ, since the mean of any decision is no longer zero but pointing toward the equilibrium point θ or x_{th} with keeping the properties associated with the variance as the same. In this respect, the bias is apparent in the first term of the differential equation and clearly visible through the sign of $-\lambda(X_t - \theta)$, and the mean reversion rate is proportional to λ for each Δt.

$$dX_t = -\lambda(X_t - \theta)dt + \sigma dW_t \tag{3.12}$$

Even if θ in Equation 3.12 is a constant representing the threshold of the spring, it can also be chosen as a stochastic process too. Then it must be denoted as a function of time θ_t, similar to the process X_t representing the dynamics of CoP_x time series. After that, this part defines the process θ_t obeys, to describe the system of stochastic differential equations involving X_t and θ_t. Similar to the discussion up to this point, θ_t can not diffuse unboundedly as X_t is pulled toward it. Therefore it has to be selected as an Ornstein Uhlenbeck process to keep the variance bounded for all $t > 0$ such as $d\theta_t = -\kappa\theta_t dt + \sigma dW_t$ with some mean reversion rate κ and its own Wiener

process denoted by W_t^2. Furthermore, the process has to be represented with terms $\sigma_2 dW_t^2$ to differentiate volatility terms σ and Wiener process from the other driving noise associated with X_t. Therefore the following system of stochastic differential equations can be written.

$$dX_t = -\lambda(X_t - \theta_t)dt + \sigma_1 dW_t^1 \tag{3.13a}$$

$$d\theta_t = -\kappa\theta_t dt + \sigma_2 dW_t^2 \tag{3.13b}$$

$$\left\langle dW_t^1 dW_t^2 \right\rangle := \rho dt = 0 \tag{3.13c}$$

The third equation dictates the covariance structure between W_t^1 and W_t^2 which must be selected $\rho \in [-1, 1]$. For the sake of simplicity, ρ is selected to be zero, but other values of ρ may yield exciting results in the model in which the CoP_x time series is correlated with the diffusive equilibrium points θ_t. At first sight, the equation may look complicated to understand, but one must not forget that it is only a "first order linear constant coefficient nonhomogenous system of stochastic differential equations" in which the analytical solution is available. Besides that Equation 3.13 is presented in matrix form in Appendix D.

After that, similar to Ornstein Uhlenbeck, the process can be analyzed by following the same recipe with the steps of determination of the solution, computation of correlation function, power spectral density, and providing a table representing the relative effects of parameters. So that the first step is providing the solution to the system of stochastic differential equations, as shown below. Please note that the solution is obtained by threading the problem like an eigenvalue problem and employing Green's function, and a detailed step-by-step solution is provided in Appendix D.

$$X_t = X_0 e^{-\lambda t} + \theta_0 \frac{\lambda}{\kappa - \lambda}\left(e^{-\lambda t} - e^{-\kappa t}\right) + \sigma_1 \underbrace{\int_0^t e^{-\lambda(t-s)} dW_t^1}_{A} + \sigma_2 \frac{\lambda}{\kappa - \lambda}\left(\underbrace{\int_0^t e^{-\lambda(t-s)} dW_t^2}_{B} - \underbrace{\int_0^t e^{-\kappa(t-s)} dW_t^2}_{C}\right) \tag{3.14}$$

In the intermediate steps of the solution, eigenvalues are found as $u_1 = -\lambda$ and $u_2 = -\kappa$, which dictates the stability of paths. Since the λ and κ are selected positive for mean reversion, eigenvalues can not be anything different than them. Therefore, eigenvalues are negative for $\lambda, \kappa > 0$, so the paths can not diverge but remain arbitrarily close to the equilibrium point θ_t at any instant, i.e., and then absolute equilibrium at zero. Also, the denominator in the solution may yield infinite if $\kappa - \lambda = 0$, yet this is not the case as shown in Appendix D due to the selection of distinct eigenvalues $\lambda \neq \kappa$. Furthermore, as mentioned in Appendix D, while $X_t = \theta_t$ is the instant equilibrium points for t that it is satisfied, zero behaves as a global equilibrium according to $-\kappa(\theta_t - 0)$ in Equation 3.13b.

After noting the points related to eigenvalues, the solution can be analyzed term by term. In order to avoid any confusion while discussing all elements of the solution, each term is denoted with A, B, and C, respectively, as shown with under braces in Equation 3.14. Yet before discussing them, it is better to keep in mind that the first and second terms are deterministic, and they dictate the relaxation of the initial condition, the current position with an exponential rate to absolute equilibrium zero. Please remind that the same term has appeared in the solution of the Ornstein Uhlenbeck process as $X_0 e^{-\lambda t}$ in the absence of a moving threshold. Therefore, $\theta \to \theta_t$ added additional decay according to initial θ_0 as a function of λ and κ.

After the deterministic part, the term A involving integral with respect to W_t^1 has nothing to do with θ_t, but it is inherent randomness of X_t as A is function of σ_1, λ and W_t^1. The same can be seen from the matrix representation of the differential equation provided in Appendix D as Equation D.8, where the lower left element of the matrix is zero. So that it is the same as the integral that one can see in the Ornstein Uhlenbeck process. On the contrary, the terms $B - C$ represent additional variance related to the moving threshold and equilibrium point as opposed to constant baseline fluctuations of X_t following the Ornstein Uhlenbeck process in the last section.

Therefore B and C are the interesting terms since the integrator is W_t^2 in each of them, so both of them are associated with the moving equilibrium point and corresponding randomness. Before the interpretation, it is better to say that $B - C$ can be rewritten as $\int_0^t e^{-\lambda(t-s)} - e^{-\kappa(t-s)} dW_s^2$ in a single integral. In this way, the time window de-

termining the influence of the distant and recent past becomes visible. Then the time window can be nothing different than the subtraction of two time windows as it rules the decay to absolute equilibrium zero. If θ_t was following a Wiener process without mean reversion, in other words, $\kappa = 0$, still B and C would appear in the solution. However, mean reversion of moving θ_t decreases variance according to the integral C, because of the minus sign in front of it compared to unbounded diffusion of θ_t. If the mean reversion of θ_t was absent, then the integrand in C would be one, and then the variance diverges with time. In the opposite case, $\kappa \to \infty$, the process θ_t turns into white noise, which is almost constant around zero. Therefore the integrand of C remains around zero except for the limit $s \to t$. In this way, the solution becomes similar to Ornstein Uhlenbeck since the denominator $\kappa - \lambda$ is almost either positive or negative infinite, which vanishes $B - C$. Besides those two limits of $\kappa \to 0$ and $\kappa \to \infty$, the opposite signs of B and C decrease the variance accordingly. Moreover, both B and C are scaled with σ_2, and it is divided by the difference $\kappa - \lambda$. The sign of $\kappa - \lambda$ may change, whether $\lambda < \kappa$ or the opposite, yet it does not matter as W_t^2 is symmetric around the mean, and the mean is not evolving in time, namely "martingale" such that $E(X_t \mid X_u) = X_u$ for $u \leq t$. In other words, as long as the mean does not evolve with time, reversion of the sign has no effect on the process since W_t^2 is symmetric around its mean in the absence of skewness and all other odd-order moments. Then inversion of the sign only makes the observed path symmetric with respect to zero, which makes no difference in probabilistic measures as all of A, B, and C are associated with the variance and squares having no direction. Therefore the inverse signs of B and C is the only relevant thing as they are related to the stealing phenomenon and constraint.

Furthermore, θ_t is nothing different than an Ornstein Uhlenbeck, so all the discussion about threshold process θ_t mentioned in the last section is still valid and applicable, except for the change of names of parameters. Therefore the discussion is not repeated.

In conclusion, the solution is a linear superposition of two deterministic exponential decays of initial conditions, together with randomness associated with W_t^1, similar to Ornstein Uhlenbeck, and two other integrals. One of them corresponds to stolen variance due to mean reversion in θ_t, but the overall B and C represent additional

variance associated with θ_t moving threshold against the Ornstein Uhlenbeck process where the rest length is constant x_{th}. In other words, the additional θ_t rather than constant θ converts the fluctuations around a baseline to a random equilibrium point determined by θ_t. In this way, the variance of X_t increases. Then the next step is the interpretation of moments, especially the second moment, as the mean is zero for all t, so there is nothing interesting about it. Also, please note that the process is linear, and X_t is normal distributed, so the rest of the moments are not applicable, but the complete description of the distribution can be handled with only the first and the second moments.

$$\left\langle X_t^2 \right\rangle = \frac{\sigma_1^2}{2\lambda} + \frac{\sigma_2^2}{(\kappa-\lambda)^2}\frac{\lambda^2}{2\lambda} + \frac{\sigma_2^2}{(\kappa-\lambda)^2}\frac{\lambda^2}{2\kappa} - \frac{\sigma_2^2}{(\kappa-\lambda)^2}\frac{2\lambda^2}{\lambda+\kappa} = \underbrace{\frac{\sigma_1^2}{2\lambda}}_{<A^2>} + \left(\frac{\sigma_2\lambda}{\kappa-\lambda}\right)^2 \underbrace{\left[\underbrace{\frac{1}{2\lambda}}_{<B^2>} + \underbrace{\frac{1}{2\kappa}}_{<C^2>} - \underbrace{\frac{2}{\lambda+\kappa}}_{<-2BC>}\right]}_{\frac{(\lambda-\kappa)^2}{2\lambda\kappa(\lambda+\kappa)}} \tag{3.15}$$

The first thing to notice in the relation is the additional term in the variance. While Ornstein Uhlenbeck has a second moment $\sigma_1^2/(2\lambda)$, now a strictly positive expression is summed up to increase the variance due to moving threshold compared to fluctuations around a constant baseline. The positive definite nature of the second term due to squares is shown with the outer underbrace.

One by one investigation of the relation requires the analysis of four distinct terms. The integral represented with A in the solution ends up with a contribution of $\sigma_1/2\lambda$ in variance, the same as the Ornstein Uhlenbeck process. Furthermore, the second term is associated with a square of B, and similarly, the third term is a square of C. The subtraction is due to the product of BC and the opposite sign, which decreases the variance, as mentioned in the interpretation of the solution. Further grouping of terms by taking them into common parenthesis makes it more suitable for comprehension. In this setting, the sign of the terms inside the parenthesis can be questioned easily, and it is strictly positive, which can be seen by bringing all fractions together under a common denominator. Therefore moving θ_t can only increase the overall variance of

X_t. Moreover, the parameter ρ indicating the correlation between W_t^1 and W_t^2 is zero. So the cross terms involving A such as AB and AC must be zero as long as W_t^1, and W_t^2 are independent. Still the generalization $\rho \in [-1, 1]$ is provided in Appendix E.

After the discussion of the variance, the correlation structure as a function of time delay $\tau := t - u$ can be explained through the relation provided below. Again its detailed derivation is given in Appendix D, and $\langle \theta_t \theta_u \rangle$ is not discussed since it is shown in the last section as the Ornstein Uhlenbeck process.

$$\langle X_t X_u \rangle = \left[\frac{\sigma_1^2}{2\lambda} + \left(\frac{\sigma_2 \lambda}{\kappa - \lambda} \right)^2 \left[\frac{1}{2\lambda} - \frac{1}{\lambda + \kappa} \right] \right] e^{-\lambda \tau} + \left[\left(\frac{\sigma_2 \lambda}{\kappa - \lambda} \right)^2 \left[\frac{1}{2\kappa} - \frac{1}{\lambda + \kappa} \right] \right] e^{-\kappa \tau} \quad (3.16)$$

The covariance function has a form of double exponential in which the time constants are determined by λ and κ, respectively. Even if there is an additional $\sigma_1^2/2\lambda$, the rest are similar except for the interchange of λ and κ in denominators. Obviously, the first exponential decay with λ involves λ in the denominator, and the same is true for the second exponential decaying with κ. Therefore the form is symmetric in terms of λ and κ.

Furthermore, one of the correlations has to be negative, while the other one is positive, either $\lambda > \kappa$ or $\kappa > \lambda$. Since the exponentials are positive definite, the opposite signs of correlations are associated with the difference $\frac{\kappa - \lambda}{2\lambda(\lambda+\kappa)}$ and $\frac{\lambda - \kappa}{2\kappa(\lambda+\kappa)}$ respectively. So the negative and positive correlations at different frequency ranges according to decay ruled by τ can be interpreted similar to persistence and antipersistence terms in Collins's article [29], even if those are completely distinct concepts related to fractal structure. The desired range of parameters $\lambda >> \kappa$ and $\sigma_1 << \sigma_2$ has to be considered for the assessment of the CoP_x. Therefore the first term involving σ_1 vanishes because of the square, and either variance or correlations become a function of the rest of the terms symmetrically. Moreover, as $\lambda >> \kappa$, the first term decaying with λ governs the negative correlations, and the second term governs positive correlations analogous to antipersistence and persistence, respectively. Once again, please note that two phenomena are completely distinct concepts, and the difference originates

from the form of the time window. In this relation, the integrands are exponential functions, yet persistence and antipersistence in a fractional sense require integrands obeying power law such as $(t-s)^{H-1/2}$ for two distinct values of H greater or less than $1/2$, respectively in different frequency ranges. Interpretation of positive and negative correlations can be clearly seen in all the tables provided in the next pages, so it may be beneficial to check any of them now.

Those two exponential decays present themselves in power spectral density too, in other words, the frequency domain. Importantly it coincides with Collins's article again. As two exponentials related to λ and κ decay with different rates, the frequency spectrum becomes modified accordingly. The one decaying faster determines the frequency content at greater frequencies, in our particular problem represented with λ and σ_1 are associated with greater frequencies in the desired range of parameters. Then, the further analysis is only possible with seeing relative effects of each parameter $\{\lambda, \kappa, \sigma_1, \sigma_2\}$. In this way, everything about the processes X_t and θ_t become clearly visible. Therefore presenting tables similar to Ornstein Uhlenbeck is necessary.

Before presenting the tables, all terms have to be interpreted one by one. Firstly, κ and σ_2 have the same effects over θ_t similar to Equation 3.7, as discussed in the last section related to ordinary Ornstein Uhlenbeck process diffusing around a constant baseline. Furthermore λ determines the decay rate of X_t to θ_t. Also, σ_1 pushes X_t away from θ_t, and greater the σ_1, X_t has more fluctuating appearance as discussed in power spectrum. In other words, σ_1 determines the smoothness of X_t. Moreover, if $\lambda \to \infty$, X_t sticks to θ_t, and they move together as the decay rate is infinite.

Furthermore for the generation of all paths given below, parameters are selected according to $\lambda << \kappa$ and $\sigma_1 << \sigma_2$ to have a greater influence of θ_t on variance rather than $\mid X_t - \theta_t \mid$ distance. In this way X_t remains close to θ_t compared to $\mid \theta_t - 0 \mid$. The relative influences on variance can be checked from Equation 3.15, as the contributions to variance are proportional to σ_i^2, then $\sigma_1^2 << \sigma_2^2$ becomes more significant. Besides that, since θ_t is only an Ornstein Uhlenbeck process, the comparison involving κ and σ_2 is not that much interesting, but the identification of λ and σ_1 is the most essential one so that it is going to be discussed at first.

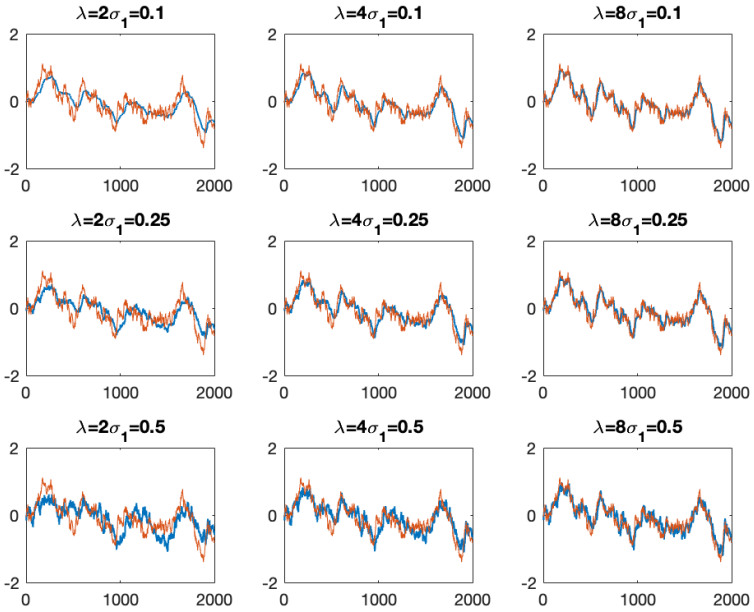

Figure 3.5: Paths Generated with Different Values of λ and σ_1. X_t is blue, θ_t is red.

In all portions, κ and σ_2 are kept constant so that the variance did not change significantly like the ones in Figure 3.3. The same can be interpreted as X_t has no other chance rather than following θ_t. Therefore it is visible that main contribution to variance is associated with θ_t and σ_2 in this parameter range, except $\sigma_1 >> \sigma_2$ and $\kappa >> \lambda$. In this case, θ_t remains almost constant around zero, and X_t becomes indistinguishable from the Ornstein Uhlenbeck process, which is not interesting in the scope of the dissertation and related literature. Furthermore, the main effect of λ and σ_1 are on the smoothness of the X_t blue curve. Please note that in the presence of the Wiener process $\sigma_1 > 0$, variation becomes infinite as mentioned before. Yet visually, increasing σ_1 decreases the smoothness of paths as shown from top to bottom. The same can be concluded from Equation 3.16 relating it with high-frequency content. As $\lambda >> \kappa$ slowly decaying exponential $e^{-\kappa\tau}$ is directly proportional to σ_1^2. Along the columns increasing λ makes X_t more sticky to θ_t through the rate of exponential decay shown in $-\lambda(X_t - \theta_t)dt$ term. The stickiness of X_t is clearly visible in the comparison of left-most and right-most columns. In this respect, X_t can be treated as an exponential smoothing of an Ornstein Uhlenbeck θ_t plus some certain integrated Brownian noise scaled by σ_1. Also, the increased wiggly appearance at greater σ_1 is visible along each column.

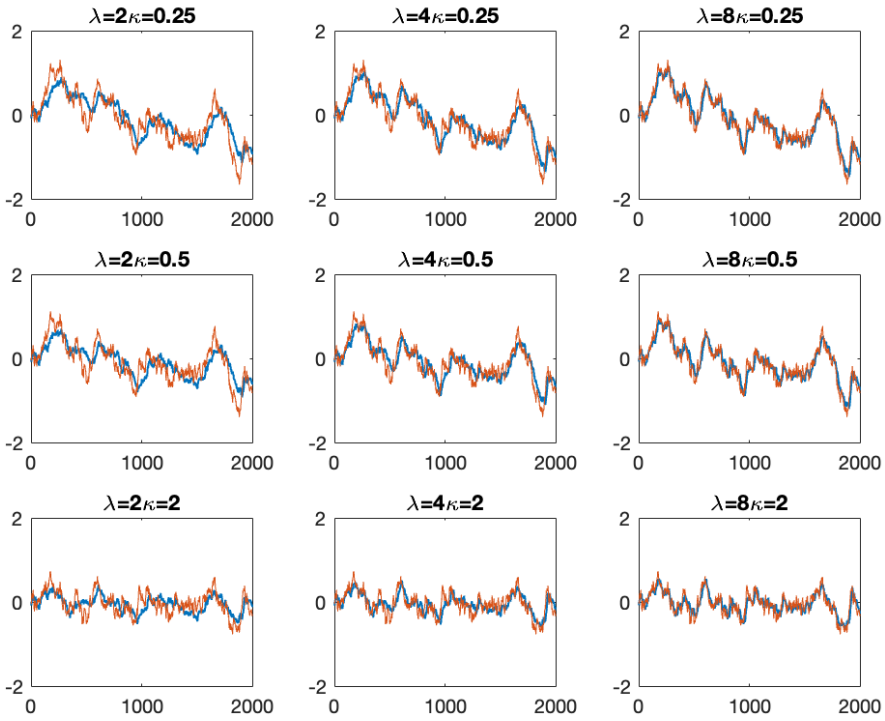

Figure 3.6: Paths Generated with Different Values of λ and κ

Another interesting comparison is the relative effects of λ and κ. While λ rules the stickiness of X_t to θ_t, the other parameter κ determines the frequency content in smaller frequencies due to different decay rates of exponentials, as it did to the regular Ornstein Uhlenbeck process. Long period navigation of the curves is determined by κ, similar to the discussion of Ornstein Uhlenbeck. Please note that the frequency content of θ_t is independent of σ_2, but decreasing κ ends up with a gain in low frequencies. Therefore along the columns, especially the right-most one, which is the stickiest as $\lambda = 8$, the effect of κ is clearly visible. Further discussion of σ_2 is not that much necessary as it has no effect on frequency content but only a scale of noise in θ_t, so it determines the area under the power spectrum. Anyone considering the effects of σ_2 may have a look at Figure 3.4. Still, visualization may seem interesting, so the related figure comparing λ stickiness and σ_2 scale of θ_t is provided below.

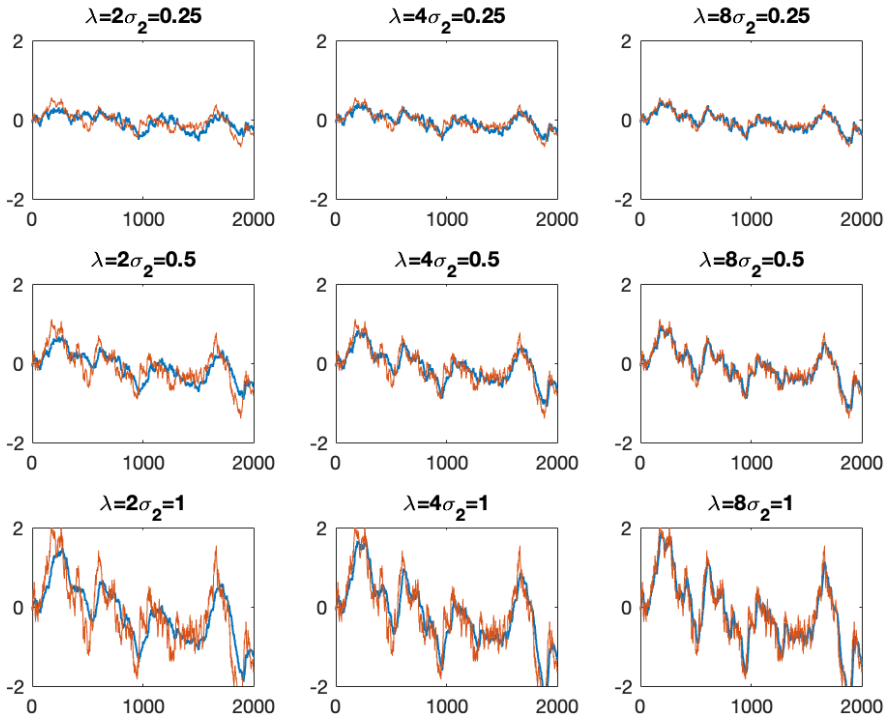

Figure 3.7: Paths Generated with Different Values of λ and σ_2

Even if σ_2 has no effect on spectral content but only a scaling, it significantly changes the variance of X_t according to $\langle \theta_t \rangle = \sigma_2^2/2\kappa$. As X_t follows θ_t with an exponential decay in this parameter range, an increasing variance of θ_t affects the scale of X_t by leaving the frequency content the same. Therefore square of σ_2 appears in the variance of X_t. Anyone looking at the bottom row may see that the curve becomes more sticky with increasing λ, as it variates with large fluctuations due to greater values of σ_2.

In conclusion, λ determines the stickiness of X_t to θ_t as it is an exponential smoothing, so it can be seen from the system of differential equations presented in Equation 3.13. The second parameter σ_1 determines the wiggliness of X_t as it is additional noise added to $(X_t - \theta_t)$ distance, besides that it pushes X_t away from θ_t in either direction. Please keep in mind that $\sigma_1 > 0$ implies infinite variation. Therefore for any value of $\sigma_1 > 0$ implies infinite jitteriness, technically variation. Furthermore, κ induces the long-range properties (power at low frequencies), as X_t has nothing to do except following θ_t, which has a frequency spectrum determined by κ. Finally σ_2

is nothing different than scaling of θ_t and it has significant effect on variance of X_t in the chosen range of parameters shown in Figure 3.5, Figure 3.6 and Figure 3.7. Moreover, the behavior can be changed if $\lambda << \kappa$. In this case, X_t behaves like an ordinary Ornstein Uhlenbeck as $\theta_t = 0$ constant threshold, i.e. constant baseline fluctuations. Then κ and σ_2 have no significant effect on the dynamics of X_t different than an Ornstein Uhlenbeck process.

Further interpretation requires the analysis of two distinct cross relations. The first one involves the relation between X_t and θ_t through $\langle X_t \theta_t \rangle$. Furthermore the difference $X_t - \theta_t$ itself and its relation with θ_t can be discussed with $\langle X_t(X_t - \theta_t) \rangle$. Secondly, the cross relation of W_t^1 and W_t^2 governed by ρ can be assessed similarly. Moreover, covariance structures involving $\tau := t - u$ is also necessary. Please note that variance is a special case of covariance in time which $\tau = 0$.

Even if up to now all steps are followed similar to Ornstein Uhlenbeck process, an additional step can be carried out by investigating relation between X_t and θ_t such that $\langle X_t \theta_t \rangle$ and $\langle X_t \theta_s \rangle$. Therefore corresponding relations are provided below in the absence of covariation between two Wiener processes $dW_t^1 dW_t^2 = \rho dt = 0$.

$$\langle X_t \theta_t \rangle = \frac{\lambda \sigma_2^2}{\kappa - \lambda} \left[\frac{1}{\lambda + \kappa} - \frac{1}{2\kappa} \right] = \frac{\lambda \sigma_2^2}{2\kappa(\kappa + \lambda)} = \frac{\sigma_2^2}{2\kappa} \frac{\lambda}{\lambda + \kappa} = \left\langle \theta_t^2 \right\rangle \frac{\lambda}{\lambda + \kappa} \tag{3.17}$$

The covariance between X_t and θ_t is found to be equal to multiplication of variance $\langle \theta_t \rangle$ and a positive constant $\frac{\lambda}{\lambda+\kappa}$. It is already mentioned that in this parameter range $\lambda >> \kappa$, the multiplied constant becomes almost one, and cross relations becomes $\langle X_t \theta_t \rangle \approx \langle \theta_t^2 \rangle$ that is directly proportional to σ_2^2. Furthermore, one may generalize it to $t \neq s$, which grasps the decay rate of covariance as follows.

$$\langle X_t \theta_u \rangle = e^{-\lambda \tau} \left[\frac{\lambda \sigma_2^2}{\kappa - \lambda} \frac{1}{\lambda + \kappa} \right] + e^{-\kappa \tau} \left[-\frac{\lambda \sigma_2^2}{\kappa - \lambda} \frac{1}{2\kappa} \right] \tag{3.18}$$

Similar to the discussion up to that point, double exponential correlations appeared again that are decaying with different time constants λ and κ. Moreover, two distinct correlations have inverse signs again. While the fast decaying correlation associated with λ has a negative sign, the other term governs the positive correlations, which

remain at greater τ. Furthermore, the different denominators $\lambda + \kappa$ and κ govern the power of respective positive and negative correlations at different time scales. Once again, please note that in this parameter range, $\lambda >> \kappa$, slow decaying correlations have a positive sign.

$$\langle (X_t - \theta_t)(X_t - \theta_t) \rangle = \frac{\sigma_1^2}{2\lambda} + \left(\frac{\sigma_2 \lambda}{\kappa - \lambda}\right)^2 \left[\frac{1}{2\lambda} + \frac{1}{2\kappa} - \frac{2}{\lambda + \kappa}\right] + \frac{\sigma_2^2}{2\kappa} + -2\frac{\sigma_2^2}{2\kappa}\frac{\lambda}{\lambda + \kappa} \tag{3.19}$$

Another exciting relation is related to the difference between X_t and θ_t. The variance of the difference can be derived from the other equations by employing the distributive property of multiplication and linearity of expectation so no additional calculation is not required such that $\langle (X_t - \theta_t)(X_t - \theta_t) \rangle = \langle X_t^2 + \theta_t^2 - 2X_t\theta_t \rangle$. For the interpretation, at first, please note that in this parameter range, the first term can be neglected as $\sigma_1 << \sigma_2$, which is associated with the square of σ_1, even smaller. Moreover, the relation explicitly shows the stolen part of the variance, which is twice of covariation $2X_t\theta_t$ which can not be neglected since most of the variance $\langle X_t^2 \rangle$ is associated with θ_t rather than $X_t - \theta_t$ in this parameter range. Therefore one can conclude that this relation yields a significantly smaller value compared to X_t similar to the figures provided in this section.

$$\langle (X_t - \theta_t)\theta_t \rangle = \left\langle X_t\theta_t - \theta_t^2 \right\rangle = \frac{\sigma_2^2}{2\kappa}\left[\frac{\lambda}{\lambda + \kappa} - 1\right] = \frac{\sigma_2^2}{2\kappa}\frac{-\kappa}{\lambda + \kappa} \tag{3.20}$$

Finally the last relation shows the negative definite cross-relation between the difference $X_t - \theta_t$ and θ_t. Furthermore, in this parameter range $\lambda >> \kappa$, this relation yields a small value due to the division of $\kappa << \lambda + \kappa$.

Further generalization of the system of stochastic differential equations can be handled through $\rho \in [-1, 1]$. However, the variances and covariance become too complicated for interpretation since they have more terms involving ρ. Still, the equations are provided for a curious reader in Appendix E without detailed explanations.

3.5 Step 4 Multimodality

At the cost of losing analytical solution and then sacrificing explicit determination of temporal correlation structure and power spectrum, the model can be brought into a multimodal distributed process. It can be reached if there exist two stable fixed points. Then one can guess that the manipulation of relation is only possible by changing the relation θ_t obeys since X_t can not do anything rather than following θ_t as discussed before.

Please remind that the phase portrait of Ornstein Uhlenbeck is a line $\dot{x} = -\lambda x$ having an intersection at zero and a slope $-\lambda$. In Ornstein Uhlenbeck, the negative slope around the equilibrium point (origin is stable equilibrium point) made it mean reverting due to opposite signs of $\dot{x}$ and x at either side. Similarly, stable fixed point is converted to a constant θ, threshold, by moving the intersection according to Equation 3.12. So that the simplest possible way to impose two stable fixed points that are symmetric around zero is the employment of a third-degree polynomial that has three roots. Therefore it is possible to use the polynomial $\dot{\theta} = -r\theta^3 + \theta$ which has roots at zero and $\pm\sqrt{r}$. Since the slope is negative at either $\pm\sqrt{r}$, those roots correspond to stable fixed points. Inevitably, the polynomial around the middle root has a positive slope, and it becomes an unstable fixed point, that is why the third-order polynomial having three roots is used. Then the following nonlinear relation can be written by keeping the first equation related to X_t the same.

$$dX_t = -\lambda(X_t - \theta_t)dt + \sigma_1 dW_t^1 \tag{3.21a}$$

$$d\theta_t = (-r\theta_t^3 + \theta_t)dt + \sigma_2 dW_t^2 \tag{3.21b}$$

$$\left\langle dW_t^1 dW_t^2 \right\rangle := \rho dt = 0 \tag{3.21c}$$

In this way, θ_t and X_t following it, hopes between two stable points at $\pm\sqrt{r}$. Figure 3.8 visualizes velocities $\dot{x}$ with respect to position x. While the directions of velocities are shown with arrows, full circles and empty circles correspond to stable and unstable fixed points, respectively. Furthermore integral of the polynomial, the red curve, is provided for the visualization of the pseudo energy surface [99] in which

the local minimums and maximums are representing the aforementioned fixed points. Therefore θ_t can be interpreted as a ball rolling over the red polynomial. As there are two symmetric local minimums at $\pm\sqrt{r}$, the imaginary ball jumps in between according to dice $\sigma_2 dW_t^2$. So that the main effect must be seen in smaller frequencies even if the analytical solution and explicit expression of variance can not be found. The detailed analysis of $d\theta_t = (-r\theta_t^3 + \theta_t)dt + \sigma_2 dW_t^2$ can be found on Grigoriu's book [100].

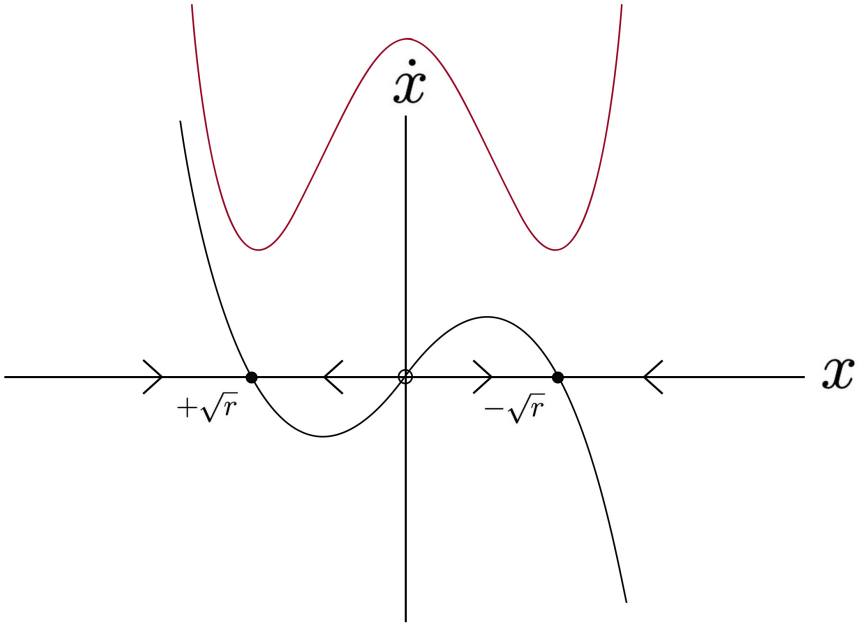

Figure 3.8: Phase Portrait

Besides that, using the new relation involving the polynomial causes giving up the analytical traceability still has an advantage from a computational perspective. While estimating the parameters from any experimentally collected time series, introducing nonlinearity to the model makes parameter identification easier as it offers freedom for model fitting. Please note that up to that step, all models were linear. Since dW_t is distributed normal, then all the processes until now have nothing to do differently than having a normal distribution as long as they all are linear. However, in this model, X_t can not be distributed normal due to the nonlinear form used. Particularly the distribution has a multimodal probability distribution which is impossible for Gaussian distributed random variables, so the modes of the new distributions are located at $\pm\sqrt{r}$. In this way, even moments with all orders $\langle X_t^n \rangle$, $n = 2, 4, 6, ...$ become free to be selected in order to match the experimentally collected time series, rather than

only the first and second moments, which are the only ones for Gaussian distribution. Please keep in mind that still, the distribution is symmetric around its mean, so the odd moments are still zero, including the third-moment skewness. Since all moments are independent of each other, five parameters, including ρ, can easily be determined by employing some of the five moments. Then the rest is the Monte Carlo simulation of an ensemble of paths to calculate moments; in other words, this is nothing but a well-defined optimization problem. In contrast to previously proposed linear models, the same fitting procedure is impossible as long as we have no more than the first and second moments.

CHAPTER 4

DISCUSSION

4.1 Probabilistic Features of Postural Sway

Human erect posture is defined as the decisive step in the transition from ape to man by Friedrich Engels [7]. As long as it has a crucial role in the existence of humankind, dynamical characterization of the never-ending sway of the erect stance is assessed with stochastic calculus throughout the thesis. Since the center of mass of the human body (a few centimeters at the front of the lumbosacral joint) is elevated from the ground by approximately one meter, the area spanned by the foot is smaller in order of magnitude depending on the ankle angle, which makes the dynamics of erect posture inherently unstable, especially in back and forth direction that is analogous to an inverted pendulum rotating around the ankle joint. Still, mankind is the only creature in the animal kingdom which maintains the proactive erect posture which is dynamically characterized in terms of never-ending sway. Postural sway can be quantified in terms of two distinct time series where a hierarchical order presents itself. While the first time series is the projection of the location of the center of mass onto the horizontal plane, CoM_x and CoM_y, it is kept inside the area spanned by the two feet with ground reaction forces (GRF) exerted through the foot, which the application point is assessed with the center of the pressure signal, CoP_x and CoP_y at the sagittal and frontal planes respectively.

Even if the dynamics of quiet stance can be understood through an inverted pendulum with a biomechanical perspective by considering the hierarchical relation between CoP_x and CoM_x, the understanding remains somehow incomplete [40] if anyone considers the dynamical elements contributing to the posture, including sensors, ac-

tuators, plant, and the nervous system. At this point, it is worth noting that each of those four elements has inherently complex natures besides the cross relations existing in between. Basically, there exist four distinct sensors somatosensory, vestibular organ, vision, and proprioception. While the first three of them are exteroceptors collecting "information" from the external world, the last one is the interoceptor responsible for gathering kinematic information related to respective joint angles and velocities. Still, any of those sensors can not be evaluated on its own. Please remind that in the second chapter, the role of proprioception in the internal construction of *self* motion is explained in terms of its relation to the vestibular apparatus. Furthermore, its relation with somatosensory is also somehow complicated, which can be discussed by mentioning three important experimental studies. While Simoneau is studying diabetic patients having sensory neuropathy, deterioration of nerves, the effects of neuropathy on subjects' balance can not be assessed clearly since diabetes does not only affect the mechanoreceptors associated with the somatosensory system under the foot sole but damages the nerves contributing to the proprioception related to the ankle joint position and velocity at the same time. So the observed changes can not be separated in a well-defined manner [13] due to the ambiguity in the sensorimotor control system and during the diagnosis. Therefore, the investigation of the effects of somatosensory on the dynamics of quiet stance is only achievable with its isolation, and it is either possible with anesthesia targeted to cutaneous foot sole somatosensory afferents or immersion of ice applied to the plantar side of the foot. After the application of anesthesia which is affecting only somatosensory afferents, Meyer observes statistically significant effects on CoP_x if and only if the eyes are closed, but he found that the effect is insignificant while the eyes of subjects' are open. In other words, when the vision is intact, two of the postural sensory systems of balance (vestibular and vision) are enough to compensate for the imposed somatosensory deficiency. This experimental finding is an indication of the two-of-the-three postural control mechanisms triggered by exteroceptors is a necessary and sufficient condition to maintain the balance. On the contrary, in the absence of vision during the aforementioned experiment, the condition of "full compensation of sensory information" with vision in the reduction of plantar sensitivity [14] is not fulfilled, which makes the cross-relation between the two distinct sensors apparent. The maintenance of balance requires sensory information, which serves as the first hierarchical level of

postural organization and control, while the second level is about the perception of the motion described as the simulation of the action [41] collectively employed for the construction of the self. Further, McKeon observes a significant increment in the area spanned by CoP together with mean excursion velocity after complete removal of plantar sensation; on the contrary partial decrement of somatosensory information ends up with the decrement of the area spanned by CoP. McKeon associates the decrement of the area under partial removal with decreasing explorative behavior of postural sway [101]. Even if it is possible to investigate those sensory cross relations with sensory reweightings [102], the findings can be treated as inherent complexities of the sensorimotor system that needs to be quantified by using "Information Theory" [20], requiring a probabilistic point of view. Since explorative search behavior with trial and error involves missing information, i.e., entropy, an understanding consisting of Shannon's information theory and statistical mechanics becomes inevitable, rather than a deterministic approach in which there is no room for either information or missing information. In this perspective, anyone can assert that the probabilistic postural sway is not tried to be minimized [103], but it is diligently escalated for the sake of learning and search for dynamic characteristization [52] with trial and error.

Besides the sensors, the actuators of quiet stance, similar to any other motor behavior, are striated muscles that obey the laws of statistical mechanics in terms of their microstates in the order of a few nanometers [104], [105], [99], [106], [107]. In terms of posture, the actuators are not only responsible for the displacement of joints, particularly the ankle joint, but also the provider of joint stiffness, which has a significant effect on the stability of the joint. Since the control of any dynamical system depends on the characteristics of its actuators, probabilistic effects observed in the consecutive biochemical reactions of actin and myosin filaments, i.e., motor proteins driving the muscle cells, are likely to manifest themselves at the macrostates of quiet stance, which can only be understood with a stochastic point of view. So that it is better to change the understanding from Newtonian determinism to probability theory and then statistical mechanics, which considers the missing information content, namely entropy of chemical reactions occurring in the microstates.

Furthermore, the plant, the human body, including ankle joints, knee joints, vertebrates stacked one on another, etc., imposes multidegrees of freedom and presents

complex dynamics. Then it serves to an opportunity for many combinations of joint angles corresponding to the same macro observable in the control of the endpoint position during the execution of a given task, such as the position of the hand in writing. Bernstein, the founder of motor control, calls this issue as "Degree of Freedom Problem", which is the reason behind the redundancy contained in the task. Therefore again, a probabilistic understanding is suitable for the investigation of the task as the joint space configurations do not map one-to-one to the endpoint task requirements.

Finally, the nervous system, which is responsible for processing and transferring information [108] is subject to noise, either in terms of sensory or motor signals acting simultaneously. Therefore not only the position and velocity estimations are erroneous [59], but also it is shown that motor signals that are responsible for the execution of tasks are subject to noise having a variance proportional to the size of the control signal [38].

Since any of the elements of the postural control; i.e., sensors having crosstalks, biochemical actuators, plant consisting of multiple degrees of freedom, and the noisy nervous system has inherent uncertainties, missing information, cross relations, redundancies, and so on, it is impossible to consider the dynamics of quiet stance as the summation of deterministic variables, yet it is a complex dynamical system involving many distinct segments working in a collective way for the maintenance of balance during quiet stance under the presence of uncertainties. Therefore a probabilistic understanding equipped with the tools of Shannon's Information Theory with an awareness of Statistical mechanics becomes more suitable than the deterministic mechanical approach, where the initial conditions make any deviation from the calculated path impossible. Rather it is better to leave some room for randomness at every time interval due to the existence of entropy in time. Besides that, Maurer and Peterka's attempt for the assessment of quiet stance with the injection of noise is also subject to problems that can be seen from their words "however, we tested the model with different sites of noise injection, and the simulation results were very similar" [109]. Please note that their model consists of a superposed noise source with a PID controller as opposed to using it at the core of the dynamics as a driving factor of the sway, which can easily be associated with biochemically driven stochastic muscles. In other words, it is more suitable to make the noise a part of the story

rather than direct addition as a disturbance, which is the commonly used method in posture research. Therefore the proposed model consists of noise as the driving factor of the sway, either denoted with W_t^1 or W_t^2 at later stages of the derivation. Then the rest is the exploitation of the proper constraints by structuring the stochastic differential equation to mimic the dynamical characteristics of postural sway, especially its bounded nature, which keeps the subjects away from falling by preserving the CoP inside the area under foot.

By employing stochastic reasoning, rather than the investigation of any particular motor execution path or sampled quiet stance time series, the attention can be focused on probabilistic features of the postural sway, including statistical moments, correlation function, and power spectrum.

4.2 Heuristic Approach to the Two-Level Dynamics of Postural Sway

Besides the rationales for the probabilistic features of quiet stance mentioned in the last section, human postural sway is a complex dynamical system by definition, the whole is more than its segments due to relations between distinct parts like the dynamics of sociology as opposed to independent individuals or materials formed by different types of atoms. Since the postural sway is a reflection of a complex dynamical system, its dissection into parts like sensors, actuators, plant, and so on may lead to misinterpretations, and pure analytical investigation of elements remains incomplete [108]. With this point of view, the proposed model considers the dynamics of postural sway as a black box that has an input of gravitational force, and the output is CoP_x time series. Still, further improvement of the model is possible, and the proposed stochastic differential equation is the first step of the deductive approach that can capture the aspects of mechanistic reasoning and control theory with further improvements. Even if a mechanical taste is absent in the stochastic differential equation written with the tools of stochastic dynamical system theory, the model has advantages in terms of mimicking the complex outputs, including the randomness of the sway [110]. While the complex outputs can be noted as search, exploration, and so on, any of those complex characteristics are trivial to associate with any particular neuromechanical element mentioned above, even if it is not impossible. There-

fore those features can be investigated by employing the proposed model involving a "wholistic approach". Yet it is better to keep in mind that, like any other model, the proposed form remains incomplete like any other model due to the nature of mathematical modeling; still, further improvements to the model are possible. As long as any biologically plausible, analytically consistent, and self-contained model provides opportunities for asking new questions, they are worth paying attention even if they are not complete.

An important characteristic of postural sway is its nature consisting of two superposed oscillations at different frequencies that are visually observed by Begbie first and later by Arnbald, as discussed before. Similar to other complex outputs, it is challenging to associate them with any of the neuromechanical elements [1]. Yet those two processes can be assessed with the proposed system of stochastic differential equations denoted as $(dX_t, d\theta_t)$ with a spatio-temporal perspective. Therefore the proposed model discusses physiological aspects of quiet stance including two levels [40], namely "conservative and operative levels" proposed by Gurfinkel [63], Feldman λ-threshold theory [5], Hogan's virtual trajectory [64], and rambling trembling decomposition of Zatsiorsky [2].

Firstly Gurfinkel constructs an experimental setup that induces superslow platform tilts to the subjects. In this way, due to imposed small velocities, even if the inherent reflex loops are not activated, higher levels are selectively addressed that are associated with the conservative level. Then it is shown that gravity vertical is not the absolute reference for orthograde posture, but the stabilization of equilibrium is maintained around a position prescribed by the second level that is slowly and continuously updated in time. In other words, Gurfinkel asserts that while the upper level is responsible for the determination of muscle activities, the lower level is responsible for providing stability around *it* corresponding to the equilibrium point. Yet those two levels, namely conservative and operative, are not associated with a single sensory input, but it is the complex output of "multiple sources", as mentioned by Gurfinkel himself [63]. While posture is following a set of dynamical points provided by conservative level rather than absolute gravitational vertical, Gurfinkel observes two superposed oscillations at different amplitudes and frequencies, and the one having a greater period and amplitude is associated with the conservative level of control

providing the equilibrium point at any instant. Following the idea in the proposed model, rather than the absolute equilibrium point located at zero for all the time, at any instant, θ_t represents the instant equilibrium point. Furthermore, the stability of either the absolute equilibrium point around zero or the instant equilibrium point around θ_t can be determined according to the signs of positive definite λ and κ system parameters, which are the eigenvalues of the proposed stochastic dynamical system, see Appendix D. This phenomenon is named "mean reversion" in the terminology of stochastic calculus.

Secondly, the proposed process reminds the Feldman equilibrium point theory, in which the trajectories are pulled toward θ_t at any instant. As explained before, the Feldman equilibrium point is the complex output of the nervous system due to the neural command to execute the voluntary motion. If the equilibrium point is to be kept constant (static equilibrium) in time, then the current equilibrium needs to be stabilized. Otherwise, when the body is forced to move, the current equilibrium point is destabilized to shift the body toward the desired direction, which is the generation of the movement explained from a dynamical perspective by Feldman [5]. While the former case, namely static equilibrium, is mimicked with the proposed system of stochastic differential equations, the latter one depending on the stability condition of the equilibrium point, has not been simulated yet with the current state of the mathematical model. The dynamic extension of the Feldman equilibrium point can be read from Hogan's article [64] as well. He defines the "virtual trajectory" from a Feldmanian perspective. Hogan employs the tools of the calculus of variations for the construction of the virtual trajectory, which is defined as the path that would be followed by the limb in the absence of damping, inertia, and any external forces [73]. Therefore the position of the limb can be considered as a sluggish response of the limb to the continuously updated virtual trajectory. Since the proposed λ is the ratio between stiffness and damping k/b with a Langevin sense, the absence of damping $b = 0$ is nothing but an infinite λ which sticks the process X_t onto θ_t, in the absence of inertial term $\ddot{X}_t = 0$ and $\sigma_1 = 0$ that vanishes the disturbance of X_t away from θ_t in any direction which is similar to the absence of external forces mentioned by Hogan. Therefore either in Feldman's or Hogan's perspective built onto Feldman's approach, the limb is kept closed around, i.e., pulled toward, a virtual trajectory de-

termined by higher levels of the central nervous system where the effector is a single muscle or multiple neuromuscular elements. Furthermore, Feldman asserts that the revealed kinematic information of the limb is with respect to the current equilibrium point specified by the brain in terms of a deviation from it rather than the absolute position [5]. In fact, the proposed model involves a lumped correction term $-\lambda(X_t-\theta_t)$ without underpinning the physiological mechanisms.

Thirdly, Zatsiorsky assesses two superposed oscillations with the rambling and trembling decomposition method [1], [2] that is the most relevant understanding to compare with the proposed stochastic differential equations where rambling and trembling are linked to θ_t and $X_t - \theta_t$ respectively. In the scheme provided by Zatsiorsky, the rambling trajectory is determined by the application of cubic splines to the CoP time series for smoothening, later used for detrending the CoP signal to extract the trembling trajectory. Even if the employment of cubic splines requires a set of points where rambling and CoP intersect, which is experimentally determined by the instants that the horizontal force equilibrium is satisfied, the proposed model can not argue it as long as it does not involve a mechanical taste and is completely independent of mechanistic reasons causing the sway. Still, both approaches involve two superposed oscillations that are consistent in terms of respective time scales (frequencies) and variances, where rambling has a variance almost three times greater than trembling trajectory [2]. Furthermore, the differentiation of time scales is possible with the time constants of $e^{-\lambda t}$ and $e^{-\kappa t}$ forming the double exponential relation in the correlation function as shown in Equation 3.16. At the desired range of parameters $\lambda >> \kappa$, almost one to eight, [53], [29] either the ratio of variances or the exponential decay rates of respective correlations become visible by the utilization of stochastic analysis.

Another issue related to the frequency content of either process is the smoothness that is worth attention. Although the smoothness of rambling is referred in the second chapter, it is crucial to recall that the rambling trajectory is much smoother than both the trembling and CoP, according to Zatsiorsky. On the other hand, the proposed process θ_t has more jitters than X_t that represents CoP_x. While Zatsiorsky calls smoothening of CoP as rambling, exponential smoothening of θ_t is called CoP in the aforementioned stochastic model. Even if it is possible to make θ_t smoother via

using a band-limited White noise W_t^2, then the dissertation would lose the capability of explicitly showing the relation between the two time constants κ, λ and jittering shown in Equation 3.16. In the proposed model, the slower decay in correlation function and power spectrum is associated with κ, while the faster frequencies are dictated by λ. Therefore θ_t dynamics govern the long-term behavior of X_t resembling equilibrium point rambling in CoP_x. Also, faster frequencies in CoP_x (named as tremble by Zatsiorsky) were simulated by λ in the model.

A further implication of rambling trembling decomposition can be seen from Figure 2.4 and Figure 2.3 where multiple stable equilibrium points of rambling are observed as opposed to a definite unipolar appearance of trembling. The unipolar structure of trembling can be associated with the term $-\lambda(X_t - \theta_t)$, linear mean reversion. Similarly, CoP definitely has at least two stable points that are also stressed out and experimentally validated by Lee [70]. As long as the understanding is probabilistic through the model, the number of stable points manifest themselves as multimodality rather than Gaussian unimodality. While trembling has one pole that is linked to $-\lambda(X_t - \theta_t)$, the multipolar structure is imposed to the stochastic differential equation in Equation 3.21 using a third order polynomial $r\theta_t - \theta_t^3$ that has two symmetric stable points and modes at $\pm\sqrt{r}$ together with an unstable fixed point at zero which corresponds to the local minimum of the probability density function, see Figure 3.8. As long as the roots are located symmetrically at $\pm\sqrt{r}$, the model does not consider the back-and-forth asymmetry seen in postural sway. Therefore rambling trembling decomposition and the proposed model (X_t, θ_t) are neither similar to a pendular motion around a fixed point nor a free drift inside the margins of stability, as explained before in the second chapter. Because the inverted pendulum motion consists of at least one unstable equilibrium point similar to the model involving third-order polynomial [24], Zatsiorsky's rambling trembling decomposition and the proposed stochastic model coincide, although they involve multiple equilibrium points, which are all stable.

In the posture literature, the closest understanding to the proposed model can be seen in the study of Dijkstra, which depends on the following differential equation [111].

$$\ddot{x} + \alpha_x \dot{x} + \omega_0^2 (x - u) + \sqrt{Q_x}\xi_t = c_x(\dot{s} - \dot{x}) \tag{4.1}$$

$$\dot{u} + \alpha_u u + \sqrt{Q_u}\xi_t = c_u(s - u) \tag{4.2}$$

The equation introduced by Dijkstra can easily be compared with the proposed stochastic differential equation. Besides that, the provided relation is in Langevin form, the differentiation of both sides of the proposed stochastic differential equation yields a similar form. At a first glance, $\sqrt{Q_x}$ and $\sqrt{Q_u}$ scales the variances of white noise as σ_1 and σ_2 does to $\frac{dW_t^1}{dt}$ and $\frac{dW_t^2}{dt}$ respectively. Dijkstra uses a single Wiener process for either x and u although the proposed model involves two distinct Wiener processes W_t^1 and W_t^2 that are related with $\langle W_t^1 W_t^2 \rangle = \rho t$. If $\rho = 1$ is selected, two Wiener process becomes the same, and the proposed relation reduces to Dijkstra's relation. However, in the proposed model, the effects of ρ were not discussed even if the solution is provided in the Appendix E, but it is selected as $\rho = 0$, which implies that W_t^1 is independent of W_t^2.

The second distinction is the existence of a second order time derivative of X_t that is denoted by $\ddot{x}$ in Dijkstra's equation, pointing to the mass effect. This makes the solution of the stochastic differential equation possible to oscillate rather than an exponential decay only. Two models can be compared with Akaike Information criteria [112], [113], which quantifies how well data is explained by the addition of the new term. In this particular case, Akaike Information criteria can be employed to see whether consideration of the mass effect contributes to expressing the model from a much more entropic point of view. The last distinction is the existence of nonhomogenous part denoted by $c_x(\dot{s} - \dot{x})$ and $c_u(s - u)$ written at the right hand side of Dijkstra's equation that is missing in the proposed model. Since Dijkstra investigates the postural sway under the existence of moving visual scene and somatosensory input, the effects are imposed to the relation with those additional terms where x and u are coupled to the input in terms of velocity and position, respectively. On the other hand, quiet stance does not involve a varying visual scene, so those terms have to be selected zero for our particular case where the dynamics are driven by the noise. Similarly, Dijkstra explains $c_x = c_u = 0$ as the case where the input is absent, i.e., eyes are closed. Besides the distinctions, α_x, and α_u are akin to λ, and κ, respectively.

Another point that is asserted by Dijkstra that is also captured with the proposed stochastic differential equation is the existence of two distinct time scales. Those time scales can be seen from the covariance function $\langle X_t X_s \rangle$ in Equation 3.16 that has a double exponential form. While λ that is greater than κ determines the behavior at higher frequencies, κ rules the behavior at longer periods, as discussed in the first paragraph of this section. Besides, this behavior is apparent in Figures 3.5, 3.6 and 3.7 provided in Chapter 3, Collins [29] associates those two time scales with persistence and anti-persistance dynamical characteristics of open-loop and closed-loop control, respectively. Two distinct processes are further scaled by their own σ_i ("average activity of stochastic process") and are employed for the evaluation of the power carried by open loop and closed loop control mechanisms referring to multiscale fractional Brownian motion [114], [115].

Before going further, it is better to stress that Gurfinkel's operative and conservative levels, Feldman's equilibrium point with Hogan's virtual trajectory, Zatsiosky's rambling trembling decomposition, and the proposed stochastic differential equations are all similar in spirit involving *"dualities"* even though the neuromechanical sources and the reasons of the everlasting postural oscillations are different.

4.3 Concluding Remarks

Throughout the thesis, a stochastic differential equation representing the dynamics of postural sway in terms of its complex output CoP_x is defined step by step with physiological reasoning. In the beginning, the zeroth step was somehow trivial as it corresponds to a zeroth order differential equation which does not allow the "accumulation of surprise", so the necessity of at least a first-order differential equation is stressed. Still, the Gaussian distribution of velocities is visually validated with Q-Q plots later used for decision makings, i.e., displacements, represented with driving noise dW_t. Therefore in the first step, σdW_t is integrated, yet it is then seen that the variance of the process increased unboundedly in time due to the absence of proper constraint. Since it is impossible for CoP_x to diffuse unboundedly, the simplest constraint, linear mean reversion, is imposed, which ends up with the Ornstein Uhlenbeck process, which is also called the Langevin equation. By considering neurophysiological motor

control mechanisms, in the following step, the system of stochastic differential equations denoted by $(dX_t, d\theta_t)$ are defined. The new set of differential equations differs from the Ornstein Uhlenbeck process proposed at the former step in terms of fluctuations around θ_t trajectory rather than oscillating around the baseline at 0. From the proposed form, thanks to the availability of the analytical solution, the variance $\langle X_t^2 \rangle$ and the covariance functions $\langle X_t X_s \rangle$ are employed for further analysis. Besides the increase of variance due to the additional fluctuations of θ_t, the covariance function revealed two distinct time scales related to the time constants of the two exponentials, κ and λ. In the desired range of parameters $\lambda \approx 8\kappa$, while fast decay is associated with λ determining the behavior at smaller periods, κ is responsible for the power at larger periods as X_t decays to θ_t faster than the rambling of θ_t. θ_t has greater power at high frequencies due to the employment of the Wiener process dW_t^2 that carries infinite energy and infinite variation because of the power at greater frequencies. Even though the employment of the Wiener process is physically implausible, band-limited noise was not used for smoothing the θ_t trajectory for analytical reasoning. On the other hand, in the last step, a cubic nonlinearity is imposed on θ_t to asses the multimodal appearance of CoP_x, which is derived from the normally distributed velocities that were visually validated by Q-Q plots.

Lastly, the answer to the question *"What is the dice ruling the sway?"* was explored through the proposed model with a spatio-temporal perspective involving Markovnian randomness at every integration step constrained by an elastic element. The elastic constraint imposed determinism in time to the particular path of the sway while throwing the dice at every displacement of the path imposed spatial variation to the ensemble of many paths of never lasting postural sway. While the former element points to the fate of a particle, the latter refers to the determinism in the probability distribution, estimated by $\langle X_t X_u \rangle$ and $\langle X_t^2 \rangle$, respectively.

REFERENCES

[1] V. M. Zatsiorsky and M. Duarte, "Instant equilibrium point and its migration in standing tasks: rambling and trembling components of the stabilogram," *Motor control*, vol. 3, no. 1, pp. 28–38, 1999.

[2] V. M. Zatsiorsky and M. Duarte, "Rambling and trembling in quiet standing," *Motor control*, vol. 4, no. 2, pp. 185–200, 2000.

[3] L. Mochizuki, M. Duarte, A. C. Amadio, V. M. Zatsiorsky, and M. L. Latash, "Changes in postural sway and its fractions in conditions of postural instability," *Journal of applied biomechanics*, vol. 22, no. 1, pp. 51–60, 2006.

[4] A. Danna-Dos-Santos, A. M. Degani, V. M. Zatsiorsky, and M. L. Latash, "Is voluntary control of natural postural sway possible?," *Journal of motor behavior*, vol. 40, no. 3, pp. 179–185, 2008.

[5] A. G. Feldman, "Space and time in the context of equilibrium-point theory," *Wiley Interdisciplinary Reviews: Cognitive Science*, vol. 2, no. 3, pp. 287–304, 2011.

[6] D. A. Winter, A. E. Patla, S. Rietdyk, and M. G. Ishac, "Ankle muscle stiffness in the control of balance during quiet standing," *Journal of neurophysiology*, vol. 85, no. 6, pp. 2630–2633, 2001.

[7] F. Engels, *Dialectics of nature*. Wellred Books, 1960.

[8] C. Darwin, *The origin of species*. PF Collier & son New York, 1909.

[9] J. M. Winters and P. E. Crago, *Biomechanics and neural control of posture and movement*. Springer Science & Business Media, 2012.

[10] R. Descartes, "A discourse of a method for the well guiding of reason and the discovery of truth in the sciences, 1649," 1966.

[11] F. E. Zajac and J. M. Winters, "Modeling musculoskeletal movement systems: joint and body segmental dynamics, musculoskeletal actuation, and neuromuscular control," in *Multiple muscle systems*, pp. 121–148, Springer, 1990.

[12] J. M. Winters, "Terminology and foundations of movement science," in *Biomechanics and neural control of posture and movement*, pp. 3–35, Springer, 2000.

[13] G. G. Simoneau, J. S. Ulbrecht, J. A. Derr, M. B. Becker, and P. R. Cavanagh, "Postural instability in patients with diabetic sensory neuropathy," *Diabetes care*, vol. 17, no. 12, pp. 1411–1421, 1994.

[14] P. F. Meyer, L. I. Oddsson, and C. J. De Luca, "The role of plantar cutaneous sensation in unperturbed stance," *Experimental brain research*, vol. 156, no. 4, pp. 505–512, 2004.

[15] B. Keim, "The marvelous physics of swarming midges," Oct 2021.

[16] L. Boltzmann, *Theoretical physics and philosophical problems: selected writings*, vol. 5. Springer Science & Business Media, 2012.

[17] A. Einstein, "Does the inertia of a body depend upon its energy-content," *Annalen der Physik*, vol. 18, no. 13, pp. 639–641, 1905.

[18] L. Bachelier, "Théorie de la spéculation," in *Annales scientifiques de l'École normale supérieure*, vol. 17, pp. 21–86, 1900.

[19] S. H. Strogatz, *Nonlinear dynamics and chaos: with applications to physics, biology, chemistry, and engineering*. CRC press, 2018.

[20] C. E. Shannon, *The Mathematical Theory of Communication by CE Shannon and W. Weaver*. 1949.

[21] J. P. Keener, *Biology in Time and Space: A Partial Differential Equation Modeling Approach*, vol. 50. American Mathematical Soc., 2021.

[22] J.-P. Eckmann and D. Ruelle, "Ergodic theory of chaos and strange attractors," *The theory of chaotic attractors*, pp. 273–312, 1985.

[23] S. Strogatz, *Infinite powers: how calculus reveals the secrets of the universe*. Eamon Dolan Books, 2019.

[24] S. Gürses, *Postural dynamics and stability*. PhD thesis, Middle East Technical University, 2002.

[25] S. Gürses, N. Akkaş, and B. Platin, "Ters dönmüş bir sarkacın doğrusal olmayan konum denetiminden en büyük lyapunov üstelinin poincare kesitinden elde edilmesi," 2006.

[26] S. Gurses and H. Celik, "Correlation dimension estimates of human postural sway," *Human movement science*, vol. 32, no. 1, pp. 48–64, 2013.

[27] S. Gurses, B. Platin, S. Tumer, and N. Akkas, "Characteristic phase plane pattern of human postural sway," *IFAC Proceedings Volumes*, vol. 39, no. 18, pp. 225–230, 2006.

[28] N. Wiener, *Cybernetics or Control and Communication in the Animal and the Machine*. MIT press, 2019.

[29] J. J. Collins and C. J. De Luca, "Open-loop and closed-loop control of posture: a random-walk analysis of center-of-pressure trajectories," *Experimental brain research*, vol. 95, no. 2, pp. 308–318, 1993.

[30] J. G. Milton, T. Ohira, J. L. Cabrera, R. M. Fraiser, J. B. Gyorffy, F. K. Ruiz, M. A. Strauss, E. C. Balch, P. J. Marin, and J. L. Alexander, "Balancing with vibration: a prelude for "drift and act" balance control," *PLoS One*, vol. 4, no. 10, p. e7427, 2009.

[31] A. Bottaro, M. Casadio, P. G. Morasso, and V. Sanguineti, "Body sway during quiet standing: is it the residual chattering of an intermittent stabilization process?," *Human movement science*, vol. 24, no. 4, pp. 588–615, 2005.

[32] A. Rosenblueth, N. Wiener, and J. Bigelow, "Behavior, purpose and teleology," *Philosophy of Science*, vol. 10, no. 1, pp. 18–24, 1943.

[33] D. J. Herzfeld and R. Shadmehr, "Motor variability is not noise, but grist for the learning mill," *Nature neuroscience*, vol. 17, no. 2, pp. 149–150, 2014.

[34] P. Tankov, *Financial modelling with jump processes*. Chapman and Hall/CRC, 2003.

[35] A. E. Kyprianou, *Introductory lectures on fluctuations of Lévy processes with applications*. Springer Science & Business Media, 2006.

[36] D. Wolpert, "The man with the golden brain," Dec 2011.

[37] E. R. Kandel, J. H. Schwartz, T. M. Jessell, S. Siegelbaum, A. J. Hudspeth, S. Mack, *et al.*, *Principles of neural science*, vol. 4. McGraw-hill New York, 2000.

[38] C. M. Harris and D. M. Wolpert, "Signal-dependent noise determines motor planning," *Nature*, vol. 394, no. 6695, pp. 780–784, 1998.

[39] Y. Ivanenko and V. S. Gurfinkel, "Human postural control," *Frontiers in neuroscience*, vol. 12, p. 171, 2018.

[40] J. Massion, "Postural control systems in developmental perspective," *Neuroscience & Biobehavioral Reviews*, vol. 22, no. 4, pp. 465–472, 1998.

[41] A. Berthoz, *The brain's sense of movement*, vol. 10. Harvard University Press, 2000.

[42] E. Pourreza, *Screening Infant's Developmental Aspects of Learning During Standing by Measuring Pressure Distribution Beneath the Feet*. PhD thesis, Middle East Technical University, 2022.

[43] J. Barela, J. J. Jeka, and J. E. Clark, "The use of somatosensory information during the acquisition of independent upright stance," *Infant Behavior and Development*, vol. 22, no. 1, pp. 87–102, 1999.

[44] H. G. Wu, Y. R. Miyamoto, L. N. G. Castro, B. P. Ölveczky, and M. A. Smith, "Temporal structure of motor variability is dynamically regulated and predicts motor learning ability," *Nature neuroscience*, vol. 17, no. 2, pp. 312–321, 2014.

[45] F. Lestienne and V. Gurfinkel, "Posture as an organizational structure based on a dual process: a formal basis to interpret changes of posture in weightlessness," *Progress in brain research*, vol. 76, pp. 307–313, 1988.

[46] J. P. Scholz and G. Schöner, "The uncontrolled manifold concept: identifying control variables for a functional task," *Experimental brain research*, vol. 126, no. 3, pp. 289–306, 1999.

[47] P. S. Archambault, P. Mihaltchev, M. F. Levin, and A. G. Feldman, "Basic elements of arm postural control analyzed by unloading," *Experimental brain research*, vol. 164, no. 2, pp. 225–241, 2005.

[48] M. L. Latash, "Motor synergies and the equilibrium-point hypothesis," *Motor control*, vol. 14, no. 3, pp. 294–322, 2010.

[49] M. L. Latash, V. Krishnamoorthy, J. P. Scholz, and V. M. Zatsiorsky, "Postural synergies and their development," *Neural plasticity*, vol. 12, no. 2-3, pp. 119–130, 2005.

[50] M. L. Latash, J. P. Scholz, and G. Schöner, "Toward a new theory of motor synergies," *Motor control*, vol. 11, no. 3, pp. 276–308, 2007.

[51] E. B. Thorp, K. P. Kording, and F. A. Mussa-Ivaldi, "Using noise to shape motor learning," *Journal of Neurophysiology*, vol. 117, no. 2, pp. 728–737, 2017.

[52] S. M. Slobounov, E. S. Slobounova, and K. M. Newell, "Virtual time-to-collision and human postural control," *Journal of motor Behavior*, vol. 29, no. 3, pp. 263–281, 1997.

[53] T. Kiemel, K. S. Oie, and J. J. Jeka, "Slow dynamics of postural sway are in the feedback loop," *Journal of neurophysiology*, vol. 95, no. 3, pp. 1410–1418, 2006.

[54] T. Mergner, "The matryoshka dolls principle in human dynamic behavior in space: a theory of linked references for multisensory perception and control of action," *Cahiers de psychologie cognitive*, vol. 21, no. 2-3, pp. 129–212, 2002.

[55] T. Mergner, C. Maurer, and R. J. Peterka, "Sensory contributions to the control of stance," in *Sensorimotor control of movement and posture*, pp. 147–152, Springer, 2002.

[56] M. Kawato, "Internal models for motor control and trajectory planning," *Current opinion in neurobiology*, vol. 9, no. 6, pp. 718–727, 1999.

[57] D. Engelhart, J. H. Pasma, A. C. Schouten, C. G. Meskers, A. B. Maier, T. Mergner, and H. van der Kooij, "Impaired standing balance in elderly: a

new engineering method helps to unravel causes and effects," *Journal of the American Medical Directors Association*, vol. 15, no. 3, pp. 227–e1, 2014.

[58] K. P. Körding and D. M. Wolpert, "Bayesian integration in sensorimotor learning," *Nature*, vol. 427, no. 6971, pp. 244–247, 2004.

[59] D. M. Wolpert and J. R. Flanagan, "Motor prediction," *Current biology*, vol. 11, no. 18, pp. R729–R732, 2001.

[60] D. M. Wolpert, "Probabilistic models in human sensorimotor control," *Human movement science*, vol. 26, no. 4, pp. 511–524, 2007.

[61] E. Akcay, *The Somatosensory and Vestibular Interaction in Human Postural Control*. PhD thesis, Middle East Technical University, 2015.

[62] M. Imir, *Postural Responses of Patients with Bilateral Vestibular Loss and Healthy Subjects to Sinusoidal Tilts*. PhD thesis, Middle East Technical University, 2017.

[63] V. Gurfinkel, Y. P. Ivanenko, Y. S. Levik, and I. Babakova, "Kinesthetic reference for human orthograde posture," *Neuroscience*, vol. 68, no. 1, pp. 229–243, 1995.

[64] N. Hogan, "An organizing principle for a class of voluntary movements," *Journal of neuroscience*, vol. 4, no. 11, pp. 2745–2754, 1984.

[65] M. Duarte, S. Freitas, and V. Zatsiorsky, "Control of equilibrium in humans—sway over sway," *Motor Control, Oxford University Press, Oxford*, pp. 219–242, 2011.

[66] A. G. Feldman, V. Goussev, A. Sangole, and M. F. Levin, "Threshold position control and the principle of minimal interaction in motor actions," *Progress in brain research*, vol. 165, pp. 267–281, 2007.

[67] I. D. Loram, H. Gollee, M. Lakie, and P. J. Gawthrop, "Human control of an inverted pendulum: is continuous control necessary? is intermittent control effective? is intermittent control physiological?," *The Journal of physiology*, vol. 589, no. 2, pp. 307–324, 2011.

[68] T. Mergner, C. Maurer, and R. Peterka, "A multisensory posture control model of human upright stance," *Progress in brain research*, vol. 142, pp. 189–201, 2003.

[69] A. Bottaro, Y. Yasutake, T. Nomura, M. Casadio, and P. Morasso, "Bounded stability of the quiet standing posture: an intermittent control model," *Human movement science*, vol. 27, no. 3, pp. 473–495, 2008.

[70] I.-C. Lee, M. M. Pacheco, and K. M. Newell, "A test of fixed and moving reference point control in posture," *Gait & Posture*, vol. 51, pp. 52–57, 2017.

[71] N. Sarabon, A. Panjan, and M. Latash, "The effects of aging on the rambling and trembling components of postural sway: Effects of motor and sensory challenges," *Gait & posture*, vol. 38, no. 4, pp. 637–642, 2013.

[72] A. Feldman, "Superposition of motor programs—i. rhythmic forearm movements in man," *Neuroscience*, vol. 5, no. 1, pp. 81–90, 1980.

[73] M. L. Latash, "Control of human movement," *Human Kinetics*, 1993.

[74] J. McIntyre, F. Mussa-Ivaldi, and E. Bizzi, "The control of stable postures in the multijoint arm," *Experimental brain research*, vol. 110, no. 2, pp. 248–264, 1996.

[75] V. M. Zatsiorsky and V. M. Zaciorskij, *Kinetics of human motion*. Human kinetics, 2002.

[76] J.-F. Pilon and A. G. Feldman, "Threshold control of motor actions prevents destabilizing effects of proprioceptive delays," *Experimental brain research*, vol. 174, no. 2, pp. 229–239, 2006.

[77] E. Bizzi, N. Accornero, W. Chapple, and N. Hogan, "Posture control and trajectory formation during arm movement," *Journal of Neuroscience*, vol. 4, no. 11, pp. 2738–2744, 1984.

[78] M. Katayama and M. Kawato, "Virtual trajectory and stiffness ellipse during multijoint arm movement predicted by neural inverse models," *Biological cybernetics*, vol. 69, no. 5, pp. 353–362, 1993.

[79] T. Flash and N. Hogan, "The coordination of arm movements: an experimentally confirmed mathematical model," *Journal of neuroscience*, vol. 5, no. 7, pp. 1688–1703, 1985.

[80] H. Mittelstaedt, "A new solution to the problem of the subjective vertical," *Naturwissenschaften*, vol. 70, no. 6, pp. 272–281, 1983.

[81] H. Mittelstaedt, "Evidence of somatic graviception from new and classical investigations," *Acta Oto-Laryngologica*, vol. 115, no. sup520, pp. 186–187, 1995.

[82] D. A. Winter, F. Prince, J. S. Frank, C. Powell, and K. F. Zabjek, "Unified theory regarding a/p and m/l balance in quiet stance," *Journal of neurophysiology*, vol. 75, no. 6, pp. 2334–2343, 1996.

[83] A. Kahveci, B. C. Cengiz, V. Alcan, M. Zinnuroğlu, and S. Gürses, "Identification of control strategies in diabetic neuropathic patients versus healthiest through kinematic trajectories," in *Orthopaedic Proceedings*, vol. 102, pp. 80–80, The British Editorial Society of Bone & Joint Surgery, 2020.

[84] O. Alkan, *Statistical Analysis of Force Distribution on the Plantar Foot During Quiet Stance*. PhD thesis, Middle East Technical University, 2015.

[85] G. G. Simoneau, J. S. Ulbrecht, J. A. Derr, and P. R. Cavanagh, "Role of somatosensory input in the control of human posture," *Gait & posture*, vol. 3, no. 3, pp. 115–122, 1995.

[86] J. Hicks, "The mechanics of the foot: I. the joints," *Journal of anatomy*, vol. 87, no. Pt 4, p. 345, 1953.

[87] J. Hicks, "The mechanics of the foot: Ii. the plantar aponeurosis and the arch," *Journal of anatomy*, vol. 88, no. Pt 1, p. 25, 1954.

[88] D. A. Winter, A. Patla, and F. Prince, "Stiffness control of balance during quiet standing," *Gait & Posture*, vol. 2, no. 5, pp. 154–155, 1997.

[89] D. L. King and V. M. Zatsiorsky, "Extracting gravity line displacement from stabilographic recordings," *Gait & Posture*, vol. 6, no. 1, pp. 27–38, 1997.

[90] V. M. Zatsiorsky and D. L. King, "An algorithm for determining gravity line location from posturographic recordings," *Journal of biomechanics*, vol. 31, no. 2, pp. 161–164, 1997.

[91] A. Nicolaï, M. Limnios, A. Trouvé, and J. Audiffren, "A langevin-based model with moving posturographic target to quantify postural control," *IEEE Transactions on Neural Systems and Rehabilitation Engineering*, vol. 29, pp. 478–487, 2021.

[92] M. Mangalam and D. G. Kelty-Stephen, "Hypothetical control of postural sway," *Journal of the Royal Society Interface*, vol. 18, no. 176, p. 20200951, 2021.

[93] N. N. Taleb, "Statistical consequences of fat tails: Real world preasymptotics, epistemology, and applications," *arXiv preprint arXiv:2001.10488*, 2020.

[94] Peyam, "Stieltjes integral," Mar 2018.

[95] S. E. Shreve *et al.*, *Stochastic calculus for finance II: Continuous-time models*, vol. 11. Springer, 2004.

[96] B. B. Mandelbrot and J. W. Van Ness, "Fractional brownian motions, fractional noises and applications," *SIAM review*, vol. 10, no. 4, pp. 422–437, 1968.

[97] F. D. Rouah, *The heston model and its extensions in VBA*. John Wiley & Sons, 2015.

[98] N. N. Taleb, *Fooled by randomness: The hidden role of chance in life and in the markets*, vol. 1. Random House Trade Paperbacks, 2005.

[99] R. Phillips, J. Kondev, J. Theriot, H. G. Garcia, and N. Orme, *Physical biology of the cell*. Garland Science, 2012.

[100] M. Grigoriu, *Stochastic calculus: applications in science and engineering*. Springer, 2002.

[101] P. O. McKeon and J. Hertel, "Diminished plantar cutaneous sensation and postural control," *Perceptual and motor skills*, vol. 104, no. 1, pp. 56–66, 2007.

[102] R. J. Peterka, "Sensorimotor integration in human postural control," *Journal of neurophysiology*, vol. 88, no. 3, pp. 1097–1118, 2002.

[103] I.-C. Lee, M. M. Pacheco, and K. M. Newell, "The precision demands of viewing distance modulate postural coordination and control," *Human Movement Science*, vol. 66, pp. 425–439, 2019.

[104] J. Keener and J. Sneyd, *Mathematical physiology: II: Systems physiology*. Springer, 2009.

[105] A. V. Hill, *First and last experiments in muscle mechanics*. CUP Archive, 1970.

[106] T. L. Hill, *Free energy transduction and biochemical cycle kinetics*. Courier Corporation, 2013.

[107] G. I. Zahalak, J. Winters, and S. Woo, "Multiple muscle systems: Biomechanics and movement organisation," 1990.

[108] T. MERGNER and W. Becker, "A modeling approach to the human spatial orientation system," *Annals of the New York Academy of Sciences*, vol. 1004, no. 1, pp. 303–315, 2003.

[109] C. Maurer and R. J. Peterka, "A new interpretation of spontaneous sway measures based on a simple model of human postural control," *Journal of neurophysiology*, vol. 93, no. 1, pp. 189–200, 2005.

[110] G. E. Riccio, "Information in movement variability about the qualitative dynamics of posture and orientation," *Variability and motor control*, pp. 317–357, 1993.

[111] T. M. Dijkstra, "A gentle introduction to the dynamic set-point model of human postural control during perturbed stance," *Human Movement Science*, vol. 19, no. 4, pp. 567–595, 2000.

[112] J. Gareth, W. Daniela, H. Trevor, and T. Robert, *An introduction to statistical learning: with applications in R*. Spinger, 2013.

[113] G. H. Givens and J. A. Hoeting, *Computational statistics*, vol. 703. John Wiley & Sons, 2012.

[114] F. Molz, H. Liu, and J. Szulga, "Fractional brownian motion and fractional gaussian noise in subsurface hydrology: A review, presentation of fundamental properties, and extensions," *Water Resources Research*, vol. 33, no. 10, pp. 2273–2286, 1997.

[115] J.-M. Bardet and P. Bertrand, "Identification of the multiscale fractional brownian motion with biomechanical applications," *Journal of Time Series Analysis*, vol. 28, no. 1, pp. 1–52, 2007.

[116] R. Shadmehr and M. A. Arbib, "A mathematical analysis of the force-stiffness characteristics of muscles in control of a single joint system," *Biological cybernetics*, vol. 66, no. 6, pp. 463–477, 1992.

[117] T. Shimba, "An estimation of center of gravity from force platform data," *Journal of biomechanics*, vol. 17, no. 1, pp. 53–60, 1984.

Appendix A

Q-Q PLOTS

A.1 Q-Qplots

Q-Q plots are used to show whether the sampled data is distributed normal or not by visual inspection. Q-Q plots are obtained by plotting quartiles of data with respect to the quartiles of Gaussian distribution derived from its probability distribution function. In other words, it is not a quantitative summary statistic that makes one able to compare the normality with further statistical tests, but the associated statistical method is called the "Kolmogorov Smirnoff test". For a deeper understanding of Q-Q plots, four data sets are generated from $uniform(0,1)$, $\mathcal{N}(0,1)$, $\mathcal{N}(1,2)$ and exponential with $\lambda = 1$ (s.t. $p(x) = \lambda e^{-\lambda x}$) are provided below.

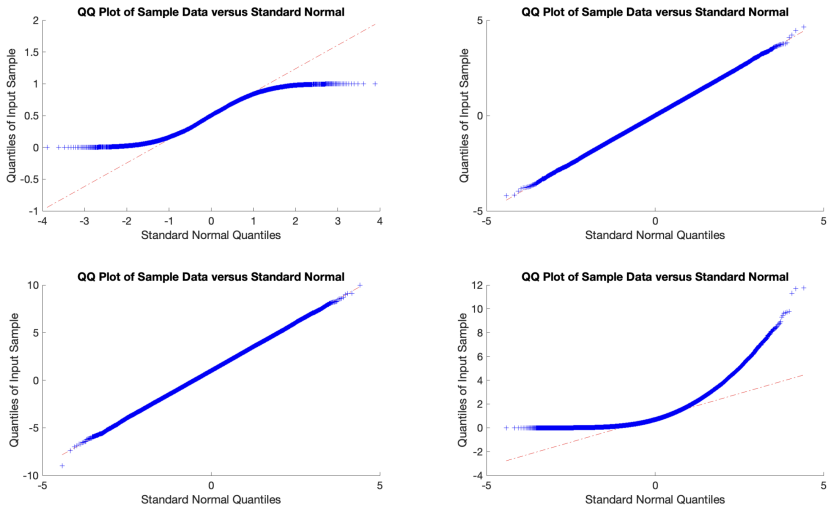

Figure A.1: Q-Q plots of Data Generated from Different Distributions
Top Left: Uniform(0,1), Top Right: N(0,1), Bottom Left: N(1,2), Bottom Right: Exp(1)

While the plot in the upper left corner shows the Q-Q plot of uniform distribution, it is a sigmoid that coincides with the cumulative distribution of Gaussian distribution. The ones at the top right and bottom left are the plots of random numbers sampled from normal distribution with different means and variances, so each appeared linear as the quartiles of data matched with the normal distribution. Still, the behavior at the tails is not good enough due to an insufficient sample size that is selected to be 100.000. Finally, the bottom right figure shows the Q-Q plot of exponentially distributed sampled data, and it has no linear appearance.

Besides that, checking the normality of data is essential for modeling since the deviations from normality may end up with significant misinterpretation of the data.

A.2 White Noise

Throughout the dissertation, white noise takes Gaussian distributed values in discrete times with specified mean and variance. In the scope of the thesis, the mean is selected to be zero in the absence of bias, and the unit standard deviation is scaled with a constant $\sigma > 0$. Therefore the histogram of white noise appears to be distributed normal, and it looks linear in the Q-Q plot. A sample path generated with Matlab is provided below for the visualization of the white noise process.

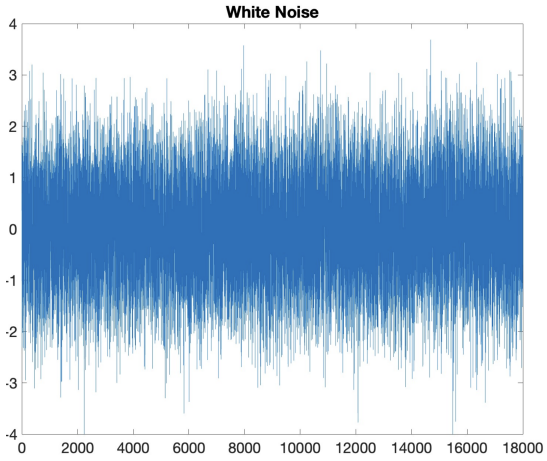

Figure A.2: A Sample Path of White Noise

One of the most critical aspects of white noise is that it has constant power among all frequencies by definition. In other words, the power spectrum in the Fourier domain

does not decay at greater frequencies which is directly proportional to the square of frequency according to $E = \frac{1}{2}I\omega^2$ where I is the moment of inertia. Therefore one can say that white noise carries equal and finite power at all frequencies, and it is physically not plausible as it requires an infinite amount of energy. The same presents itself in the Wiener process W_t, too, as it has infinite variation in any finite time interval according to $\lim_{\Delta t \to 0} \frac{\Delta t}{\sqrt{\Delta t}} \to \infty$, which necessitates an infinite amount of energy.

Appendix B

INVERTED PENDULUM

Since the rambling trembling analysis heavily depends on the instant equilibrium of horizontal forces $\sum F_{hor} = 0$ [90], [1], [2], [75], [89], the models proposed by Winter [88], [6], together with the thought experiment about holding a pen at the tip of the finger, are related to classical mechanics, it is inevitable to use a mathematical model involving an inverted pendulum which covers the issue. Also, by using a single inverted pendulum, one may understand the control of the posture easier with keeping the plant as simple as possible. In this way, the attention can be focused on the other aspects of the control scheme involving sensors, actuators, etc. Besides those, the discussion throughout the dissertation can be improved to have a mechanical taste since the thesis only considers the stochastic characteristics of the dynamical output of the complex system without mentioning control theory and classical mechanics. Therefore, the further understanding of the control of the pendulum has a central position for future work. After that, like any other mechanical problem, the first step is drawing the free body diagram by separating it into two as the foot and the body represented by a single inverted pendulum with a mass m at the tip of the pendulum with length l. Furthermore, the angular displacement from the absolute verticle is defined as θ, and the control torque at the ankle joint is denoted as T_a as shown in Figure B.1.

The first thing to notice in the free body diagram is that the discussion is restricted to the anteroposterior direction, back-and-forth, which is inherently unstable. In this plane, the sagittal plane, the inverted pendulum is an open kinematic chain. However, in the mediolateral direction, frontal plane, the structure is a closed kinematic chain, a four-bar linkage, which is stable. Yet the discussion is restricted to R^1 in forth-and-back for the sake of simplicity, so only CoP_x and CoM_x are going to be analyzed.

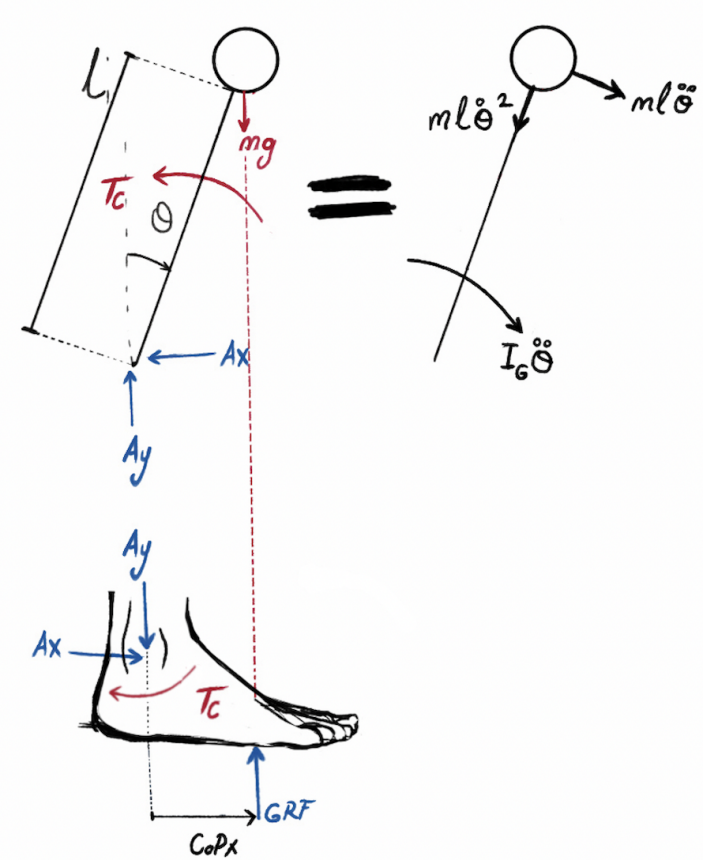

Figure B.1: Free Body Diagram

According to the provided inverted pendulum, the mass oscillates around an unstable fixed point at $\theta = 0$ without leaving the confined area spanned by the foot comparatively small to the height of the center of mass elevated almost one meter from the ground. While even an infinitesimal deviation from $\theta = 0$ induces further acceleration in either direction, on the contrary, the torque generated by the muscles around the ankle joint, T_c in the opposite direction, keeps the θ at moderate values close to zero. By keeping in mind that CoM_x spans one or two centimeters in anteroposterior directions, one can see that θ is on the order of one degree such that $sin\theta = x/l$ which makes the local linearization (small angle approximation) of $sin\theta \approx \theta$ possible. By considering the inverted pendulum provided in Figure B.1 and the control torque T_c defined, one can write down the following relation according to the moment around the ankle joint.

$$-T_c + mglsin\theta = \left(I_G + ml^2\right)\ddot{\theta} \tag{B.1}$$

While the control torque T_c and the torque induced by gravity due to weight mg with a moment arm $lsin\theta$ is presented on the left-hand side of the equation, the right-hand side involves the angular acceleration multiplied with the superposition of moment of inertia and additional rotation with respect to the ankle joint according to the *"parallel axis theorem"*. As I_G represents the moment of inertia of distributed mass m, the additional term ml^2 represents the effect of rotation around the ankle joint, so that $I_a := I_G + ml^2$ can be defined around the ankle joint. Then the next step is the supposition of a proper form for control torque T_c around the ankle joint. In this respect, one of the most straightforward supposition is $T_c = k_t\theta + b_t\dot{\theta}$, involving two terms that consider torsional spring to keep the θ at relatively small values around zero, together with a parallel connected torsional damper representing the actuator viscosity spanning the joint. By substituting the supposed relatively simple T_c, one can find the following relation governing the temporal evolution of sway (equation of motion) in terms of angular displacement θ.

$$-k_t\theta - b_t\dot{\theta} + mglsin\theta = \left(I_G + ml^2\right)\ddot{\theta} \tag{B.2}$$

It is already mentioned that θ is not only bounded by the area spanned by foot, but it takes relatively small values in time, so the linearization of θ around zero is possible $sin\theta \approx \theta$ for the simplification of the relation, namely small angle approximation. Then the following equation can be written in terms of some constants and two variables involving angular position θ and its time rate of change θ, angular velocity denoted by $\dot{\theta}$.

$$\underbrace{\left(I_G + ml^2\right)}_{I_A}\ddot{\theta} + b_t\dot{\theta} + (k_t - mgl)\theta = 0 \tag{B.3}$$

According to Equation B.3, finding the roots is descriptive, whether they are complex or real, to understand the characteristics of the type of damping that is possible to be underdamped, overdamped, or critically damped Since the everlasting dynamics of postural sway is oscillatory, the nonoscillatory response is out of question [116]. Then $\Delta = b^2 - 4ac$, it can be easily shown that $b_t^2 - 4I_A(k_t - mgl)$ which is the responsible term for the characteristics of roots to be complex. This implies that

the sign of $k_t - mgl$ and the magnitude of b_t [104] are the critical terms that can be controlled. In this way, the critical value of k_t with respect to the rest can be determined, which makes the roots complex for assessing postural sway, and it is named critical ankle stiffness.

Besides the moment equilibrium around ankle ΣM_A, equality of forces under dynamic conditions in either direction is also necessary so that the related equations around the ankle joint are provided below according to tangential and radial accelerations.

$$\vec{a}_{tot} = (\ddot{r} - r\dot{\theta}^2)\hat{e}_r + (2\dot{r}\dot{\theta} + r\ddot{\theta})\hat{e}_\theta \implies \tag{B.4a}$$

$$\Sigma F_x : -A_x = ml\ddot{\theta}cos\theta - ml\dot{\theta}sin\theta \tag{B.4b}$$

$$\Sigma F_y : A_y - mg = -ml\ddot{\theta}sin\theta - ml\dot{\theta}^2cos\theta \tag{B.4c}$$

Please keep in mind that $\dot{r} = \ddot{r} = 0$ as the length of the pendulum carrying the mass at the tip is held constant, and the local linearization around $\theta \approx 0$ (small angle approximation) is always valid throughout the Appendix. Therefore the term involving $sin\theta \approx 0$ in Equation B.4. Furthermore, under static conditions, force equalities can be written as follows for the foot in Figure B.1.

$$\Sigma F_x = 0 : A_x = \mu_s GRF \tag{B.5a}$$

$$\Sigma F_y = 0 : A_y = GRF = mg := W \tag{B.5b}$$

$$\Sigma M_A = 0 : -T_c + CoP_x GRF = 0 \implies T_c = CoP_x W \tag{B.5c}$$

While the first subequation represents that the force at the ankle is equal to static friction with a coefficient of friction is μ_s, the second equation dictates the equilibrium between GRF, ground reaction force, and mg. Furthermore, the last relation is written according to the moment around the ankle joint for the foot, and it is the only relation involving CoP_x, which is the temporal variable under interest throughout the dissertation. Moreover, for the calculation of ΣM_A, the horizontal frictions are neglected as its moment arm is too short, the height of the ankle joint is so close

to the ground, and the frictional forces are very small. Still, it is better to keep in mind that any human can not stand on a piece of perfect ice without friction, $\mu_s = 0$, due to the fact that even an infinitesimal small $\dot{\theta}$ leads to falling down according to Equation B.4 and B.5. On the other hand, almost surely, never-ending postural sway $P(\dot{\theta}(t) \neq 0) = 1$ can be carried on under the presence of friction. In other words, if $\dot{\theta} \neq 0$, friction forces are necessary for the force equilibrium in x direction.

Please note that geometrically $lsin\theta := CoM_x$, and employing it together with Equation B.5c to substitute into Equation B.3, it is possible to write down the following equation without considering the damping term.

$$-T_c + mglsin\theta = -T_c + mgCoM_x = mgCoP_x - mgCoM_x = I_A\ddot{\theta} \tag{B.6}$$

By keeping in mind that $GRF = mg = W$, the final division of both sides with mg yields the following relation. Please note that after linearization $\theta = CoM_x/l$ implies $\ddot{\theta} = \ddot{CoM}_x/l$.

$$(CoM_x - CoP_x) = -\frac{I_A}{mg}\ddot{\theta} \approx -\frac{I_A}{mgl}\ddot{CoM}_x \tag{B.7}$$

This equation is nothing but the relation used by Winter [6] to determine the linear correlation between $l\ddot{\theta} \approx \ddot{CoM}_x$ and the moment arm $CoM_x - CoP_x$. Therefore one can say that CoP_x controls CoM_x by oscillating either side of it [82]. According to the sign of $CoM_x - CoP_x$, the convexity of CoM_x (i.e., the second derivative with respect to time, $\ddot{CoM}_x$) must be reversed to keep the subject away from falling. Figure B.2 clearly shows the inverse relation between the direction of the difference between CoP_x and CoM_x and convexity around that instant. Therefore Winter [88] shows that the linear correlation $\left\langle (CoM_x - CoP_x)\ddot{CoM}_x \right\rangle$ is between -0.96 and -0.99, which is employed for the validation of the single degree of freedom inverted pendulum model.

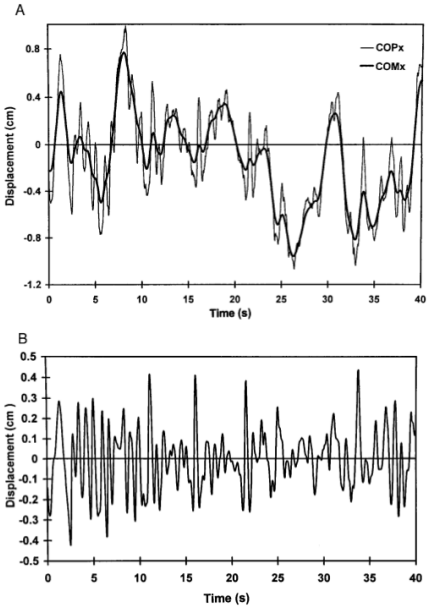

Figure B.2: Time Series of CoP_x and CoM_x Retrieved from Winter [6]

Besides Winter, the instant equilibrium points of rambling trembling are the locations of CoP_x at any instant where $\Sigma F_x = 0$, which is nothing but the equilibrium of forces in the related directions. According to the aforementioned inverted pendulum model Equations B.5a and B.4b, at any instant where $\sum F_x = 0$, Zatsiorsky defines the corresponding position of the CoM as an instantaneous equilibrium point [89], [90], [75]. Therefore we can say that equilibrium is instantly maintained when the moment arm is instantly zero $CoM_x - CoP_x = 0$, see Equation B.7. So that Zatsiorsky [2] estimates the location of CoM_x according to Newton's second law by using the following relation involving two initial conditions.

$$CoM_x(t) = CoM(0) + \dot{CoM}_x(0)t + \int_0^t \int_0^s \frac{F_x(u)}{m} duds \tag{B.8}$$

Equation B.8 estimates the location of $CoM_x(t)$ from the measurements of force plate F_x from one instant equilibrium point to the next as $F_x = ma_x$ at any instant t. CoM trajectory estimated in between two equilibrium points [89] can be linked to the rambling trajectory [2]. In this respect, the same method can be employed for the estimation of CoM trajectory in the absence of CoM recordings [117]. In conclusion, the CoM trajectory manifests itself as the smoothened version of the CoP signal in all aforementioned posture models.

Appendix C

ORNSTEIN UHLENBECK PROCESS

C.1 Ito Isometry Property

Before solving the stochastic differential equation representing the Ornstein Uhlenbeck process, it is better to state the Ito Isometry property, which will be used in Appendix C and Appendix D frequently for the calculation of variance and covariance function.

$$\left\langle \left(\int_0^T f(t, X_t) dW_t \right)^2 \right\rangle = \int_0^T f^2(t, X_t) dt \tag{C.1}$$

Equation C.1 asserts that the second moment of an integral with respect to the Wiener process boils down to a deterministic time integral of the squared function. It can be shown by the discretization of the integral as follows.

$$\left\langle \left(\int_0^T f(t, X_t) dW_t \right)^2 \right\rangle = \lim_{N \to \infty} \left\langle \left(\sum_{i=1}^{N} f(t_i, X_{t_i}) \Delta W_{t_i} \right)^2 \right\rangle \tag{C.2}$$

After that, the square of the terms of the series can be multiplied by employing a new index j as shown.

$$\left\langle \left(\int_0^T f(t, X_t) dW_t \right)^2 \right\rangle = \lim_{N \to \infty} \left\langle \left(\sum_{i=1}^{N} f(t_i, X_{t_i}) \Delta W_{t_i} \right) \left(\sum_{j=1}^{N} f(t_j, X_{t_j}) \Delta W_{t_j} \right) \right\rangle \tag{C.3}$$

At this point, it is better to note that the Wiener process has Markov property which

means one-step memory. Therefore the steps in the mutually disjoint time intervals are independent such that $\left\langle \Delta W_{t_i} \Delta W_{t_j} \right\rangle = 0$ if $i \neq j$ and $\left\langle \Delta W_{t_i} \Delta W_{t_j} \right\rangle = \Delta t$ if $i = j$. So that all of the cross terms in the summation vanishes, and the equation yields the following form involving the square of each term.

$$\lim_{N\to\infty} \left\langle \left(\sum_{i=1}^{N} f(t_i, X_{t_i}) \Delta W_{t_i} \right) \left(\sum_{j=1}^{N} f(t_j, X_{t_j}) \Delta W_{t_j} \right) \right\rangle = \lim_{N\to\infty} \left\langle \sum_{i=1}^{N} f^2(t_i, X_{t_i}) \left(\Delta W_{t_i} \right)^2 \right\rangle \tag{C.4}$$

It is possible to change the order of summation and expectation by exploiting the linearity of expectation. Furthermore, $f^2(t_i X_{t_i})$ can be taken outside the expectation since it is deterministic. In this way, the following relation can be obtained.

$$\lim_{N\to\infty} \left\langle \sum_{i=1}^{N} f^2(t_i, X_{t_i}) \left(\Delta W_{t_i} \right)^2 \right\rangle = \lim_{N\to\infty} \sum_{i=1}^{N} f^2(t_i, X_{t_i}) \left\langle \left(\Delta W_{t_i} \right)^2 \right\rangle \tag{C.5}$$

As a final step, the term inside the expectation is the variance of the increments of the Wiener process, and it is known that $\left\langle \left(\Delta W_{t_i} \right)^2 \right\rangle = \Delta t$. Accordingly, the discrete summation can be converted back to the time integral to reach the statement of Ito Isometry Property in Equation C.1.

$$\lim_{N\to\infty} \sum_{i=1}^{N} f^2(t_i, X_{t_i}) \left\langle \left(\Delta W_{t_i} \right)^2 \right\rangle = \lim_{N\to\infty} \sum_{i=1}^{N} f^2(t_i, X_{t_i}) \Delta t = \int_0^T f^2(t, X_t) dt \tag{C.6}$$

C.2 Analysis of Ornstein Uhlenbeck Process

By keeping in mind the sketch of the proof of the Ito Isometry property that will be used for later calculations, we can start to solve the stochastic differential equation provided below.

$$dX_t = -\lambda X_t dt + \sigma dW_t \tag{C.7}$$

Before solving the differential equation, it may be beneficial for a reader to see the differential equation in discrete form for interpretation.

$$\Delta X_t = -\lambda X_t \Delta t + \underbrace{\sigma \Delta W_t}_{\sigma(\Delta t)^{1/2} N(0,1)} \tag{C.8}$$

In the discrete form, the probabilistic decision at every time interval Δt becomes apparent. While the probabilistic part characterized by standard deviation is the second term which is absent in deterministic calculus, the first term is the deterministic constraint. For the second term, positive constant σ scales the variance at any single Δt. Therefore the increasing standard deviation can be seen as $\sqrt{\Delta t} N(0,1)$ analogous to a dice thrown at every Δt for the decision-making of the next step. In the absence of the first term, the summation of discrete steps ends up with a linear increment of variance as time passes. Evergrowing variance in time can be interpreted as "accumulation of chance" and entropy where the paths are diverging from the initial position according to linearly increasing variance, as shown in Figure 3.3. On the other hand, the first term with $\lambda > 0$ restricts the increment of variance to a constant finite value that is independent of time. Due to the presence of $-\lambda X_t \Delta t$, any path diverging to the positive side at any instant $X_t > 0$ pulled back toward the long-term mean zero as $-\lambda X_t \Delta t < 0$. Similarly, the paths diverging in the negative direction are also pulled toward zero due to the positive sign of $-\lambda X_t \Delta t > 0$. Since the mean reversion is only a function of X_t, the process remains to have one-step memory, the Markov property, and $\lambda > 0$ determines the rate of linear mean reversion. In other words, the first term $-\lambda X_t \Delta t$ is the linear constraint that makes the decision biased toward zero according to their current value X_t. According to the dice analogy constraint imposed through the first moment of displacements as $N(-\lambda X_t \Delta t, \sigma^2 \Delta t)$.

In this point of view, considering the phase space where the position is considered with respect to displacements, the Ornstein Uhlenbeck process can also be interpreted as a search of the line that has a slope $-\lambda$ and horizontal intercept at zero. For any position, $X_t > 0$, the decisions gain bias toward the intercept (zero), and for $X_t < 0$ same magnitude bias is observed toward the long-term mean again. Therefore Ornstein Uhlenbeck can be interpreted as the noise driven search of the line $\dot{x} = -\lambda x$. In this perspective, Ornstein Uhlenbeck process can be understood as similar to a

parallel connected spring and damper driven by Gaussian noise, which is named the Fokker Plank equation in the physics literature. Therefore mean reversion rate λ is nothing different than ratio of stiffness to damping k/b which can be determined by differentiation of both sides of Equation C.7 with respect to time as $\dot{x} = -k/bx + \sigma B_t$.

After the interpretation, as the first step of the solution, $\lambda X_t dt$ must be added to both sides. Consecutively, the right-hand side only involves the nonhomogenous part, which is particularly the Wiener process scaled with constant $\sigma > 0$.

$$dX_t + \lambda X_t dt = \sigma dW_t \tag{C.9}$$

Then the next step is the multiplication of both sides with the integrating factor $e^{\lambda t}$ as shown.

$$e^{\lambda t} dX_t + e^{\lambda t} \lambda X_t dt = e^{\lambda t} \sigma dW_t \tag{C.10}$$

After that, anyone can deduce the next relation as usual by observation.

$$d\left(e^{\lambda t} X_t\right) = e^{\lambda t} \sigma dW_t \tag{C.11}$$

By using Equation C.11, the integral can be computed from 0 to t by employing a dummy variable s for integration.

$$\int_0^t d\left(e^{\lambda s} X_s\right) = \int_0^t e^{\lambda s} \sigma dW_s \tag{C.12}$$

Even if it is possible to compute the integral on the left-hand side, the integral on the right must be left as it is, which will be crucial for the interpretation of the solution.

$$e^{\lambda t} X_t - X_0 = \int_0^t e^{\lambda s} \sigma dW_s \tag{C.13}$$

The addition of the initial condition X_0 to both sides and a multiplication with constant $e^{-\lambda t}$ yields the solution of the Ornstein Uhlenbeck process.

$$X_t = X_0 e^{-\lambda t} + \sigma e^{-\lambda t} \int_0^t e^{\lambda s} dW_s \tag{C.14}$$

Another representation of the solution is given below, which frequently appears in textbooks and articles. Please note that $e^{-\lambda t}$ is constant, therefore, the exponentials can be fused together.

$$X_t = X_0 e^{-\lambda t} + \sigma \int_0^t e^{-\lambda(t-s)} dW_s \tag{C.15}$$

Whether the solution is represented as Equation C.14 or Equation C.15 the integrand requires attention. Contrary to an ordinary diffusion equation $X_t = \sigma W_t$, the integrand behaves as an exponential time window which determines the respective effects of ΔW_i in *"distant past"* and *"recent past"*. Particularly for the Ornstein Uhlenbeck process, the constraint imposed from the first term in differential form reveals itself in the integrated, furthermore effect of the time window reveals itself in the correlation function that will be shown in Equation C.31. In this way, integrated respective influences according to $e^{\lambda s}$ are normalized with $e^{-\lambda t}$, which is outside the integral in Equation C.14. In this way, the variance can be kept bounded for large t.

Besides the exponential time window in the solution of Ornstein Uhlenbeck, another time window $(t-s)^{H-1/2}$ is the integrand in fractional Brownian motion in which the steps are dependent on time accordingly. Contrary to exponential form, power law $f(x) = x^{\alpha}$ fractal structure of diffusion can be modified with the generalization of Hurst exponent H. [96] Even if it is out of scope for the dissertation, it is better for the reader to keep in mind that through the integrand, time dependence can be imposed on the model.

After finding the solution, the first and second moments have to be calculated as X_t is distributed Gaussian, and its distribution can be completely characterized by the first and second moments.

Calculation of the first moment does not involve any steps as $\langle \Delta W_s \rangle = 0$ by definition. For further information, please refer to Shreve Theorem 11.4.5 [95] related to integrations with respect to martingales. Intuitively, as long as all $< \Delta W_s >= 0$,

then by changing the order of summation and expectation, one can find that the first moment is zero.

$$\langle X_t \rangle = 0 \tag{C.16}$$

For the calculation of the second moment, the Ito isometry property derived in Section C.1 should be used. Firstly start by taking the squares and expectations of both sides of the solution presented in Equation C.14.

$$\left\langle X_t^2 \right\rangle = \left(X_0 e^{-\lambda t}\right)^2 + \left\langle \left(\sigma e^{-\lambda t} \int_0^t e^{\lambda s} dW_s\right)^2 \right\rangle \tag{C.17}$$

The first term involving initial condition X_0 is taken outside the expectation as it is deterministic. Furthermore one can take $\left(\sigma e^{-\lambda t}\right)^2$ outside the expectation as it is deterministic too.

$$\left\langle X_t^2 \right\rangle = \left(X_0 e^{-\lambda t}\right)^2 + \left(\sigma e^{-\lambda t}\right)^2 \left\langle \left(\int_0^t e^{\lambda s} dW_s\right)^2 \right\rangle \tag{C.18}$$

Then Ito Isometry property is applicable for the part inside the expectation as shown in Equation C.1. Therefore the relation reduces into the following simple deterministic form involving integration with respect to time. Please note that even if the process is random, the moments are still deterministic which can be seen explicitly in this step.

$$\left\langle X_t^2 \right\rangle = X_0^2 e^{-2\lambda t} + \sigma^2 e^{-2\lambda t} \int_0^t e^{2\lambda s} ds \tag{C.19}$$

Then the definite integral with an exponential integrand can be computed as usual to find the next relation.

$$\left\langle X_t^2 \right\rangle = X_0^2 e^{-2\lambda t} + \sigma^2 e^{-2\lambda t} \frac{1}{2\lambda} \left(e^{2\lambda t} - 1\right) \tag{C.20}$$

After that, for a better form $e^{-2\lambda t}$ must be distributed into the paranthesis to differentiate the term decaying to zero from the remaining constant value.

$$\left\langle X_t^2 \right\rangle = X_0^2 e^{-2\lambda t} + \frac{\sigma^2}{2\lambda}\left(1 - e^{-2\lambda t}\right) \tag{C.21}$$

For greater values of time $t >> 0$, exponential terms decay, and the variance can be computed as the ratio of σ and λ as follows.

$$\left\langle X_t^2 \right\rangle = \frac{\sigma^2}{2\lambda} \tag{C.22}$$

Please remind that at the beginning σ is mentioned as the scale of standard deviation of displacements, so in the variance its squared appeared at the nominator. Furthermore as long as λ is determining the rate of mean reversion it is inversely proportional to variance of the Ornstein Uhlenbeck process.

In a similar way, covariance function can be computed which is the expectation $\langle X_t X_u \rangle$ for some $u < t$. In addition to variance, *"independence of increments in mutually disjoint time intervals"* must be considered for the proof. Then it is better to start with the following statement. Please note that for the sake of simplicity, only the stochastic terms are considered as the deterministic one has nothing to do with expectation and it will decay for $t >> 0$ due to the exponential term it is multiplied with. Also the cross multiplications are zero similar to calculation of mean of Ornstein Uhlenbeck process, i.e. integration with respect to martingale.

$$\langle X_t X_u \rangle = \left\langle \left(\sigma e^{-\lambda t} \int_0^t e^{\lambda s} dW_s \right) \left(\sigma e^{-\lambda u} \int_0^u e^{\lambda s} dW_s \right) \right\rangle \tag{C.23}$$

As a first step, the deterministic exponentials together with constant σ can be taken outside the expectation.

$$\langle X_t X_u \rangle = \sigma^2 e^{-\lambda(t+u)} \left\langle \left(\int_0^t e^{\lambda s} dW_s \right) \left(\int_0^u e^{\lambda s} dW_s \right) \right\rangle \tag{C.24}$$

It is already chosen that $u < t$, so the integral between 0 and t can be written as a summation of two integrals one is from zero to u and the other one is between u and t, as shown below.

$$\langle X_t X_u \rangle = \sigma^2 e^{-\lambda(t+u)} \left\langle \left(\int_0^u e^{\lambda s} dW_s + \int_u^t e^{\lambda s} dW_s \right) \left(\int_0^u e^{\lambda s} dW_s \right) \right\rangle \tag{C.25}$$

Applying distributive properties inside the expectation yields the following relation.

$$\langle X_t X_u \rangle = \sigma^2 e^{-\lambda(t+u)} \left\langle \left(\int_u^t e^{\lambda s} dW_s \right) \left(\int_0^u e^{\lambda s} dW_s \right) + \left(\int_0^u e^{\lambda s} dW_s \right)^2 \right\rangle \tag{C.26}$$

Then as an intermediate step, due to the linearity of the expectation operator, one can write the following relation.

$$\langle X_t X_u \rangle = \sigma^2 e^{-\lambda(t+u)} \left[\left\langle \left(\int_u^t e^{\lambda s} dW_s \right) \left(\int_0^u e^{\lambda s} dW_s \right) \right\rangle + \left\langle \left(\int_0^u e^{\lambda s} dW_s \right)^2 \right\rangle \right] \tag{C.27}$$

Please carefully look at the first expectation, which involves the multiplication of Wiener processes at disjoint time intervals. Since the disjoint intervals are independent, the first term must be zero. For the second expectation, the Ito Isometry property can be applied similarly to the computation of variance. Then the following equation can be obtained.

$$\langle X_t X_u \rangle = \sigma^2 e^{-\lambda(t+u)} \left\langle \left(\int_0^u e^{\lambda s} dW_s \right)^2 \right\rangle = \sigma^2 e^{-\lambda(t+u)} \int_0^u e^{2\lambda s} ds \tag{C.28}$$

After that, the rest is the computation of the integral on time as usual.

$$\langle X_t X_u \rangle = \frac{\sigma^2}{2\lambda} e^{-\lambda(t+u)} \left(e^{2\lambda u} - 1 \right) \tag{C.29}$$

Finally, the terms on the left-hand side of the parenthesis can be distributed into subtraction, and defining delay as $\tau := t - u$ yields the final form of the covariance

function.

$$\langle X_t X_u \rangle = \frac{\sigma^2}{2\lambda} e^{-\lambda(t+u)} = \frac{\sigma^2}{2\lambda} e^{-\lambda\tau} \tag{C.30}$$

Since the correlation function is the normalization of the covariance with respect to variances, the correlation function can be found as shown in the next relation, which is only an exponential decay with delay $\tau := t - s$.

$$\frac{\langle X_t X_u \rangle}{\sqrt{\langle X_t^2 \rangle \langle X_u^2 \rangle}} = e^{-\lambda\tau} \tag{C.31}$$

The correlation function found is nothing different than the time window in the integrand of Equation C.15, which was mentioned as the influence of distant and recent pasts.

Finally, the Fourier transform of the exponential correlation function can be computed with usual methods, so the Fourier integration is not shown but directly provided in the next relation.

$$\mathcal{F}\left\{\langle X_t X_u \rangle\right\}(\omega) := \int_{-\infty}^{\infty} e^{-j\omega\tau} e^{-\lambda\tau} d\tau = \frac{\lambda}{\pi\left(\lambda^2 + \omega^2\right)} \tag{C.32}$$

The relation is named power spectral density, and it shows the partition of variance among frequencies ω. Therefore the area under power spectral density is variance $\langle X_t^2 \rangle$. Since σ is only the scale of the standard deviation of displacements, as mentioned before, it does not affect the shape of power spectral density, i.e., decay rate, but it only determines the area under the curve. On the other hand, decay in the frequency spectrum is associated with λ. For smaller, the λ decay becomes slower, and greater power is observed in longer periods, as shown in Figure 3.4. Therefore greater power in longer periods is visible on the right-hand side of the figure.

Furthermore long term mean of Ornstein Uhlenbeck process can be changed from zero to other constant values by subtracting X_t from θ as shown in the equation provided below.

$$dX_t = -\lambda(X_t - \theta)dt + \sigma dW_t \tag{C.33}$$

In the equation the new parameter θ shifts the direction of bias without changing the variance. If $\theta \neq 0$ then the trajectories diverging away becomes pulled toward θ as the first term changes sign accordingly $X_t < \theta$ or $X_t > \theta$. In phase portrait the change shifts the intercept of the line from zero to θ with keeping the slope λ constant. Also the new form appears as the equilibrium point of the spring in Langeving form as follows.

$$\dot{x} + \underbrace{\frac{k}{b}}_{\lambda}(x - \theta) = \underbrace{\sigma B_t}_{\frac{d}{dt}(\sigma dW_t)} \tag{C.34}$$

Similarly if the equilibrium point of the spring is considered as θ than the dynamics of x changes as a shift from zero to θ.

Appendix D

DOUBLE ORNSTEIN UHLENBECK PROCESS

Before solving the system of the stochastic differential equations shown in Equation 3.13, equations are provided below to keep the reader away from going back and forth during reading. Besides that, it may be beneficial to read Appendix C related to the Ornstein Uhlenbeck process since some methods are going to be used in the same way whenever they are needed.

$$dX_t = -\lambda(X_t - \theta_t)dt + \sigma_1 dW_t^1 \tag{D.1a}$$

$$d\theta_t = -\kappa\theta_t dt + \sigma_2 dW_t^2 \tag{D.1b}$$

$$\left\langle dW_t^1 dW_t^2 \right\rangle = \rho dt \tag{D.1c}$$

Before starting to solve, first and second relations can be expressed in matrix form, as shown below. If anyone employs a Σ_{2x2} then the third relation can also be considered, yet $\rho = 0$ is selected, which makes the nondiagonal elements of variance-covariance matrix zero, $\Sigma_{i \neq j} = 0$.

$$\begin{bmatrix} dX_t \\ d\theta_t \end{bmatrix} = \begin{bmatrix} -\lambda & \lambda \\ 0 & -\kappa \end{bmatrix} \begin{bmatrix} X_t \\ \theta_t \end{bmatrix} dt + \begin{bmatrix} \sigma_1 dW_t^1 \\ \sigma_2 dW_t^2 \end{bmatrix} \tag{D.2}$$

It is also possible to consider the given system of stochastic differential equations as follows, similar to the stochastic differential equation of the Ornstein Uhlenbeck process and the corresponding Fokker Plank equation.

$$\dot{\vec{y}} = A\vec{y} + F_t \iff d\vec{y} = A\vec{y}dt + F_t dt \tag{D.3}$$

Then the next step is to follow the well-known route to solve Equation D.3, which involves computation of eigenvalues, eigenvectors, fundamental matrix, and finally, Green's function for the nonhomogenous part. Please note that it is similar to the solution of the Ornstein Uhlenbeck process given below but in vector form.

$$X_t = X_0 e^{-\lambda t} + \sigma e^{-\lambda t} \int_0^t e^{\lambda s} dW_s \tag{D.4}$$

Please remind that after determining eigenvalues and eigenvectors, the solution of the homogenous system of differential equations can be found as $\vec{x_t} = \psi_t \vec{c}$ with some integration constant vector $\vec{c}$. After that, applying the initial condition by substitution of $\vec{x_0} = \psi_0 \vec{c}$ and multiplication of both sides with the inverse of ψ_0^{-1} from left yields $\psi_0^{-1} \vec{x_0} = \vec{c}$. Then found $\vec{c}$ can be substituted back to determine $\vec{x_t}$ as $\vec{x_t} = \psi_t \psi_0^{-1} \vec{x_0}$ in terms of initial initial conditions. As a final step, the definition $\phi_t := \psi_t \psi_0^{-1}$ yields the solution of the homogenous part as given below.

$$\vec{x_t} = \phi_t \vec{x_0} \tag{D.5}$$

For the sake of simplicity, further derivation of Green's function is skipped for the nonhomogenous part, but anyone can notice the similarities between Equation D.5 and Equation D.4. Besides the first one being scalar and the second one in vector form, both equations are analogous such that $e^{-\lambda t}$ corresponds to ϕ_t. Therefore the solution of Equation D.8 can be written as follows as a function of ϕ_t and ϕ_s^{-1} similar to the solution of Ornstein Uhlenbeck process shown in Equation C.14. Still, please note that matrix multiplication is not commutative.

$$\vec{y} = \phi_t \vec{y_0} + \phi_t \int_0^t \phi_s^{-1} d\vec{F}_t \tag{D.6}$$

In order to avoid any kind of confusion, all terms have to be defined one by one. Firstly the coefficient matrix in the homogenous part is $A = \begin{bmatrix} -\lambda & \lambda \\ 0 & -\kappa \end{bmatrix}$ which ϕ_t is computed accordingly, and remind that it is analogous to $e^{-\lambda t}$ in the solution of

Ornstein Uhlenbeck. Furthermore $d\vec{F}_t := \begin{bmatrix} \sigma_1 dW_t^1 \\ \sigma_2 dW_t^2 \end{bmatrix}$ is going to be integrated with a Riemann-Stieltjes sense.

After that, the first step is finding the eigenvalues and corresponding eigenvectors associated with matrix A.

$$det(A-uI) = 0 \implies det\left(\begin{bmatrix} -\lambda - u & \lambda \\ 0 & -\kappa - u \end{bmatrix}\right) = 0 \implies u_1 = -\lambda, u_2 = -\kappa \tag{D.7}$$

Found eigenvalues give an idea about the stability, and $\lambda, \kappa > 0$ are chosen for the model. The mean reversion property associated with $\lambda, \kappa > 0$ with the terms of stochastic calculus also determines the stability since they correspond to the eigenvalues. Furthermore, by equating velocities to zero in the absence of second derivatives, it is possible to find the equilibrium points as follows.

$$\begin{bmatrix} \dot{X}_t \\ \dot{\theta}_t \end{bmatrix} = \begin{bmatrix} 0 \\ 0 \end{bmatrix} = \begin{bmatrix} -\lambda & \lambda \\ 0 & -\kappa \end{bmatrix} \begin{bmatrix} X_t \\ \theta_t \end{bmatrix} + \begin{bmatrix} \sigma_1 B_t^1 \\ \sigma_2 B_t^2 \end{bmatrix} \tag{D.8}$$

After taking the expectation of both sides, $\langle \sigma_1 B_t^1 \rangle = \langle \sigma_2 B_t^2 \rangle = 0$ vanishes and two equations, $X_t = \theta_t$ and $\theta_t = 0$, shows the equilibrium points. While $\theta_t = 0$ is the global equilibrium point, $X_t = \theta_t$ for any t shows the instants that the equilibrium is satisfied. The same can be directly concluded from Equation D.1. Since X_t is pulled toward θ_t due to $-\lambda(X_t - \theta_t)$ and θ_t is pulled toward zero because of $-\kappa(\theta_t - 0)$ those two correspond to different kinds of equilibriums. Once again, please note that the real equilibrium is at $X_t = \theta_t = 0$ globally, further $X_t = \theta_t$ is something about the equilibrium instants in terms of X_t in time.

Then, the next step is the determination of corresponding eigenvectors, as shown below.

$$\vec{v}_1 = \begin{bmatrix} 1 \\ 0 \end{bmatrix}, \vec{v}_2 = \begin{bmatrix} \frac{\lambda}{\lambda - \kappa} \\ 1 \end{bmatrix} \tag{D.9}$$

According to eigenvectors and eigenvalues, ψ_t can be defined as follows.

$$\psi_t := \left[e^{u_1 t}\vec{v}_1, e^{u_1 t}\vec{v}_2\right] = \begin{bmatrix} e^{-\lambda t} & \frac{\lambda}{\lambda-\kappa}e^{-\kappa t} \\ 0 & e^{-\kappa t} \end{bmatrix} \tag{D.10}$$

After that, the matrix has to be inverted, which requires $det(\psi_t) = e^{(\lambda+\kappa)t}$, therefore, the following matrices can be obtained.

$$\psi_t^{-1} = \begin{bmatrix} e^{\lambda t} & \frac{\lambda}{\kappa-\lambda}e^{\lambda t} \\ 0 & e^{\kappa t} \end{bmatrix} \implies \psi_0^{-1} = \begin{bmatrix} 1 & \frac{\lambda}{\kappa-\lambda} \\ 0 & 1 \end{bmatrix} \tag{D.11}$$

Please be careful about the difference of sign in the denominator involving λ and κ to avoid wrong calculation. After finding ψ_t and ψ_0^{-1}, it is possible to find ϕ_t as shown below.

$$\phi_t := \psi_t\psi_0^{-1} = \begin{bmatrix} e^{-\lambda t} & \frac{\lambda}{\kappa-\lambda}\left(e^{-\lambda t} - e^{-\kappa t}\right) \\ 0 & e^{-\kappa t} \end{bmatrix} \tag{D.12}$$

Moreover, for the nonhomogenous part, ϕ_t has to be inverted, which is denoted as ϕ_s^{-1} with dummy variable s for time, similar to $e^{\lambda s}$ in the solution of the Ornstein Uhlenbeck process.

$$\phi_s^{-1} = \begin{bmatrix} e^{\lambda s} & \frac{\lambda}{\kappa-\lambda}\left(e^{\lambda s} - e^{\kappa s}\right) \\ 0 & e^{\kappa s} \end{bmatrix} \tag{D.13}$$

As everything required for the determination of the solution, Equation D.12 and Equation D.13 must be substituted into Equation D.6 to solve Equation D.8. The substitution yields the following relation.

$$\begin{bmatrix} dX_t \\ d\theta_t \end{bmatrix} = \begin{bmatrix} e^{-\lambda t} & \frac{\lambda}{\kappa-\lambda}\left(e^{-\lambda t}-e^{-\kappa t}\right) \\ 0 & e^{-\kappa t} \end{bmatrix} \begin{bmatrix} X_0 \\ \theta_0 \end{bmatrix} + \begin{bmatrix} e^{-\lambda t} & \frac{\lambda}{\kappa-\lambda}\left(e^{-\lambda t}-e^{-\kappa t}\right) \\ 0 & e^{-\kappa t} \end{bmatrix} \int_0^t \begin{bmatrix} e^{-\kappa s} & \frac{\lambda}{\kappa-\lambda}\left(e^{\lambda s}-e^{\kappa s}\right) \\ 0 & e^{\kappa s} \end{bmatrix} \begin{bmatrix} \sigma_1 dW_t^1 \\ \sigma_2 dW_t^2 \end{bmatrix} \tag{D.14}$$

Finally, the matrix multiplications in Equation D.14 can be handled as usual. Please note that similar to the Ornstein Uhlenbeck process, the integrals in the nonhomogenous part are left as they are as it is impossible to do so.

$$X_t = X_0 e^{-\lambda t} + \theta_0 \frac{\lambda}{\kappa-\lambda}\left(e^{-\lambda t}-e^{-\kappa t}\right) + \sigma_1 \int_0^t e^{-\lambda(t-s)} dW_s^1 + \sigma_2 \frac{\lambda}{\kappa-\lambda}\left(\int_0^t e^{-\lambda(t-s)} dW_s^2 - \int_0^t e^{-\kappa(t-s)} dW_s^2\right) \tag{D.15}$$

$$\theta_t = e^{-\kappa t}\theta_0 + \sigma_2 \int_0^t e^{-\kappa(t-s)} dW_s^2 \tag{D.16}$$

Please note that θ_t is nothing different than an Ornstein Uhlenbeck.

For the rest of the explanations, θ_t is not going to be considered to find the variance and covariance since it is already found in the Appendix C in the scope of the Ornstein Uhlenbeck process. Moreover, for the determination of $\langle X_t^2 \rangle$ and $\langle X_t X_s \rangle$ the deterministic terms are not going to be considered to keep the calculations short, as mentioned in Appendix C, so the relation representing X_t is given below by denoting all three integrals with A, B and C. Please note that expectations involving the deterministic part are zero because after taking deterministic terms out of the expectation, the remaining part is integral with respect to martingale dW_t, which yields zero, similar to Appendix C.

$$X_t = \underbrace{\sigma_1 \int_0^t e^{-\lambda(t-s)} dW_s^1}_{A} + \sigma_2 \frac{\lambda}{\kappa-\lambda}\left(\underbrace{\int_0^t e^{-\lambda(t-s)} dW_s^2}_{B} - \underbrace{\int_0^t e^{-\kappa(t-s)} dW_s^2}_{C}\right) \tag{D.17}$$

It is already given that W_t^1 and W_t^2 are independent in Equation D.1c as $\rho = 0$. While $\langle X_t^2 \rangle = \langle A^2 \rangle + \langle B^2 \rangle + \langle C^2 \rangle + 2\langle AB \rangle + 2\langle BC \rangle + 2\langle AC \rangle$ due to linearity of expectation, covariances involving A are zero $\langle AB \rangle = \langle AC \rangle = 0$ because of the independence of W_t^1 and W_t^2. Hence we only need the squared terms and $2\langle BC \rangle$.

Furthermore, $\langle A^2 \rangle$ is already computed in the Ornstein Uhlenbeck part Appendix C. Then the required terms can be found as shown below by following the same procedure involving Ito Isometry Property shown in Appendix C.

$$\langle A^2 \rangle = \frac{\sigma_1^2}{2\lambda} \tag{D.18a}$$

$$\langle B^2 \rangle = \frac{\sigma_2^2}{(\kappa - \lambda)^2} \frac{1}{2\lambda} \tag{D.18b}$$

$$\langle C^2 \rangle = \frac{\sigma_2^2}{(\kappa - \lambda)^2} \frac{1}{2\kappa} \tag{D.18c}$$

$$2\langle BC \rangle = -\frac{\sigma_2^2}{(\kappa - \lambda)^2} \frac{2}{\lambda + \kappa} \tag{D.18d}$$

Summation of calculated terms yields the following relation which is the variance and the second moment of X_t as the mean is zero.

$$\langle X_t^2 \rangle = \frac{\sigma_1^2}{2\lambda} + \frac{\sigma_2^2}{(\kappa - \lambda)^2} \frac{1}{2\lambda} + \frac{\sigma_2^2}{(\kappa - \lambda)^2} \frac{1}{2\kappa} - \frac{\sigma_2^2}{(\kappa - \lambda)^2} \frac{2}{\lambda + \kappa} \tag{D.19}$$

Moreover, the variance can be shown in the following form after grouping the terms. Please remind that exponential terms decayed to zero to find this simple relation for large t such that $t >> 0$ as explained in the previous appendix about Ornstein Uhlenbeck. Therefore the newly proposed system of stochastic differential equations has a variance independent of time, in other words, a bounded variance opposed to unbounded diffusive dynamics of $X_t = \sigma dW_t$.

$$\langle X_t^2 \rangle = \frac{\sigma_1^2}{2\lambda} + \left(\frac{\sigma_2 \lambda}{\kappa - \lambda} \right)^2 \left[\frac{1}{2\lambda} + \frac{1}{2\kappa} - \frac{2}{\lambda + \kappa} \right] \tag{D.20}$$

Please remind that if θ_t was constant, the variance would be $\sigma_1^2/2\lambda$, yet due to the varying equilibrium point θ_t, the variance is increased, which is the second term in

Equation D.20. The positive definiteness of the second term can be seen by equating the denominators as follows.

$$\left(\frac{\sigma_2\lambda}{\kappa-\lambda}\right)^2\left[\frac{1}{2\lambda}+\frac{1}{2\kappa}-\frac{2}{\lambda+\kappa}\right]=\left(\frac{\sigma_2\lambda}{\kappa-\lambda}\right)^2\frac{2\lambda\kappa+2\kappa^2+2\lambda^2+2\lambda\kappa-8\lambda\kappa}{4\lambda\kappa\left(\lambda-\kappa\right)}$$
$$=\left(\frac{\sigma_2\lambda}{\kappa-\lambda}\right)^2\frac{2\lambda^2+2\kappa^2-4\lambda\kappa}{4\lambda\kappa\left(\lambda-\kappa\right)}=\left(\frac{\sigma_2\lambda}{\kappa-\lambda}\right)^2\frac{\lambda+\kappa}{2\lambda\kappa}>0 \quad \text{(D.21)}$$

After that, the next step is finding the covariance function for reaching the temporal correlation structure of the process X_t in time. Therefore the covariance function can be defined as given below.

$$\langle X_tX_u\rangle =< \left[\underbrace{\sigma_1\int_0^t e^{-\lambda(t-s)}dW_s^1}_{A_t}+\sigma_2\frac{\lambda}{\kappa-\lambda}\left(\underbrace{\int_0^t e^{-\lambda(t-s)}dW_s^2}_{B_t}-\underbrace{\int_0^t e^{-\kappa(t-s)}dW_s^2}_{C_t}\right)\right]$$
$$\left[\underbrace{\sigma_1\int_0^u e^{-\lambda(u-s)}dW_s^1}_{A_u}+\sigma_2\frac{\lambda}{\kappa-\lambda}\left(\underbrace{\int_0^u e^{-\lambda(u-s)}dW_s^2}_{B_u}-\underbrace{\int_0^u e^{-\kappa(u-s)}dW_s^2}_{C_u}\right)\right]> \quad \text{(D.22)}$$

Similar to determination of the variance, again $\langle A_tB_u\rangle = \langle A_tC_u\rangle = 0$ due to independence of W_t^1 and W_t^2 where $\rho = 0$, so we only need $\langle A_tA_u\rangle$, $\langle B_tB_u\rangle$, $\langle C_tC_u\rangle$ and $\langle B_tC_u\rangle$. By following the same procedure of computation of covariance of Ornstein Uhlenbeck and the variance found in Equation D.18, one can write the following relations where $\tau := t-u$ is the delay.

$$\langle A_t A_u \rangle = \frac{\sigma_1^2}{2\lambda} e^{-\lambda\tau} \tag{D.23a}$$

$$\langle B_t B_u \rangle = \frac{\sigma_2^2}{(\kappa-\lambda)^2} \frac{1}{2\lambda} e^{-\lambda\tau} \tag{D.23b}$$

$$\langle C_t C_u \rangle = \frac{\sigma_2^2}{(\kappa-\lambda)^2} \frac{1}{2\kappa} e^{-\kappa\tau} \tag{D.23c}$$

$$\langle B_t C_u \rangle = -\frac{\sigma_2^2}{(\kappa-\lambda)^2} \frac{1}{\lambda+\kappa} e^{-\lambda\tau} \tag{D.23d}$$

$$\langle B_u C_t \rangle = -\frac{\sigma_2^2}{(\kappa-\lambda)^2} \frac{1}{\lambda+\kappa} e^{-\kappa\tau} \tag{D.23e}$$

$$\tag{D.23f}$$

The summation of found terms yields the covariance of the stochastic process X_t.

$$\begin{aligned}\langle X_t X_u \rangle = \frac{\sigma_1^2}{2\lambda} e^{-\lambda\tau} + \frac{\sigma_2^2}{(\kappa-\lambda)^2} \frac{1}{2\lambda} e^{-\lambda\tau} + \frac{\sigma_2^2}{(\kappa-\lambda)^2} \frac{1}{2\kappa} e^{-\kappa\tau} \\ - \frac{\sigma_2^2}{(\kappa-\lambda)^2} \frac{1}{\lambda+\kappa} e^{-\lambda\tau} - \frac{\sigma_2^2}{(\kappa-\lambda)^2} \frac{1}{\lambda+\kappa} e^{-\kappa\tau}\end{aligned} \tag{D.24}$$

Similar to variance, the terms can be taken into common parenthesis for the simplicity of the representation. In this way, the double exponential form of the covariance structure reveals clearly.

$$\langle X_t X_u \rangle = \left[\frac{\sigma_1^2}{2\lambda} + \left(\frac{\sigma_2 \lambda}{\kappa-\lambda} \right)^2 \left[\frac{1}{2\lambda} - \frac{1}{\lambda+\kappa} \right] \right] e^{-\lambda\tau} + \left[\left(\frac{\sigma_2 \lambda}{\kappa-\lambda} \right)^2 \left[\frac{1}{2\kappa} - \frac{1}{\lambda+\kappa} \right] \right] e^{-\kappa\tau} \tag{D.25}$$

Compared to the Ornstein Uhlenbeck process, new correlations emerged, decaying with $e^{-\kappa t}$. In the desired parameter range, $\lambda \approx 8\kappa$ correlations of new process decay slower than the correlations associated with λ. Hence the newly defined θ_t governs the behavior at lower frequencies.

Appendix E

GENERALIZED DOUBLE ORNSTEIN UHLENBECK PROCESS

In this Appendix, the Double Ornstein Uhlenbeck process represented by Equation 3.13 and Equation D.1 is generalized in terms of $\rho \in [-1, 1]$, and the associated variances and covariances are provided below without explanations due to their complicated appearances.

$$\left\langle X_t^2 \right\rangle = \frac{\sigma_1^2}{2\lambda} + \frac{\lambda\sigma_1\sigma_2}{\kappa-\lambda}\rho\left(\frac{1}{\lambda} - \frac{2}{\lambda+\kappa}\right) + \left(\frac{\lambda\sigma_2}{\kappa-\lambda}\right)^2\left(\frac{1}{2\lambda} + \frac{1}{2\kappa} - \frac{2}{\lambda+\kappa}\right) \quad \text{(E.1)}$$

$$\begin{aligned}\langle X_t X_u \rangle = &\left[\frac{\sigma_1^2}{2\lambda} + \frac{\lambda\sigma_1\sigma_2}{\kappa-\lambda}\rho\left(\frac{1}{\lambda} - \frac{1}{\lambda+\kappa}\right) + \left(\frac{\sigma_2\lambda}{\kappa-\lambda}\right)^2\left[\frac{1}{2\lambda} - \frac{1}{\lambda+\kappa}\right]\right]e^{-\lambda\tau} + \\ &\left[-\frac{\lambda\sigma_1\sigma_2}{\kappa-\lambda}\rho\frac{1}{\lambda+\kappa} + \left(\frac{\sigma_2\lambda}{\kappa-\lambda}\right)^2\left[\frac{1}{2\kappa} - \frac{1}{\lambda+\kappa}\right]\right]e^{-\kappa t} \quad \text{(E.2)}\end{aligned}$$

$$\langle X_t\theta_t \rangle = \sigma_1\sigma_2\rho\frac{1}{\lambda+\kappa} + \frac{\lambda\sigma_2^2}{\kappa-\lambda}\left(\frac{1}{\lambda+\kappa} - \frac{1}{2\kappa}\right) \quad \text{(E.3)}$$

$$\langle X_t\theta_u \rangle = e^{-\lambda\tau}\left[\sigma_1\sigma_2\rho\frac{1}{\lambda+\kappa} + \frac{\lambda\sigma_2^2}{\kappa-\lambda}\frac{1}{\lambda+\kappa}\right] + e^{-\kappa\tau}\left[-\frac{\lambda\sigma_2^2}{\kappa-\lambda}\frac{1}{2\kappa}\right] \quad \text{(E.4)}$$

$$\begin{aligned}\langle X_t\left(X_t - \theta_t\right)\rangle = &\frac{\sigma_1^2}{2\lambda} + \frac{\lambda\sigma_1\sigma_2}{\kappa-\lambda}\rho\left(\frac{1}{\lambda} - \frac{2}{\lambda+\kappa}\right) + \left(\frac{\lambda\sigma_2}{\kappa-\lambda}\right)^2\left(\frac{1}{2\lambda} + \frac{1}{2\kappa} - \frac{2}{\lambda+\kappa}\right) - \\ &\sigma_1\sigma_2\rho\frac{1}{\lambda+\kappa} + \frac{\lambda\sigma_2^2}{\kappa-\lambda}\left(\frac{1}{\lambda+\kappa} - \frac{1}{2\kappa}\right) \quad \text{(E.5)}\end{aligned}$$

$$\langle X_t \left(X_u - \theta_u \right) \rangle = \left[\frac{\sigma_1^2}{2\lambda} + \frac{\lambda \sigma_1 \sigma_2}{\kappa - \lambda} \rho \left(\frac{1}{\lambda} - \frac{1}{\lambda + \kappa} \right) \right] e^{-\lambda \tau} +$$
$$\left[\left(\frac{\sigma_2 \lambda}{\kappa - \lambda} \right)^2 \left(\frac{1}{2\lambda} - \frac{1}{\lambda + \kappa} \right) - \sigma_1 \sigma_2 \rho \frac{1}{\lambda + \kappa} - \frac{\lambda \sigma_2^2}{\kappa - \lambda} \frac{1}{\lambda + \kappa} \right] e^{-\lambda \tau} +$$
$$\left[-\frac{\lambda \sigma_1 \sigma_2}{\kappa - \lambda} \rho \frac{1}{\lambda + \kappa} + \left(\frac{\sigma_2 \lambda}{\kappa - \lambda} \right)^2 \left[\frac{1}{2\kappa} - \frac{1}{\lambda + \kappa} \right] + \frac{\lambda \sigma_2^2}{\kappa - \lambda} \frac{1}{2\kappa} \right] e^{-\kappa t} \quad \text{(E.6)}$$